



2  
2009



This is to certify that the  
dissertation entitled

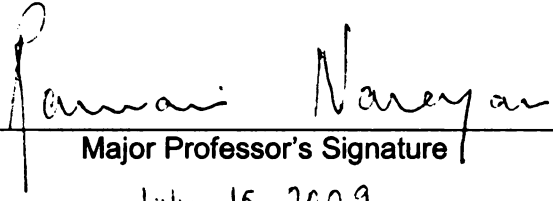
**PRODUCTION AND CHARACTERIZATION OF NOVEL  
STARCH AND POLY(BUTYLENE ADIPATE-CO-  
TEREPHTHALATE) – BASED MATERIALS AND THEIR  
APPLICATIONS**

presented by

Jacqueline Ann Stagner

has been accepted towards fulfillment  
of the requirements for the

Ph.D. degree in Materials Science and Engineering

  
Major Professor's Signature

July 15, 2009.

Date

**PLACE IN RETURN BOX** to remove this checkout from your record.  
**TO AVOID FINES** return on or before date due.  
**MAY BE RECALLED** with earlier due date if requested.

DATE DUE	DATE DUE	DATE DUE
NOV 21 2011		

**PRODUCTION AND CHARACTERIZATION OF NOVEL STARCH AND  
POLY(BUTYLENE ADIPATE-CO-TEREPHTHALATE) – BASED MATERIALS  
AND THEIR APPLICATIONS**

**By**

**Jacqueline Ann Stagner**

**A DISSERTATION**

**Submitted to  
Michigan State University  
in partial fulfillment of the requirements  
for the degree of**

**DOCTOR OF PHILOSOPHY**

**Materials Science and Engineering**

**2009**

## **ABSTRACT**

### **PRODUCTION AND CHARACTERIZATION OF NOVEL STARCH AND POLY(BUTYLENE ADIPATE-CO-TEREPHTHALATE) – BASED MATERIALS AND THEIR APPLICATIONS**

By

Jacqueline Ann Stagner

This work focuses on the production and characterization of blends of maleated thermoplastic starch (MTPS) and poly(butylenes adipate-co-terephthalate) and their application for use as thermoformed objects, films, and foams.

First, by the production and characterization of maleated thermoplastic starch (MTPS) synthesized by reactive extrusion in a twin-screw extruder, a better understanding of MTPS was gained. This reactive thermoplastic starch was prepared with glycerol as the plasticizer, maleic anhydride (MA), and free-radical initiator, 2,5-bis(tert-butylperoxy)-2,5-dimethylhexane (Luperox 101). Dynamic light scattering (DLS), differential scanning calorimetry (DSC), Fourier transform infrared spectroscopy (FTIR), soxhlet extraction in acetone, and environmental scanning electron microscopy (ESEM) were performed to determine the effect of maleation, extrusion temperature, initiator concentration, and maleic anhydride concentration on the resulting MTPS.

Next, maleated thermoplastic starch (MTPS) and thermoplastic starch (TPS) were reactively blended in a twin-screw extruder with a biodegradable polyester, poly(butylene adipate-co-terephthalate) (PBAT). The blends were extruded to

produce thermoformable sheets. The mechanical properties of the sheets were characterized by tensile and puncture tests. Proof of grafting was determined by soxhlet extraction in dichloromethane and FTIR analysis. Observations of the thermal properties were made using DSC, while the surface of the sheets was imaged using ESEM.

Blends of MTPS and PBAT were also extruded to produce films. Mechanical testing (tensile and puncture tests) and barrier performance testing (carbon dioxide, oxygen, and water vapor permeability) were performed on the films. Transmission electron microscopy (TEM) was used to image the blends and to view the dispersion of the various phases.

Finally, blends of MTPS and PBAT were extruded with an endothermic chemical blowing agent to produce foams. The foams were characterized by measuring density, expansion ratio, specific length, compressive strength, resiliency, and moisture sorption. Also, digital light microscopy was used to image the cell structure of the foams.

This work demonstrates that blends of starch and PBAT can be produced and formed into thermoformed objects, films, and foams. These objects can replace current objects made from non-biodegradable, petroleum-based plastics. By blending the starch and PBAT together, one receives advantages over using either component separately.

**To Dan and Lindsay, for all of your love and support.**

## **ACKNOWLEDGMENTS**

There are many people who have helped me over the past four years. I would like to thank my advisor, Dr. Ramani Narayan, and my guidance committee; Dr. Andre Lee, Dr. Krishnamurthy Jayaraman, and Dr. Rafael Auras, for their time, advice, guidance, and encouragement during the course of my Ph.D.

There have also been many other people who have provided their assistance. I would like to thank the members of the Biobased Materials Research Group, past and present; Dr. Daniel Graiver, Ken Farminer, Dr. Vanessa Dias Alves, Leann Lerie Matta, Laura Patrick, Dr. Alison Fowlks, Dr. Weipeng Liu, Madhusudan Srinivasan, Mamud Dako, Maria Darsono, Rebecca Frear, Elizabeth Brown, Siva Chalasani, and Zhiguan Yang. You provided much support, help, and valuable input.

The many other individuals who have helped me with various aspects of my research include Mike Rich, Per Askeland, Brian Rook, Ed Drown, and Hazel-Ann Hosein in the CMSC; Kelby Thayer, Sukeewan Detyothin, Pankaj Kumar, Isinay Yuzay, and Siriyupa Netramai in the School of Packaging; Alicia Pastor and Ewa Danielewicz in the Center for Advanced Microscopy; Rui Huang in the Department of Chemistry; Nicole Hall, Nancy Raney, John Mills, and Dan Drazkowski.



Finally, I would like to thank my family. Dan, Lindsay, Chris, Kelly, mom and dad, your love and support helped me more than you will ever know. Audra, your smiles are a great pick-me-up. Finally, our little Bambino, I can't wait to meet you.

Although I have mentioned only a few names, there are many more people who have helped me throughout this venture. I would like to extend my appreciation to all of the other people who I have inadvertently left out.

## TABLE OF CONTENTS

List of Tables.....	x
List of Figures.....	xi
Chapter 1.....	1
1.1 Problem Statement.....	1
1.2 Objectives.....	2
1.3 Specific Objectives.....	3
1.4 Structure of Dissertation.....	5
Chapter 2.....	7
2.1 Biobased and Biodegradable Plastics Rationale.....	7
2.2 Starch.....	12
2.3 Poly(butylene adipate-co-terephthalate) (PBAT).....	14
2.4 Extrusion Theory.....	15
2.5 Polymer Blends and Alloys.....	18
2.6 Review of Literature.....	20
Chapter 3.....	29
3.1 Rationale.....	29
3.2 Materials and Methods.....	30
3.2.1 Materials.....	30
3.2.2 Equipment.....	30
3.2.3 Procedure.....	32
3.2.3.1 Sample Preparation.....	32
3.2.3.2 Dynamic Light Scattering (DLS) Analysis.....	37
3.2.3.3 Fourier Transform Infrared Spectroscopy (FTIR) Analysis.....	38
3.2.3.4 Thermal Analysis (DSC).....	38
3.2.3.5 Soxhlet Extraction Analysis.....	38
3.2.3.6 Environmental Scanning Electron Microscopy (ESEM) Analysis.....	39
3.2.3.7 Statistical Analysis.....	39
3.3 Results and Discussion.....	40
3.3.1 Dynamic Light Scattering (DLS) Analysis.....	40
3.3.2 Fourier Transform Infrared Spectroscopy (FTIR) Analysis.....	44
3.3.3 Thermal Analysis (DSC).....	46
3.3.4 Soxhlet Extraction Analysis.....	50
3.3.5 Environmental Scanning Electron Microscopy (ESEM) Analysis.....	52
3.4 Conclusions.....	55
Chapter 4.....	56
4.1 Rationale.....	56
4.2 Materials and Methods.....	57
4.2.1 Materials.....	57
4.2.2 Equipment.....	57
4.2.3 Procedure.....	58

4.2.3.1 Production of Thermoplastic Starch (TPS) and Maleated Thermoplastic Starch (MTPS).....	58
4.2.3.2 Blend Production of TPS and MTPS with PBAT.....	59
4.2.3.3 Sheet Production.....	62
4.2.3.4 Thermoforming Process.....	63
4.2.3.5 Fourier Transform Infrared Spectroscopy (FTIR) Analysis.....	64
4.2.3.6 Tensile Tests.....	64
4.2.3.7 Puncture Tests.....	65
4.2.3.8 Thermal Analysis (DSC).....	65
4.2.3.8 Environmental Scanning Electron Microscopy (ESEM) Analysis.....	66
4.2.3.10 Statistical Analysis.....	66
4.3 Results and Discussion.....	66
4.3.1 Fourier Transform Infrared Spectroscopy Analysis (FTIR).....	66
4.3.2 Tensile Tests.....	69
4.3.3 Puncture Tests.....	73
4.3.4 Thermal Analysis (DSC).....	75
4.3.5 Environmental Scanning Electron Microscopy (ESEM) Analysis.....	77
4.4 Conclusions.....	80
Chapter 5.....	82
5.1 Rationale.....	82
5.2 Materials and Methods.....	83
5.2.1 Materials.....	83
5.2.2 Equipment.....	83
5.2.3 Procedure.....	84
5.2.3.1 Production of Maleated Thermoplastic Starch (MTPS).....	84
5.2.3.2 Blend Production of MTPS with PBAT.....	85
5.2.3.3 Film Production.....	86
5.2.3.4 Determining Biobased Content.....	86
5.2.3.5 Mechanical Properties.....	87
5.2.3.5.1 Tensile Tests.....	87
5.2.3.5.2 Puncture Tests.....	87
5.2.3.6 Barrier Properties.....	88
5.2.3.6.1 Carbon Dioxide Permeability.....	88
5.2.3.6.2 Oxygen Permeability.....	89
5.2.3.6.3 Water Vapor Permeability.....	90
5.2.3.7 Transmission Electron Microscopy (TEM).....	91
5.2.3.8 Statistical Analysis.....	91
5.3 Results and Discussion.....	91
5.3.1 Determining Biobased Content.....	91
5.3.2 Mechanical Properties.....	92
5.3.2.1 Tensile Tests.....	92
5.3.2.2 Puncture Tests.....	95
5.3.3 Barrier Properties.....	96
5.3.4 Transmission Electron Microscopy (TEM).....	99
5.4 Conclusions.....	101

Chapter 6.....	102
6.1 Rationale.....	102
6.2 Materials and Methods.....	103
6.2.1 Materials.....	103
6.2.2 Equipment.....	103
6.2.3 Procedure.....	104
6.2.3.1 Production of Maleated Thermoplastic Starch (MTPS).....	104
6.2.3.2 Blend Production of MTPS with PBAT.....	104
6.2.3.3 Foam Production.....	105
6.2.3.4 Chemical Blowing Agent Thermal Decomposition.....	107
6.2.3.5 Extensional Viscosity.....	107
6.2.3.6 Foam Characterization.....	108
6.2.3.6.1 Density.....	108
6.2.3.6.2 Expansion Ratio.....	108
6.2.3.6.3 Specific Length.....	109
6.2.3.6.4 Compressive Strength and Resiliency.....	109
6.2.3.6.5 Moisture Sorption Analysis.....	110
6.2.3.6.6 Digital Light Microscopy.....	110
6.2.3.7 Statistical Analysis.....	111
6.3 Results and Discussion.....	111
6.3.1 Chemical Blowing Agent Thermal Decomposition.....	111
6.3.2 Extensional Viscosity.....	113
6.3.3 Density, Expansion Ratio, and Specific Length.....	116
6.3.4 Compressive Strength and Resiliency.....	119
6.3.5 Moisture Sorption Analysis.....	121
6.3.6 Digital Light Microscopy.....	124
6.4 Conclusions.....	127
Chapter 7.....	128
7.1 Summary.....	128
7.2 Conclusions.....	129
7.2.1 Maleated Thermoplastic Starch by Reactive Extrusion Processing.....	129
7.2.2 MTPS-PBAT Blends by Reactive Extrusion Processing and Their Application and Performance for Thermoformed Articles.....	130
7.2.3 Application and Performance of MTPS-PBAT Blends for Films.....	132
7.2.4 Application and Performance of MTPS-PBAT Blends for Foams.....	133
Chapter 8.....	135
8.1 Recommendations for Future Work.....	135
References.....	138

## LIST OF TABLES

Table 1. Composition of the maleated and non-maleated thermoplastic starch (MTPS and TPS) samples.....	34
Table 2. Hydrodynamic radii as measured by dynamic light scattering.....	41
Table 3. Percentage of glycerol grafted to the starch after soxhlet extraction of maleated thermoplastic starch in acetone for 72 hours.....	52
Table 4. Composition of the blends of TPS and MTPS with PBAT.....	61
Table 5. Thickness and mechanical properties (determined by tensile tests) of sheets of blends of TPS and MTPS with PBAT.....	70
Table 6. Mechanical properties determined by puncture tests of the thermoformed pieces of the blends of TPS and MTPS with PBAT.....	74
Table 7. DSC parameters: glass transition temperature ( $T_g$ ), crystallization temperature ( $T_c$ ), crystallization enthalpy ( $\Delta H_c$ ), and melting temperature ( $T_m$ ) of the blends of MTPS and TPS with PBAT.....	76
Table 8. Composition of films of blends of MTPS with PBAT.....	85
Table 9. Thickness and mechanical properties (determined by tensile tests) of films of blends of MTPS with PBAT.....	93
Table 10. Puncture test results of films of blends of MTPS with PBAT.....	95
Table 11. Barrier properties of films of blends of MTPS with PBAT.....	97
Table 12. Composition of foams of blends of MTPS and PBAT.....	106
Table 13. Density, expansion ratio, and specific length of foams of blends of MTPS and PBAT.....	118
Table 14. Resiliency of foams of blends of MTPS and PBAT.....	121
Table 15. Moisture sorption steady-state weight gain, diameter, and length of foams of blends of MTPS and PBAT.....	123

## LIST OF FIGURES

Figure 1. The global carbon cycle.....	9
Figure 2. Degradation versus biodegradation of materials.....	11
Figure 3. Structure of amylose and amylopectin.....	13
Figure 4. Chemical structure of PBAT.....	14
Figure 5. Schematic diagram of dispersive and distributive mixing.....	17
Figure 6. Relationship between property values and blend composition.....	19
Figure 7. Screw configuration of the Century CX-30 co-rotating twin-screw extruder.....	31
Figure 8. Process schematic for extrusion of MTPS.....	35
Figure 9. Proposed reaction of starch with maleic anhydride.....	35
Figure 10. Hydrolysis (a) and glucosidation (b) reactions occurring during the reactive extrusion of maleated thermoplastic starch.....	36
Figure 11. Graph of dynamic light scattering measurements for sample 6 (MTPS high amylose starch, with 30% glycerol and 135°C).....	37
Figure 12. Picture of maleated thermoplastic starch pellets.....	40
Figure 13. FTIR Spectra for High Amylose Corn Starch, TPS 135°C 30% Glycerol, and MTPS 135°C 0.1% L101 2% MA 30% Glycerol.....	45
Figure 14. FTIR relative intensities of the carbonyl peak for the MTPS samples.....	46
Figure 15. DSC thermogram of the MTPS (at 135°C and 30% glycerol) and TPS (at 135°C and 30% glycerol) samples.....	49

Figure 16. Environmental scanning electron microscope images of extrudate samples. Images shown at 750x magnification (50 $\mu\text{m}$ scale bar). a) MTPS, at 165°C, 0.1% L101, 2% MA, 20% glycerol, b) MTPS, at 165°C, 0.25% L101, 2% MA, 20% glycerol, c) MTPS, at 165°C, 0.50% L101, 2% MA, 20% glycerol, d) MTPS, at 165°C, 0.25% L101, 6% MA, 20% glycerol, e) MTPS, at 135°C, 0.1% L101, 2% MA, 30% glycerol and f) TPS, at 135°C, 70% starch and 30% glycerol.....	54
Figure 17. Proposed reaction scheme for MTPS and PBAT .....	62
Figure 18. Picture of the object formed in the Labform thermoformer.....	63
Figure 19. FTIR Spectra for HA Starch, PBAT, and MTPS 165°C 2%MA 0.1%L101 20%G-PBAT(50:50).....	67
Figure 20. FTIR Spectra for film made after soxhlet of MTPS 165°C 0.1% L101 2%MA 20%G-PBAT(60:40), pellets left in thimble after soxhlet of MTPS 165°C 0.1%L101 2%MA 20%G-PBAT (60:40), and as extruded pellets of MTPS 165°C 0.1%L101 2%MA 20%G-PBAT (60:40).....	68
Figure 21. ESEM images of the samples extruded at 165°C and 20% glycerol at 750x magnification (50 $\mu\text{m}$ scale bar): (a) MTPS high amylose-PBAT (60:40), (b) MTPS high amylose-PBAT (50:50) and (c) MTPS corn starch-PBAT (50:50).....	78
Figure 22. ESEM images of the samples extruded at 135°C and 30% glycerol at 750x magnification (50 $\mu\text{m}$ scale bar): (a) TPS high amylose-PBAT (50:50), (b) MTPS high amylose-PBAT (50:50), (c) TPS corn starch-PBAT (50:50) and (d) MTPS corn starch-PBAT (50:50).....	79
Figure 23. TEM images of the samples at 20,000x magnification (1 $\mu\text{m}$ scale bar): (a) PBAT, (b) MTPS:PBAT (10:90), (c) MTPS:PBAT (20:80), (d) MTPS:PBAT (30:70), (e) MTPS:PBAT (40:60), and (f) MTPS:PBAT (50:50). MTPS is the light phase and PBAT is the dark phase.....	100
Figure 24. TGA graph of thermal decomposition of chemical blowing agent.....	112
Figure 25. Extensional viscosity plot of PBAT at 150°C.....	114
Figure 26. Extensional viscosity of blends at 140°C and 1 <sup>-s</sup> .....	115
Figure 27. Logarithmic plot of compressive strength as a function of foam density.....	120

**Figure 28. Digital light microscope images of foams of blends of MTPS and PBAT (250  $\mu\text{m}$  scale bar) showing the cell structure of the foams..... 126**



# **CHAPTER 1**

## **INTRODUCTION**

---

### **1.1 PROBLEM STATEMENT**

In recent years, there has been growing concern over society's dependence on petroleum, not only for fuel, but also as the basis for many single-use plastic items. There are many biobased, biodegradable materials that have the potential to be replacements for petroleum-based polymers. Biobased and biodegradable plastics can form the basis for a sustainable and environmentally preferable alternative to current materials based exclusively on petroleum. Recent cost increases for petroleum are also forcing end-users to look more aggressively for alternative products that provide the required performance characteristics, while having a reduced carbon footprint, and an environmentally responsible design.

With this in mind, the work presented here aims to show that biodegradable plastics that are partly biobased, can be produced to meet the needs of end-users.

## **1.2 OBJECTIVES**

This study focuses on the design and engineering of blends of maleated thermoplastic starch (MTPS) with poly(butylene adipate-co-terephthalate) (PBAT) through reactive extrusion, and the characterization of the resulting polymers. Furthermore, the application of these polymers for products such as thermoformed articles, films, and foams is studied. Specifically, the study focuses on the following:

- Maleated thermoplastic starch by reactive extrusion processing.
- MTPS-PBAT blends by reactive extrusion processing.
- Application and performance of MTPS-PBAT blends for thermoformed articles, films, and foams.

### 1.3 SPECIFIC OBJECTIVES

- **Maleated thermoplastic starch by reactive extrusion processing.**
  - Extrusion processing to graft maleic anhydride, glycerol, and starch using free radical initiation chemistry.
  - Characterization of the resulting MTPS.
    - Soxhlet extraction, Thermal Analysis, Environmental Scanning Electron Microscopy (ESEM), Fourier Transform Infrared Spectroscopy (FTIR) analysis, and Dynamic Light Scattering (DLS) analysis.
  
- **MTPS-PBAT blends by reactive extrusion processing.**
  - MTPS-PBAT blends by reactive extrusion processing using maleic acid as a trans-esterification catalyst.
  - Characterization of the resulting blends
    - Soxhlet extraction, Thermal Analysis, Environmental Scanning Electron Microscopy (ESEM), and Fourier Transform Infrared Spectroscopy (FTIR) analysis.

- **Application and performance of MTPS-PBAT blends for thermoformed articles, films, and foams.**
  - Extrusion of sheets of MTPS-PBAT and subsequent thermoforming of the sheets.
  - Characterization of the resulting thermoformed articles.
    - Tensile Testing and Puncture Testing.
  - Extrusion of films of MTPS-PBAT.
  - Characterization of the resulting films.
    - Tensile Testing, Puncture Testing, Permeability Testing.
  - Extrusion of foams of MTPS-PBAT using a chemical blowing agent.
  - Characterization of the resulting foams.
    - Density, Expansion Ratio (ER), Specific Length (SL), Compressive Strength, Resiliency, Moisture Sorption, and Digital Light Microscopy.

## **1.4 STRUCTURE OF DISSERTATION**

This dissertation has been divided into chapters in order to organize the information.

Chapter 2 presents the relevant background needed to read this dissertation. It includes information on biobased and biodegradable plastics, starch, poly(butylene adipate-co-terephthalate) (PBAT), and extrusion theory. Chapter 2 also includes a review of literature pertinent to the subsequent chapters.

Chapters 3, 4, 5, and 6 contain the experimental details of this dissertation.

Chapter 3 deals with maleated thermoplastic starch (MTPS) production and characterization. The characterization methodologies include soxhlet extraction, thermal analysis, environmental scanning electron microscopy (ESEM), Fourier transform infrared spectroscopy (FTIR) analysis, and dynamic light scattering (DLS) analysis. Chapter 4 deals with MTPS-PBAT blends production using reactive extrusion processing and their application and performance for thermoformed articles. The characterization of the blends and thermoformed sheets using DSC, FTIR, ESEM, and mechanical testing, which includes tensile and puncture tests are discussed. Chapter 5 deals with the application and performance of MTPS-PBAT blends for films. The methodologies used to characterize the films are tensile and puncture testing, and carbon dioxide, oxygen, and water vapor permeability testing. Also, transmission electron microscopy is used to characterize the morphology of the blends. Chapter 6

deals with the application and performance of MTPS-PBAT blends for foams and their subsequent characterization through density, expansion ratio, and specific length measurements, compressive strength, resiliency, and moisture sorption tests, and imaging using digital light microscopy. Summary and conclusions are presented in Chapter 7, while recommendations for future work are discussed in Chapter 8.

## **CHAPTER 2**

### **BACKGROUND**

---

#### **2.1 BIOBASED AND BIODEGRADABLE PLASTICS RATIONALE**

Topics which are receiving much attention lately are the issues of global warming, greenhouse gases, and products' carbon footprint. Also, petroleum dependence and peak oil are of much concern to governments, scientists, and policy-makers. Much work is being done to produce “environmentally-friendly” products that are solutions to the above concerns. Using starch as a polymeric material is a way in which these issues can be addressed. First, let us consider the carbon cycle. Carbon in the atmosphere, in the form of carbon dioxide, is fixed by plants through the process of photosynthesis. Over many years ( $>10^6$  years), these plants become fossilized and are converted into petroleum and

natural gas. These fossil fuels are extracted from the earth's core and used to make fuels, polymers, and chemicals. In doing so, CO<sub>2</sub> is released back into the atmosphere. This release of carbon dioxide back into the atmosphere happens over a period of one to ten years.<sup>1</sup> As one can see, the rate at which carbon dioxide is fixed by plants and converted into petroleum is much slower than the rate at which carbon dioxide is liberated. This leads to an accumulation of carbon dioxide in the atmosphere. In their summary, the Intergovernmental Panel on Climate Change concluded that global warming is occurring, that carbon dioxide and other greenhouse gases cause global warming, and that human activity has caused an increase in the amount of atmospheric carbon dioxide and greenhouse gases.<sup>2</sup>

As shown in Figure 1, making polymeric materials, fuels, and chemicals from annually renewable biomass crops instead of petroleum can balance out the rate of carbon fixation and the rate of carbon liberation.<sup>1</sup> Furthermore, if more plants are grown than are harvested to produce the polymers, fuels, and chemicals, the CO<sub>2</sub> rate equation can actually be reversed.

From the above discussion, one can assert that the benefits of using renewable crops/biomass feedstocks to produce polymers are three-fold:

- Enabling sustainable development of biobased polymeric materials
- Helping to meet the CO<sub>2</sub> emission standards set by the Kyoto protocol<sup>3</sup>
- Improving the environmental profile of materials



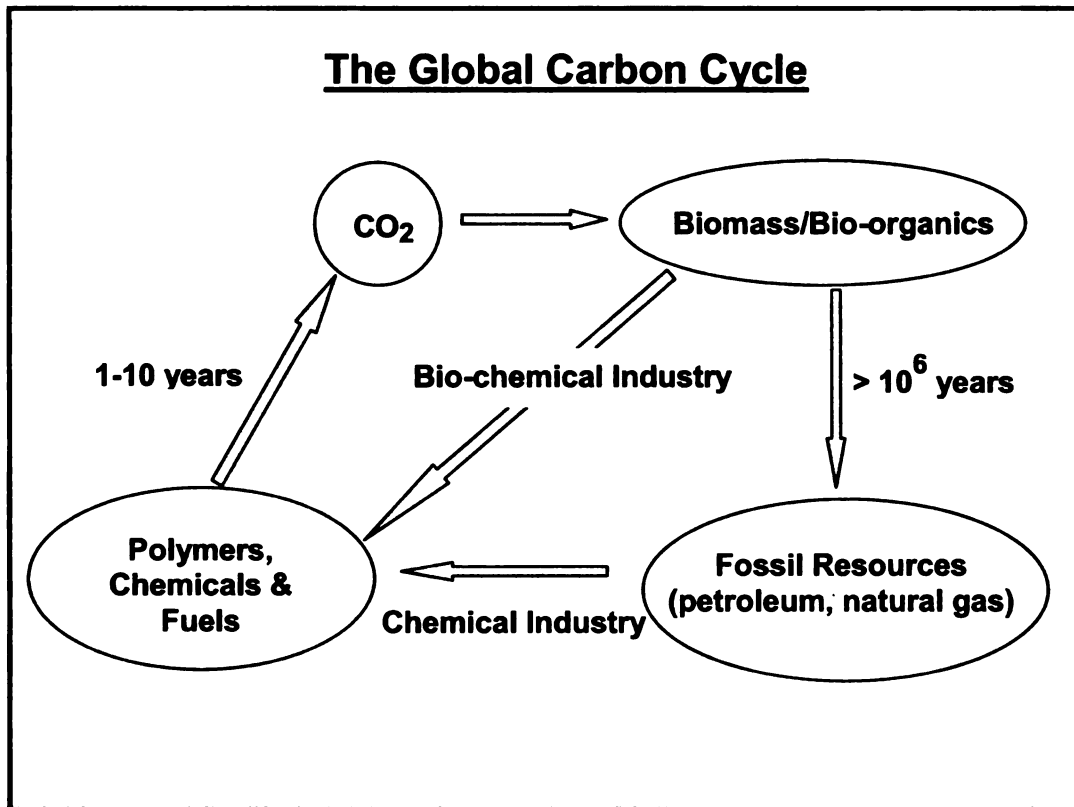


**Figure 1.** The global carbon cycle. [Adapted from Narayan<sup>1</sup>]

Using a holistic approach to producing materials means that products should be designed and engineered from “conception to reincarnation”.<sup>4</sup> Not only must the ecological impact of the raw materials used in producing a product be considered, but also how the product will be disposed of and where it will enter the waste stream. Consideration must be given to whether or not a product is biodegradable or recyclable. Many new market opportunities have opened up for engineering biobased, biodegradable products to meet the demand for sustainable materials that fulfill both economic and ecological requirements. This method of designing a product with consideration for its end-of-life is not currently given a great deal of focus, especially in the case of single-use, disposable

consumer goods and packaging. It is environmentally and ecologically sound to design these products so that they are biodegradable, and also to ensure that the products end up in the correct waste stream. By composting biodegradable plastics and paper wastes, as well as food, yard, and agricultural wastes, carbon-rich compost (humic material) can be created. This humic material can then be placed on farmland, thereby re-initiating the carbon cycle.

When one discusses the term biodegradable, one must have a clear understanding of the exact meaning of the term. Biodegradability means that there exists a microbially, oxidatively or hydrolytically susceptible linkage in the backbone of a polymer, or a catalyst that can break down the polymer chains in a specific environment. Furthermore, the products present after the breakdown process should not persist in the environment or be toxic, and should be used by microorganisms in a defined time frame.<sup>5,6</sup> The typical time frame would be one growing season or one year. A product that is designed to be degradable (fragment into small pieces), and not biodegradable, can be quite harmful to the environment. Although a degraded material may be invisible to the naked eye, it may persist in the environment. Thompson *et al.*<sup>7</sup> have reported that degraded plastic debris from around the world is accumulating in the oceans. The plastic debris has broken down into microscopic granular and fiber-like fragments. Furthermore, the Algalita Marine Research Foundation<sup>8</sup> has reported that the degraded plastics in the oceans attract and hold hydrophobic elements such as

PCB and DDT. The concentrations of these elements in the high surface area plastic residues can be up to one hundred times the background levels.

As shown in Figure 2, heat, moisture, sunlight and/or enzymes can shorten polymer chains and cause fragmentation and some cross-linking of plastic, resulting in intractable persistent residues.<sup>9</sup> If the degraded fragments are not completely assimilated by microbes in the waste stream, within a short period of time, then the material can be more harmful in the environment than if it had not degraded at all. For this reason, biodegradation, not just degradation, is a very important characteristic of compostable polymers.

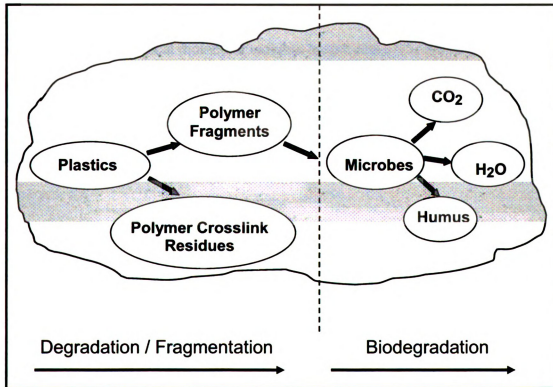


**Figure 2.** Degradation versus biodegradation of materials. [Adapted from Narayan<sup>9</sup>]

## 2.2 STARCH

Starch is a natural, biodegradable, polymeric material. The structure of starch is that of a polymer of anhydroglucose units linked by alpha-1,4 linkages. Starch is found in granules of 2 to 50 microns in diameter. The granules consist of starch polymer in two forms. The first form of starch is amylose, a predominantly linear  $\alpha$ -1,4 glucan polymer. The second form of starch is amylopectin, a  $\alpha$ -1,6 branched  $\alpha$ -1,4 glucan polymer. The ratio of amylose to amylopectin in starch can vary, depending on the origin of the starch.<sup>10</sup> In the United States, corn is the predominant source of starch, however, starch can come from sources such as wheat, rice, cassava, or tapioca as well. Figure 3 shows the structure of amylose and amylopectin. Typical molecular weights for amylose and amylopectin are approximately 1 million and 10 million, respectively. Within the granules of starch, the amylose and amylopectin form ordered arrangements, giving crystallinity to the granules.

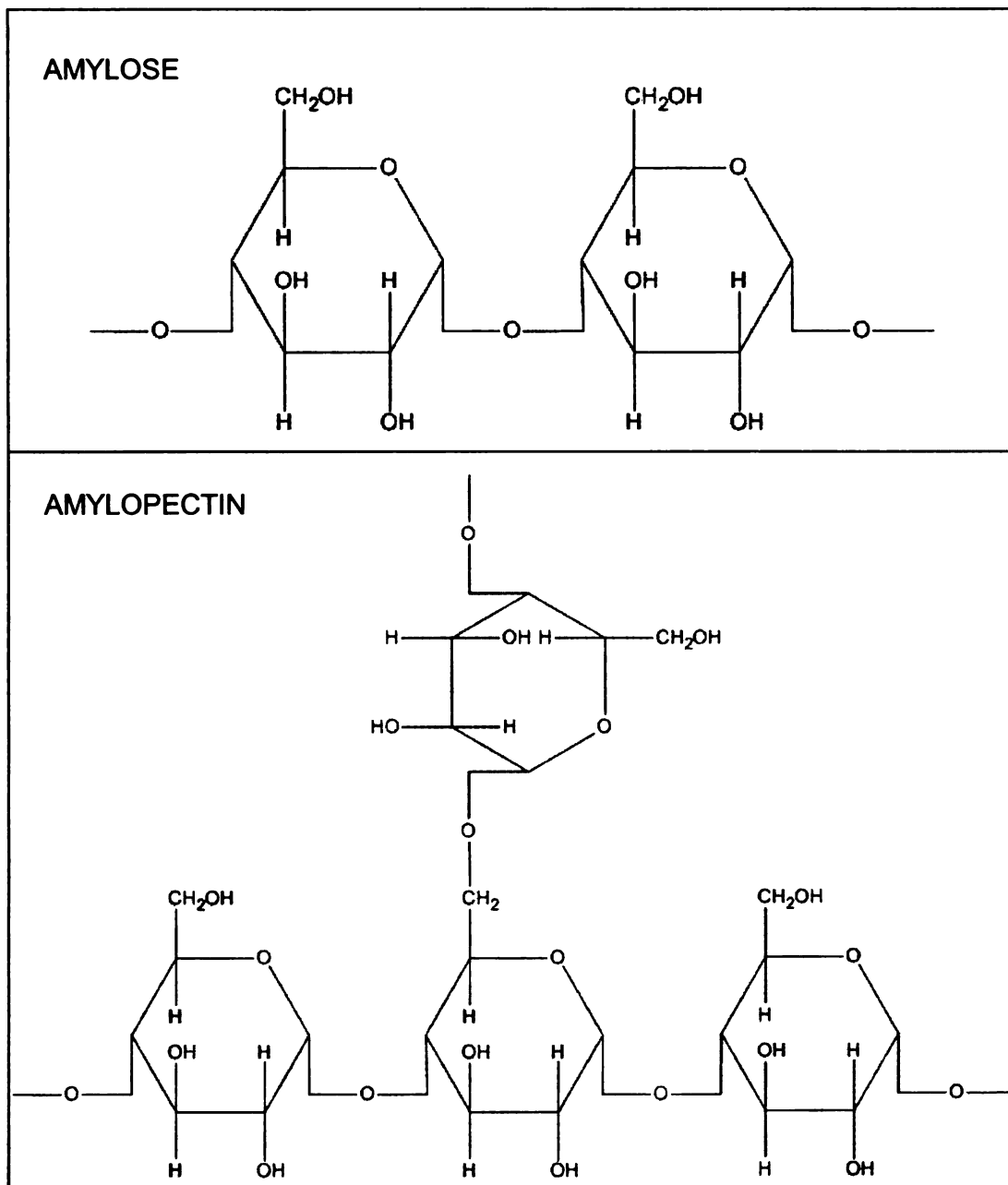


**Figure 3.** Structure of amylose and amylopectin. [Adapted from Narayan<sup>10</sup>]

Due to the hydroxyl groups on the surface of the starch granules, starch shows hydrophilic properties and strong inter-molecular association in the form of hydrogen bonding. This strong hydrogen bonding, along with the crystallinity of the granules, causes poor thermal processing of starch. The melting temperature

of starch is higher than the thermal decomposition temperature. As a result, starch begins to degrade prior to melting, during thermal processing.<sup>10</sup> These issues of hydrophilicity and thermal sensitivity make starch unsuitable for thermoplastic applications.

Nevertheless, thermoplastic starch can be produced through the use of an appropriate plasticizer. The plasticizer breaks the hydrogen bonds within the granules and allows the starch molecules to flow like a thermoplastic material. Using glycerol as a plasticizer, starch has been plasticized in a twin screw extruder.<sup>9</sup> However, the resultant material is brittle and does not provide acceptable performance characteristics.

### 2.3 POLY(BUTYLENE ADIPATE-CO-TEREPHTHALATE) (PBAT)

Poly(butylene adipate-co-terephthalate) (PBAT) is manufactured by BASF, under the trade name Ecoflex. The chemical structure of PBAT is shown in Figure 4. It is an aliphatic-aromatic copolyester comprised of 1,4-butanediol, terephthalic acid, and adipic acid.<sup>11</sup> It is a synthetic, biodegradable polyester.

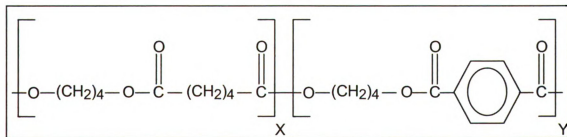


**Figure 4.** Chemical structure of PBAT. [Adapted from Nabar<sup>12</sup>]

Ecoflex can be degraded by micro-organisms and fulfills the requirements for biodegradable and compostable polymers set by the US standard ASTM D6400-04, the European standard DIN EN13432, and the Japanese GreenPla standard.<sup>13</sup>

Ecoflex is quite compatible with natural materials such as starch and cellulose<sup>12</sup> and its low melting temperature (110-120°C)<sup>13</sup> makes processing it with starch very easy. By blending Ecoflex with starch, there is the opportunity to produce materials that are much better suited for making consumer products than using starch alone, while having the added benefit of decreasing the price of using Ecoflex alone.

## **2.4 EXTRUSION THEORY**

Extruders are very useful machines and have been used for many years in industries as wide ranging as mining, petroleum, food processing, and polymers. Extruders are used in the polymer industry (1) as plasticating pumps that convey melts to profile dies, (2) for continuous compounding and blending, (3) as continuous chemical reactors, and (4) as devolatilizers.<sup>14</sup>

An extruder allows the use of shear, heat, and pressure to change a solid resin into a melt that can then be used in another process. Oftentimes, additives such

as

re

Th

wh

di

se

co

an

Th

ex

co

de

of

pr

ex

th

th

sh

Th

di



as fillers, colors, and blending resins are also mixed in an extruder.<sup>15</sup> The final requirements of the products to be made dictate what additives are used.

The basic components of an extruder include a hollow tube, called the barrel, which contains a screw. The screw has helical channels and, in general, is divided into three sections; the solids conveying section, the compression section, and the metering or pumping section.<sup>16</sup> Extruders can be more complicated, involving features such as vents, multiple feeders, multiple screws, and dies to produce various shapes, however, the basic concept is still the same.

The raw materials, usually plastic pellets, are fed into the feed port of the extruder from a hopper. This section then conveys the material to the compression section. It is in this stage that the plastic material is melted. A decrease in the depth of the screw channels forces the material against the walls of the barrel and builds up pressure in this zone. The friction from this shearing process increases the temperature of the plastic. As well, external heating of the extruder also increases the temperature of the plastic. These processes cause the material to soften and melt. Finally, in the metering section of the extruder, the channel depth is constant and the melt is conveyed at a constant rate to the shaping apparatus.<sup>15</sup>

The screws of an extruder are composed of screw elements. There are many different screw elements that aid in the extrusion process. Forwarding elements

move material forward past various sections such as feed and vent ports. Mixing of the polymer occurs once the material begins to melt and lasts until it reaches the die. Proper mixing must occur before the material reaches the die. The screw elements which aid in the mixing of the materials are called mixing elements. Mixing can either be dispersive or distributive. Dispersive mixing elements include fluted or splined elements, annular blister rings, wide kneaders, and shaped lobal elements. Distributive mixing elements include pin mixer, slotted screw flight, narrow kneaders, and sleeve mixer elements.<sup>16,17</sup> The difference between dispersive and distributive mixing is shown schematically in Figure 5. In general, mixing occurs due to shear flow and elongational flow. If the fluids that are being mixed are compatible and do not exhibit a yield point, then distributive mixing occurs. However, if the material is a solid and exhibits a yield point, this is referred to as dispersive mixing.

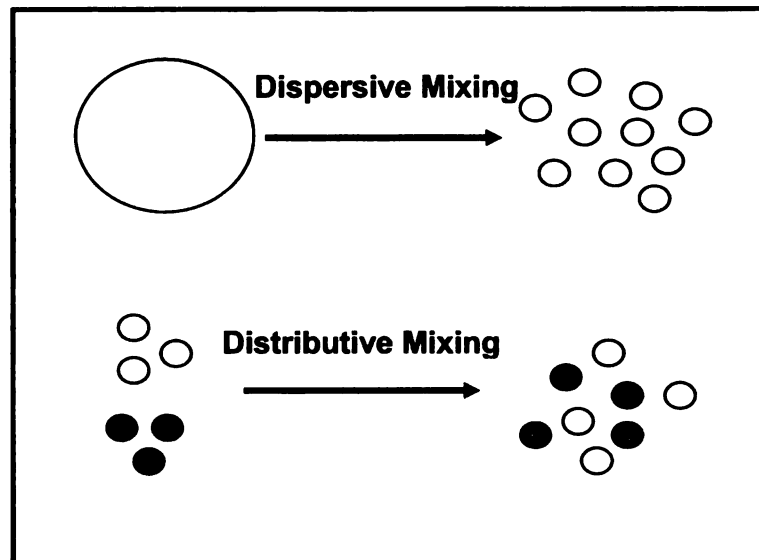


**Figure 5.** Schematic diagram of dispersive and distributive mixing. [Adapted from Balakrishnan<sup>16</sup>]

1

2  
T  
C  
C  
S  
E  
V  
A  
C

## 2.5 POLYMER BLENDS AND ALLOYS

The terms blend and alloy are often used synonymously; however, they can be distinguished based on the thermodynamic compatibility between their components, leading to different physical and mechanical properties.<sup>18</sup> In general, a property value,  $P$ , of a polymer blend or alloy of two components can be described by the following equation:

$$P = P_1C_1 + P_2C_2 + IP_1P_2$$

Where  $P_1$  and  $P_2$  are the property values for the two individual components,  $C_1$  and  $C_2$  are the concentrations of the two components, and  $I$  is an interaction coefficient for the thermodynamic compatibility between the two components.

It is the value of  $I$  that determines the property values of the blend or alloy. If  $I$  is positive ( $I > 0$ ), the property values of the polymer combination are greater than the weighted arithmetic average of the components' properties. This is termed a synergistic blend. An alloy is a synergistic polymer combination. If  $I$  is zero, the property values of the polymer combination are the weighted arithmetic average of the components' properties. This is termed an additive blend. If  $I$  is negative ( $I < 0$ ), the property values of the polymer combination are less than the weighted arithmetic average of the components' properties. This is termed a nonsynergistic blend.<sup>18</sup> The effect of the interaction coefficient on the properties of polymer combinations is shown in Figure 6.<sup>19</sup>

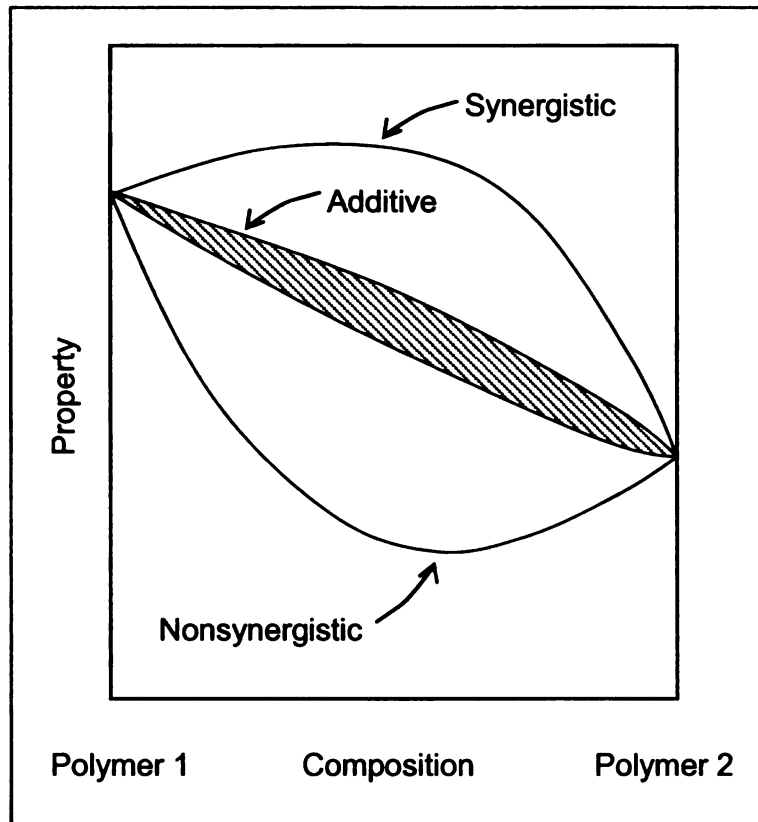


**Figure 6.** Relationship between property values and blend composition. [Adapted from Paul and Barlow<sup>19</sup>]

Thermodynamic compatibility or miscibility is determined by balancing the entropic and enthalpic contributions of the free energy of mixing.<sup>20</sup> The change in the free energy upon mixing ( $\Delta G$ ) is given by the following equation:

$$\Delta G = \Delta H - T\Delta S$$

Where H, S, and T are enthalpy, entropy, and temperature, respectively. Also, for mixing to occur spontaneously,  $\Delta G$  must be negative, thus:

$$\Delta H - T\Delta S < 0$$

In polymers, the entropy is almost zero, thus the value of enthalpy determines the miscibility, and if  $\Delta H < 0$ , then the mixture will spontaneously mix.<sup>20</sup>

## 2.6 REVIEW OF LITERATURE

Plastic materials are widely used for many applications due to their processability and cost-effectiveness.<sup>21</sup> However, plastics are almost entirely petroleum-based and, therefore, made from non-renewable resources. Much research is being done to produce plastics from alternative, biobased, materials. The two requirements of such “eco-friendly” polymers are: (1) production of the polymer from a renewable resource, and (2) biodegradability.<sup>21</sup> Polymers made from starch can thus be considered “eco-friendly”, since they meet both criteria.

Starch may be sourced from many different agricultural products. For example, potato, corn, cassava, and wheat starch have all been used to produce thermoplastic starch.<sup>22-25</sup> There exists some mutant genotypes of maize, barley, rice and wheat that produce starches containing an increased amylose content (i.e. high amylose with up to 70% amylose) or an increased amylopectin content (i.e. “waxy starch” with 99-100% amylopectin). Variations in the ratio of amylose to amylopectin within these starches causes differences in granular structure, physiochemical properties, and quality of end-use products.<sup>26</sup> The crystallinity of starch granules is affected by the amount of amylose and amylopectin within the granules. For example, high amylose starches are approximately 15% crystalline while waxy starches can be up to 45-50% crystalline.<sup>27</sup> Starch is arranged into growth rings within the granules. The concentric growth rings have alternating crystalline and amorphous regions with higher and lower density, respectively.

The crystalline regions have a lamellar structure containing crystalline and amorphous layers that alternate. Amylopectin chains pack into an ordered structure within the crystalline layers, while amylose, amylopectin, and amylopectin branching points exist in a random conformation within the amorphous layers.<sup>27, 28</sup>

Starch is not a thermoplastic material, but in the presence of a plasticizer such as water, glycerol, or sorbitol, high temperatures (90-180°C), and shear, it will become thermoplastic.<sup>12, 29, 30</sup> In the production of thermoplastic starch (TPS), the starch loses its semi crystalline granular structure and acquires thermoplastic behavior.<sup>31</sup>

The production of thermoplastic starch by extrusion of starch and glycerol has been demonstrated<sup>22</sup> and several researchers, including the Narayan group, have successfully manufactured starch that behaves like a pure thermoplastic material.<sup>32, 33</sup>

It has been shown that thermoplastic starch can have improved processability and reactivity if it is modified by reacting it with an organic dibasic acid or an anhydride in the presence of a plasticizer, using a free radical initiator. This produces a chemically modified plasticized starch (US patent 7153354)<sup>34</sup> which is biodegradable, reactive, and chemically modified allowing it to have a lower viscosity and good processability. It should also be noted that during the



pr  
th  
th  
F  
re  
th  
fi  
a  
p  
  
l  
T  
n  
F  
a  
n  
t  
n  
n  
l  
l



processing, there is no water added. This patent claims that chemically modifying thermoplastic starch prevents problems such as high viscosity, clogging of the thermoplastic starch melt at the die, or foaming of the thermoplastic starch melt. Furthermore, the resulting chemically modified thermoplastic starch is highly reactive and can form graft copolymers with polyesters. An important aspect of these starch-polyester graft copolymers is that they are able to be formed into films and molded products using conventional plastics processing equipment, and the resulting product has the most preferred balance in mechanical properties, water resistance, processability, and rate of biodegradation.<sup>34</sup>

In the present work, maleic anhydride is the anhydride used to produce modified TPS. This maleated thermoplastic starch is thus referred to as MTPS. Since maleated thermoplastic starch can be used in blends with other biodegradable polymers for different applications such as films and sheets, or injection molded and thermoformed materials, it is necessary to understand the effect that maleation has on starch. The maleation of starch has been shown to decrease the molecular weight of starch when no initiator was used, however, the molecular weight increased when an initiator was used.<sup>34</sup> The decrease in molecular weight was attributed to the fact that starch is hydrolyzed in the presence of maleic acid. The increase in molecular weight was attributed to branching or cross-linking occurring with the addition of the initiator.<sup>35</sup>

As a packaging material, starch alone does not form films with adequate mechanical properties such as high percentage of elongation, tensile, and flexural strength.<sup>36</sup> Starch also has the disadvantages of exhibiting: a) brittleness when no plasticizers are utilized; b) hydrophilicity and poor water resistance; c) deterioration of mechanical properties when exposed to environmental conditions such as humidity and d) soft and weak tendencies when plasticizers are utilized.<sup>37</sup>

Thermoplastic starch has weaknesses that limit its utilization in packaging applications as a film, but also for thermoforming applications. Thermoformed objects often have low wall thickness and the drawbacks of using starch create additional issues.<sup>38</sup> Major drawbacks are water sensitivity, change of mechanical properties with time, crystallization due to aging, water adsorption, and low impact strength resistance.<sup>39, 40</sup>

In order to make starch a more feasible option for packaging applications, thermoplastic starch (TPS) can be blended with biodegradable polyester to improve its mechanical properties and decrease its water sensitivity.

Furthermore, commercial biodegradable polyesters are expensive (3.5 to 5.0 euro/kg),<sup>41</sup> thus, by blending starch with biodegradable polyesters the price of the material can be reduced. There has been extensive investigations into blending starch with various polymers, thereby creating possible replacements for

conventional plastics, mainly in the area of packaging as films or injection molded materials.

Issues arise due to the poor compatibility of high loadings of starch with biodegradable polyesters. This results in poor physical and mechanical properties of the materials. An effective way to improve the compatibility between starch and the polyester matrix is to functionalize the polyester matrix by grafting highly reactive functional groups. By functionalizing carbonyl, anhydride, epoxy, urethane, or oxazoline groups to synthetic polymers, reactive blending with starch has been performed. The functional groups on the synthetic polymers can react with the hydroxyl or carboxyl groups in the starches and modified starches.<sup>37</sup>

In order to functionalize polymers, maleic anhydride (MA) has been grafted onto many different hydrophobic polymers, both biodegradable<sup>12, 42-48</sup> and non-biodegradable.<sup>49, 50</sup> These functional polymers can then be blended with thermoplastic starch (TPS), allowing the maleated polymers to act as compatibilizers between the non-functional polymer and the starch.

Another option for compatibilization of starch and polymers (biodegradable or non-biodegradable) is to functionalize the TPS and then to blend the chemically modified starch with various polyesters.<sup>34</sup> It has been shown that these starch-polyester graft copolymers are readily processable into films, and molded

products using conventional plastics processing equipment. As well, the mechanical and material properties of these blends are improved, due to the compatibilization of the starch and polymer.<sup>29</sup>

There are many different biodegradable polymers. They can be categorized in various ways, such as the way in which they are polymerized (biologically or synthetically): a) biosynthetic (starch, cellulose, PHB, PHBV), b) semi-biosynthetic (PLA) and (c) chemo-synthetic polymers (PCL, PBSA, PBS, PBAT).<sup>41</sup> Poly(butylene adipate-co-terephthalate) (PBAT), is a chemo-synthetic biodegradable aliphatic aromatic co-polyester. It is produced in a condensation polymerization reaction between 1,4-butanediol, terephthalic acid, and adipic acid. It has been used in several applications, such as for producing films, in blends with thermoplastics starch,<sup>51</sup> blends with biobased polymers such as poly(lactide),<sup>52</sup> and in lignin-cellulosic-based composites.<sup>53-55</sup>

This work reports on the reactive blending of thermoplasticized starch with the biodegradable polyester, poly(butylene adipate-co-terephthalate), to produce sheets of material that can be thermoformed. Both maleated thermoplastic starch (MTPS) and thermoplastic starch (TPS) are investigated. Thermoformed articles are often single-use, disposable products. Making these items biodegradable would be environmentally responsible and preferable.

Starch has been considered for many years as an attractive polymer for use in packaging film applications due to its low cost, renewability and biodegradability. Several studies have been performed to analyze the properties of starch-based films.<sup>48, 56-60</sup> Edible and/or biodegradable films will not replace all synthetic packaging films; however they do have potential to replace conventional packaging in some applications.

The hydrophilic nature of starch polymers makes them sensitive to environmental humidity and the presence of glycerol in thermoplastic starch also strengthens this behavior.<sup>29</sup> Blending thermoplastic starch with biodegradable polymers that are less hydrophilic is one option to produce film materials that are more water resistant.

In the present work, biodegradable films of blends of high amylose corn starch with poly(butylene adipate co-terephthalate) are produced and their mechanical and barrier properties, and microstructure are characterized.

Foam packaging, by design is lightweight but bulky. The high transportation costs of transporting and disposing of foam articles after their useful life makes it a suitable application in which biodegradability and compostability would be very beneficial. The Narayan group<sup>32, 61-63</sup> has reported on the rationale, design, and engineering of biodegradable polymer materials previously.

In order to impart hydrophobic characteristics to starch-based foam materials, while maintaining the beneficial biodegradable properties of starch, many researchers have investigated producing foam that is blended with hydrophobic biodegradable polymers. Bastioli *et al.*<sup>64-67</sup> have patented foams comprised of starch blended with 10-30% biodegradable polymers such as PVA, PCL, and CA. Willett and Shogren<sup>68</sup> extruded foams of starches blended with thermoplastic resins such as PVA and CA, and biodegradable polyesters such as PLA, PCL, poly(hydroxyester ether) (PHEE), poly(ester amide) (PEA), poly(hydroxybutyrate-co-valerate) (PHBV), PBAT, and others. Both regular corn starch and high amylose corn starch, wheat starch, and potato starch were used. High levels of starch and its poor compatibility with the various polymers, lead to poor properties such as density, compressibility, and resilience. Fang *et al.*<sup>69</sup> showed that the densities and expansion of the foams depended on the PBAT content. Nabar *et al.*<sup>12</sup> compatibilized starch and PBAT through the addition of maleated PBAT and reported a reduction in density and improved resilience.

The above mentioned results have been produced through the use of water as the physical blowing agent in the extrusion of the foam. The work presented here describes the use of chemical blowing agents. Work by Zirkel *et al.*<sup>70</sup> has been performed using chemical blowing agents for the extrusion on polymeric foams at high temperatures. Compression foaming of PVC using a chemical blowing agent, azodicarboxamide, has been reported by Demir *et al.*,<sup>71</sup> while

compression foaming of biodegradable poly(propylene carbonate) using a composite chemical blowing agent has been reported by Guan *et al.*<sup>72</sup>

Chemical or physical blowing agents may be used to produce foam. A chemical blowing agent (CBA) is a chemical that will decompose at elevated temperatures to produce gases. Physical blowing agents (PBAs) are usually gases that are injected during the processing of foams, and they require special equipment for their use.<sup>72</sup>

Chemical blowing agents can be divided into two categories: exothermic and endothermic.<sup>73</sup> During thermal decomposition, exothermic CBAs release heat while endothermic CBAs absorb heat. Also, in general, exothermic CBAs generate N<sup>2</sup> gas and endothermic CBAs generate CO<sub>2</sub> gas.

As was discussed previously, water (a PBA) has been used as the blowing agent for many starch-based foams. In this work, CBAs have been used to produce foams of blends of modified starch and PBAT. The properties of the foams are characterized and presented.

## **CHAPTER 3**

# **MALEATED THERMOPLASTIC STARCH BY REACTIVE EXTRUSION PROCESSING**

---

### **3.1 RATIONALE**

This work was performed to better understand the effect of the amount of maleic anhydride and initiator, and the effect of extrusion temperature on maleated thermoplastic starch (MTPS) produced through reactive extrusion.

Characterization of the MTPS samples was performed through dynamic light scattering (DLS), differential scanning calorimetry (DSC), and environmental scanning electron microscopy (ESEM). Also, proof of reactive extrusion was determined by Fourier transform infrared spectroscopy (FTIR) and soxhlet extraction in acetone.



## **3.2 MATERIALS AND METHODS**

### **3.2.1 Materials**

High amylose corn starch was used in this work. The corn starch was purchased from National Starch and Chemicals (Indianapolis, IN). Anhydrous glycerol, 99.9% assay, was purchased from J.T. Baker (Phillipsburg, NJ). Maleic anhydride was purchased from Sigma-Aldrich, Inc (St. Louis, MO). The initiator, 2,5-bis(tert-butylperoxy)-2,5-dimethylhexane, also referred to as Luperox 101, was purchased from Sigma-Aldrich, Inc (St. Louis, MO). The solvent used in the studies was dimethyl sulfoxide, and was purchased from J.T. Baker (Phillipsburg, NJ).

### **3.2.2 Equipment**

A Century CX-30 co-rotating twin-screw extruder, having a length/diameter ratio (L/D) of 42 and a screw diameter of 30 mm was used to prepare the thermoplastic starch and maleated thermoplastic starch. The screw configuration for the Century CX-30 extruder is shown in Figure 7.<sup>16</sup> A pelletizer was used to cut the extrudate strands into small pellets.

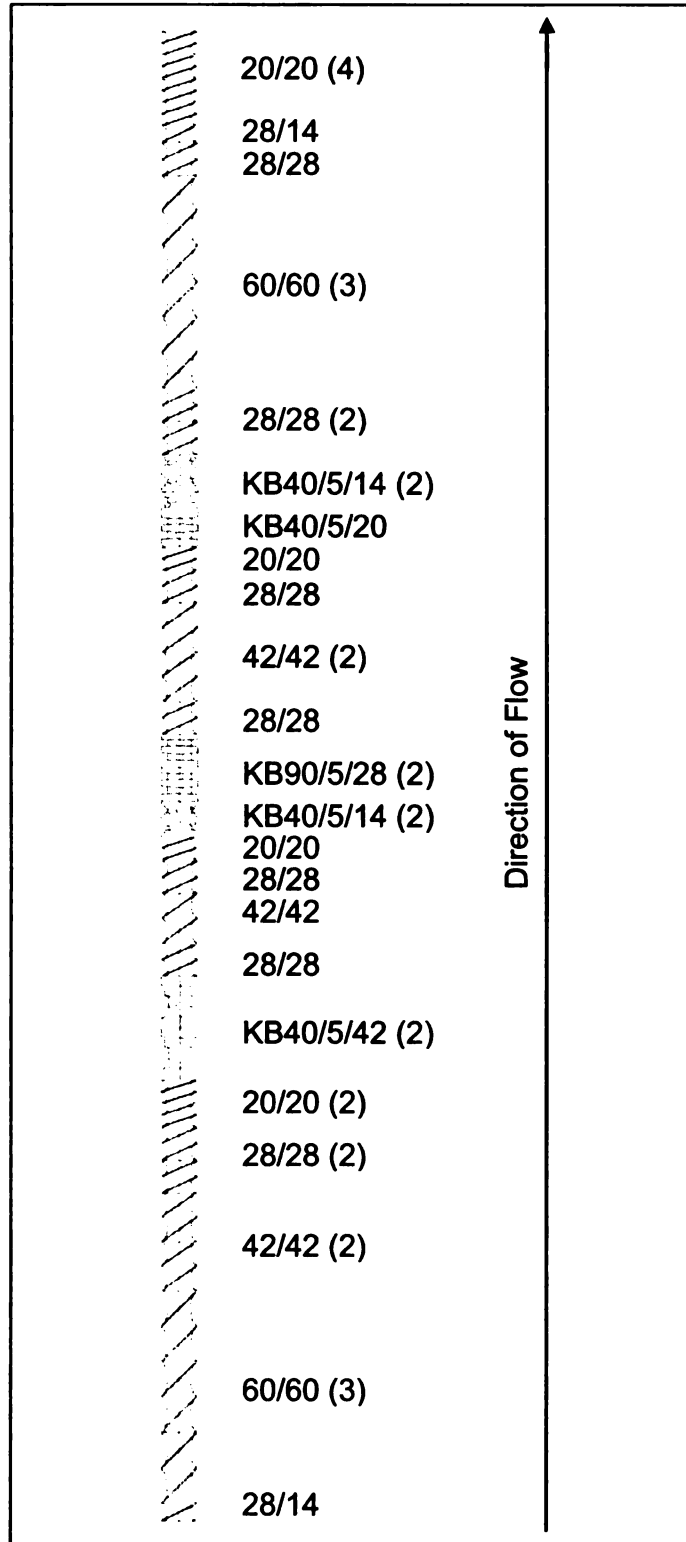


**Figure 7.** Screw configuration of the Century CX-30 co-rotating twin-screw extruder. [Adapted from Balakrishnan<sup>16</sup>]

### **3.2.3 Procedure**

#### **3.2.3.1 Sample Preparation**

Maleated thermoplastic starch was produced in a Century CX-30 co-rotating twin-screw extruder, having a length/diameter ratio (L/D) of 42 and a screw diameter of 30 mm. Maleic anhydride was ground into a fine powder using a mortar and pestle and pre-blended with the corn starch, placed in the external feeder of the extruder, which fed into the feed port of the extruder. Luperox 101 was pumped into the feed throat of the extruder using a peristaltic pump.

Glycerol, which was warmed in a water bath, was also pumped into the extruder using a peristaltic pump. The extruder was electrically heated and the maximum temperature of the extruder was set to 165°C, with a temperature profile of 25/95/125/145/160/165/165/165/150/145°C from the feed throat to the die.

Cooling water was circulated through the extruder in order to maintain the set temperatures during the extrusion process. The feed rates of the external feeder containing the starch and the peristaltic pump for the glycerol were set so as to accomplish a composition of 80 wt% starch and 20 wt% glycerol and a total flow of all material through the extruder of approximately 11 kg/h. The screw speed was set to 125 rpm. A vacuum was pulled on the vent port of the extruder in order to remove unreacted maleic anhydride and moisture. The extruded strand exiting from the die was air cooled, pelletized in line, and collected.

Table 1 shows the composition of the samples. To produce these samples, first the amount of maleic anhydride (as weight percentage of starch and glycerol) was varied while the amount of initiator (Luperox 101) was held constant at 0.25 wt% of starch and glycerol. The amount of maleic anhydride in the samples was 2 wt%, 4 wt%, or 6 wt%. Next, samples were extruded with varying amounts of initiator, while the amount of maleic anhydride was held constant at 2 wt% of starch and glycerol. These samples contained 0.1 wt%, 0.25 wt%, or 0.5 wt% of free-radical initiator.

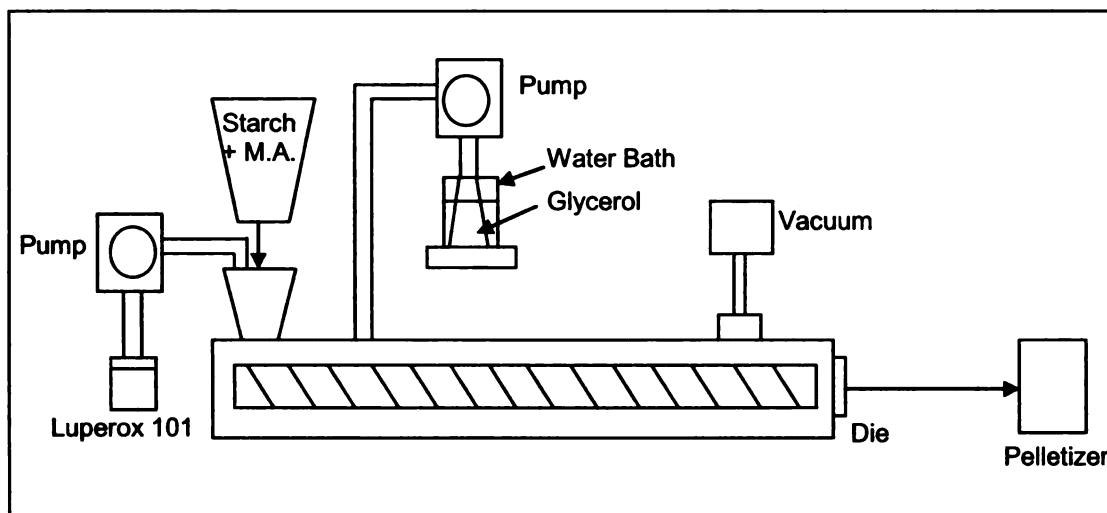
To compare the effect of temperature and maleation on the properties of the samples, TPS and MTPS containing 30 wt% glycerol were produced in the twin-screw extruder, with a maximum temperature of 135°C (25/115/120/125/130/135/135/135/130/130°C).

Figure 8 shows the process schematic for the extrusion of MTPS.

The proposed reaction of maleic anhydride with starch<sup>16</sup> is shown in Figure 9. Also, it has been shown that in the presence of maleic anhydride, starch is hydrolyzed and glycerol and maleic anhydride are grafted to the starch backbone. This is shown in Figure 10.<sup>74</sup>

**Table 1.** Composition of the maleated and non-maleated thermoplastic starch (MTPS and TPS) samples.

Sample	Max. Processing Temperature	Corn Starch	Glycerol	Maleic Anhydride	Luperox 101
	(°C)	(weight %)		(weight % of corn starch + glycerol)	
1	165	80	20	2	0.1
2	165	80	20	2	0.25
3	165	80	20	2	0.5
4	165	80	20	4	0.25
5	165	80	20	6	0.25
6	135	70	30	2	0.1
7	135	70	30	-	-



**Figure 8.** Process schematic for extrusion of MTPS.

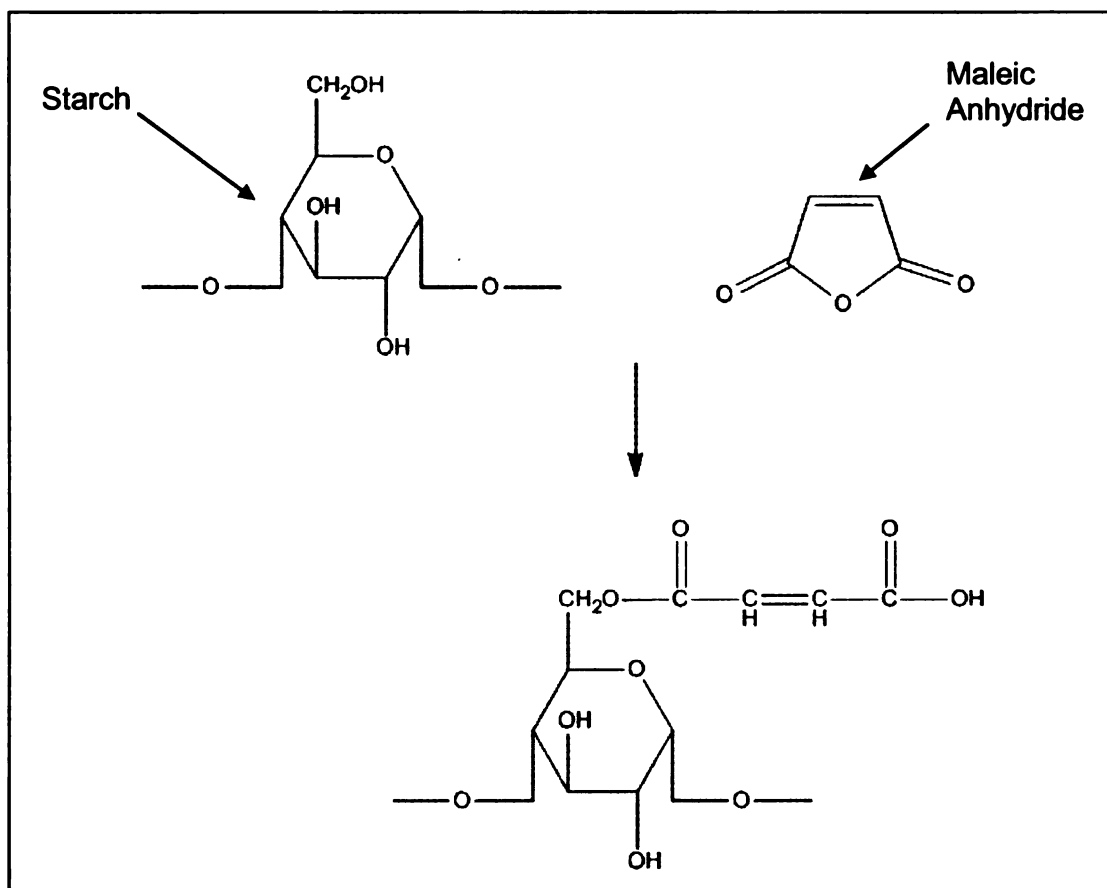


**Figure 9.** Proposed reaction of starch with maleic anhydride. [Adapted from Balakrishnan<sup>16</sup>]

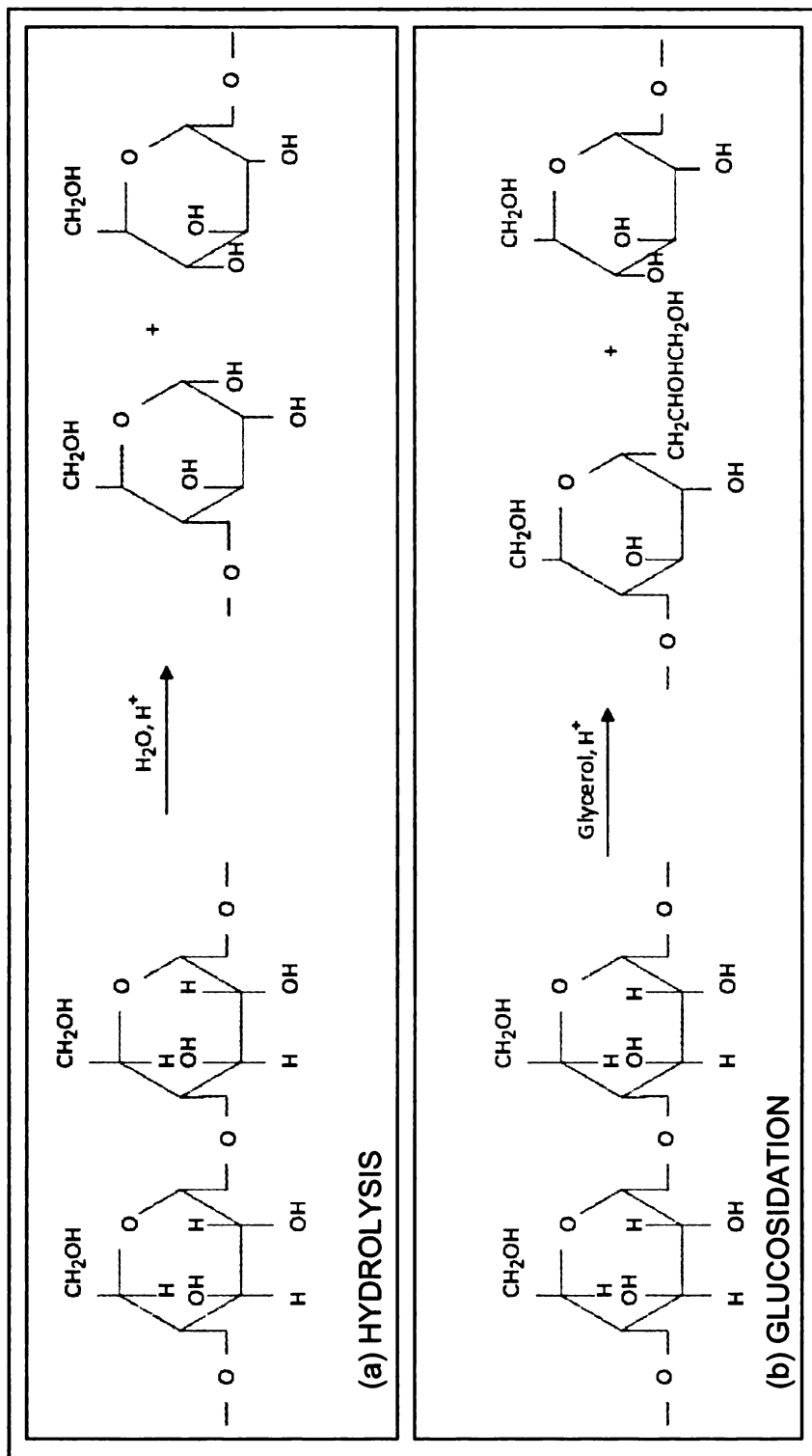


**Figure 10.** Hydrolysis (a) and glucosidation (b) reactions occurring during the reactive extrusion of maleated thermoplastic starch. [Adapted from Raquez *et al.*<sup>74</sup>]

### 3.2.3.2 Dynamic Light Scattering (DLS) Analysis

The MTPS and TPS samples were ground into a powder using a mortar and pestle. The powder was dissolved in dimethyl sulfoxide at a concentration of 10 mg/mL. A sample of high amylose corn starch was also tested in order to compare its hydrodynamic radius with those of the extruded samples. Dynamic light scattering measurements were performed in a Dynapro dynamic light scattering apparatus by Protein Solutions. This equipment has a wavelength of 827.1 nm and scatters at an angle of 90 degrees, the temperature was held constant at 25°C and the laser intensity was set to 100% for all samples.

The dynamic light scattering equipment calculated the hydrodynamic radius of each sample using a regularization algorithm. A distribution is calculated based on the mass percentage of various fractions having varying hydrodynamic radii. Figure 11 shows a graph obtained for the DLS test.

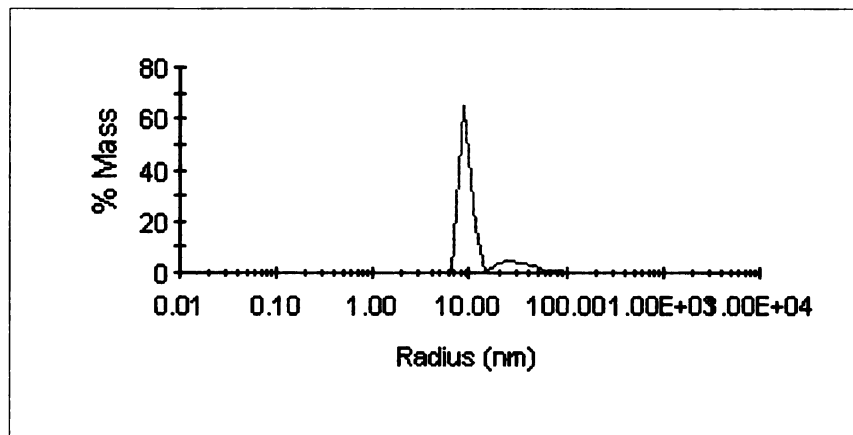


**Figure 11.** Graph of dynamic light scattering measurements for sample 6 (MTPS high amylose starch, with 30% glycerol and 135°C).



### **3.2.3.3 Fourier Transform Infrared Spectroscopy (FTIR) Analysis**

The FTIR spectra of TPS, MTPS and starch were scanned from  $650\text{ cm}^{-1}$  to  $4000\text{ cm}^{-1}$  using a Perkin Elmer Spectrum One FT-IR Spectrometer. This testing was performed in order to determine the reactions that occurred in TPS during the reactive extrusion with MA and a free-radical initiator.

### **3.2.3.4 Thermal Analysis (DSC)**

Differential scanning calorimetry (DSC) was performed using a high resolution DSC 2920 from TA Instruments. The purge gas used was nitrogen. It had a flow rate of 50 ml/min. Samples of the extruded pellets were cooled to  $-50^{\circ}\text{C}$  and then heated to  $200^{\circ}\text{C}$  at a rate of  $10^{\circ}\text{C}/\text{min}$ , cooled to  $-50^{\circ}\text{C}$  and then reheated to  $200^{\circ}\text{C}$ . Analysis of the thermograms produced shows the thermal transitions that occurred during the test.

### **3.2.3.5 Soxhlet Extraction Analysis**

Soxhlet extraction in acetone was used to determine the amount of glycerol that was grafted to the starch during the extrusion process. The MTPS and TPS samples were ground into a powder using a mortar and pestle. The ground powder samples were dried in an oven set at  $65^{\circ}\text{C}$  for 72 hours. A piece of filter paper, measuring  $10\times 10\text{cm}$  was cut, folded, and stapled at the bottom. Approximately 2 grams of the thermoplastic starch powder was accurately weighed into the folded filter paper and then the top was stapled shut. The

packet was placed into an extraction thimble holder. Evaporated solvent (acetone) condensed onto the packet containing the sample. The extraction was run for 72 hours. After extraction, the packet was removed and dried to constant weight. The top staple was then removed from the packet and the sample and filter paper (with bottom staple) were accurately weighed to determine the amount of material extracted during the soxhlet extraction. Since glycerol is soluble in acetone, but starch is not, glycerol that has not reacted with the starch will be extracted during the test; however, any glycerol that has reacted with the starch will remain in the sample in the filter paper.

#### **3.2.3.6 Environmental Scanning Electron Microscopy (ESEM) Analysis**

An environmental scanning electron microscope (ESEM) (Phillips Electroscan 2020) was used to make observations of the fractured surface of the thermoplastic starch. Pieces of the extruded samples were immersed in liquid nitrogen, frozen, and then fractured. The fractured surface was viewed in the environmental scanning electron microscope.

#### **3.2.3.7 Statistical Analysis**

Analysis of variance (ANOVA) and Tukey mean comparison tests ( $p \leq 0.05$ ) were performed using Statistica software (Statsoft, Oklahoma – USA).

### 3.3 RESULTS AND DISCUSSION

Observations made during the extrusion of the samples include the fact that MTPS had improved processability over the TPS sample. The maleation process permitted formulations with less than 30 wt% of glycerol to be extruded in the twin-screw extruder. The resulting MTPS pellets were more transparent than the TPS pellets. Figure 12 shows an image of MTPS pellets after extrusion and pelletization.



**Figure 12.** Picture of maleated thermoplastic starch pellets.

#### 3.3.1 Dynamic Light Scattering (DLS) Analysis

For each sample, the value of the hydrodynamic radius which has the largest mass percentage has been used for comparison purposes in this paper. Table 2 shows the hydrodynamic radii that were measured for the samples.

**Table 2.** Hydrodynamic radii as measured by dynamic light scattering.

<b>Sample</b>	<b>Composition</b>	<b>Hydrodynamic Radius (nm)</b>
1	MTPS, 0.10% Luperox 101, 2% MA, 20% glycerol	4.2
2	MTPS, 0.25% Luperox 101, 2% MA, 20% glycerol	2.1
3	MTPS, 0.50% Luperox 101, 2% MA, 20% glycerol	1.2
4	MTPS, 0.25% Luperox 101, 4% MA, 20% glycerol	2.5
5	MTPS, 0.25% Luperox 101, 6% MA, 20% glycerol	2.8
6	MTPS, 0.10% Luperox 101, 2% MA, 30% glycerol	9.1
7	TPS, 30% glycerol	11.9
	High amylose corn starch	12.6

As the percentage of maleic anhydride increases, there is negligible change in the hydrodynamic radius; however, as the percentage of Luperox 101 increases, the hydrodynamic radius decreases. The decrease in hydrodynamic radius as the percentage of Luperox 101 increases could be the result of chain scission occurring, as shown in Figure 10 in Section 3.2.3.1. Chain scission would decrease molecular weight and thus decrease the hydrodynamic radius of the samples.

By comparing the high amylose starch with the thermoplastic and maleated thermoplastic starch, we can observe the effect of extrusion and maleation on starch. Extruding TPS caused a decrease in the hydrodynamic radius of the starch from 12.6 to 11.9nm. When 2% of maleic anhydride and 0.1% of Luperox 101 was used, the hydrodynamic radius decreased from 11.9 to 9.1nm. These results could indicate that the extrusion and maleation processing degrade the samples and one could infer that there is a decrease in the molecular weight.

When comparing the maleated samples at 165°C and 135°C, we can observe the effect of temperature profile on the hydrodynamic radius. The values for the samples at 135°C are much larger than for the samples at 165°C. Using 165°C may degrade the samples and cause a drastic decrease in the hydrodynamic radius (9.1 to 4.2 nm). Thus, temperature has a high influence on the molecular weight of the maleated thermoplastic starch.

In comparison to other studies that have been performed to understand the effect of Luperox 101 on the molecular weight of biobased polymers, there is not a consistent trend. Carlson *et al.*<sup>75</sup> showed that branching and chain scission depended not only on the amount of Luperox 101 in the process, but also on the extrusion temperature in the reactive extrusion of polylactide.

Work done by Nabar *et al.*<sup>12</sup> suggests that the effect of increasing the amount of maleic anhydride in maleated poly(butylene adipate-co-terephthalate) (PBAT) is

to decrease the intrinsic viscosity of the samples (ie: decrease the molecular weight) and increasing the amount of initiator, Luperox 101, also decreases the intrinsic viscosity of the samples. These results of the effect of maleic anhydride on molecular weight do not show the same trends as the data presented in the present work; however, the material that was maleated was PBAT, not high amylose corn starch. Other work by Nabar<sup>35</sup> shows that when using regular corn starch, the intrinsic viscosity of TPS is lower than the intrinsic viscosity of the starch, and that when the starch is maleated, the intrinsic viscosity reduces even more. This is in agreement with the work presented here.

In other work, using regular corn starch without an initiator, the intrinsic viscosity decreased as the MA content increased.<sup>74</sup> This trend is not consistent with the present work; however, no initiator was used and the starch was regular corn starch, not high amylose corn starch.

Possible explanations for the present results showing negligible change in hydrodynamic radii as the percentage of MA increased as opposed to decreasing hydrodynamic radii could be that as the percentage of MA increased there was more swelling of the molecules in DMSO, or that aggregation of molecules occurred.

Furthermore, as was discussed by Roger *et al.*,<sup>76</sup> measuring the hydrodynamic radius of starch in DMSO can lead to some uncertainties in measurements of

pure amylose starch. This must be taken into consideration when viewing the hydrodynamic radius data from the DLS measurements. Nevertheless, in this study, all measurements were made under the same conditions so any errors due to the solvent/starch solution will be constant for all measurements. In this way, the DLS data gives one an understanding of how the hydrodynamic radius has changed due to the varying amounts of MA and Luperox 101, as well as different extrusion temperatures and glycerol contents.

### **3.3.2 Fourier Transform Infrared Spectroscopy (FTIR) Analysis**

The FTIR spectra for TPS, MTPS, and high amylose corn starch are shown in Figure 13. The spectra for TPS and MTPS are quite similar; however, proof of grafting of maleic anhydride to the starch backbone is exhibited by the fact that MTPS shows a band at  $1700\text{ cm}^{-1}$ . This band corresponds to the carbonyl group present in maleic anhydride and which is not present in either the high amylose corn starch or the TPS samples. Also, since glycerol was used as the plasticizer, two additional peaks at  $2928$  and  $2886\text{ cm}^{-1}$  are present in the TPS and MTPS samples due to the formation of inter and intramolecular bonding hydroxyl group bands between starch and glycerol. It should also be noted that the MTPS sample showed no peak at  $1787\text{ cm}^{-1}$ . This peak would correspond to a ring anhydride being present. Its absence suggests that the maleic anhydride ring was fully open.

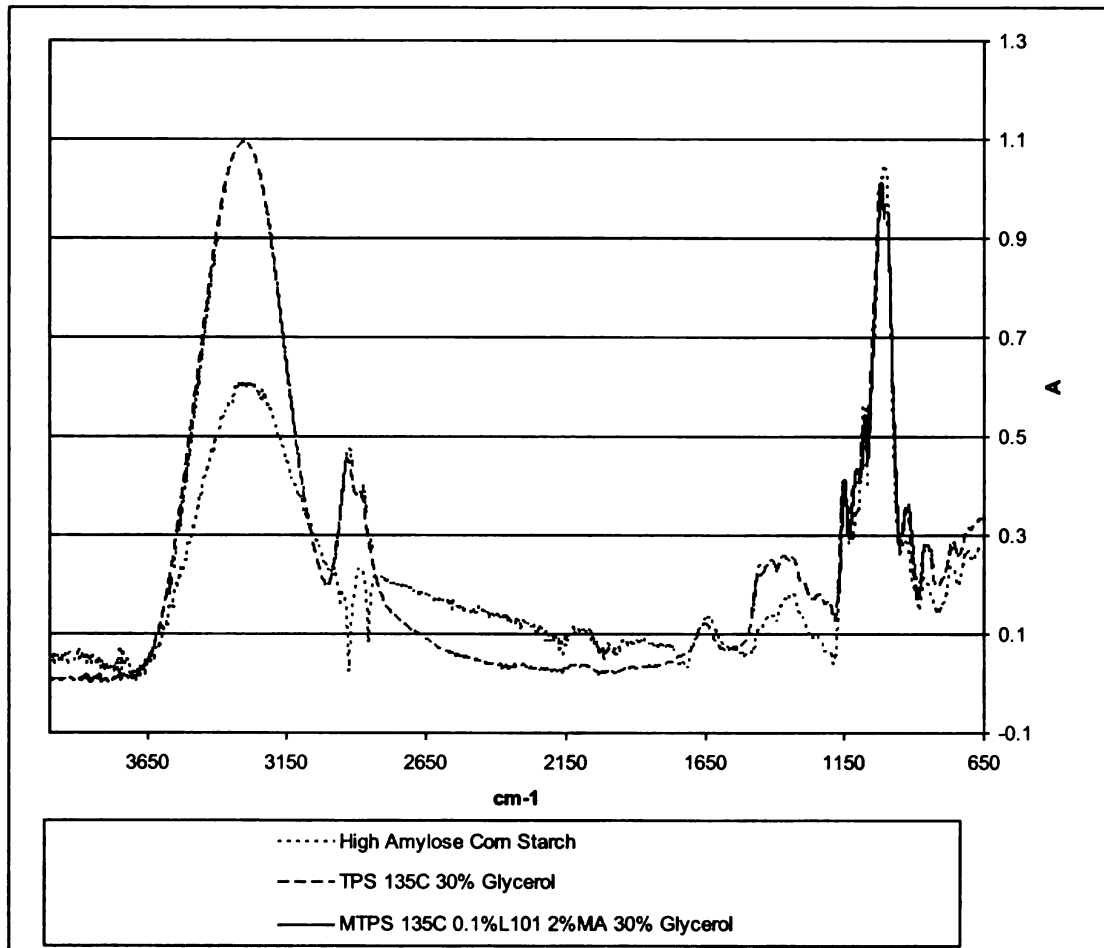


**Figure 13.** FTIR Spectra for High Amylose Corn Starch, TPS 135°C 30% Glycerol, and MTPS 135°C 0.1% L101 2% MA 30% Glycerol.

From analysis of the FTIR spectra for the MTPS samples, one is able to compare the relative intensities of the carbonyl peak in each of the MTPS samples. This is shown in Figure 14. This peak is more intense for the samples containing 4% and 6% maleic anhydride (Sample 4 and Sample 5, respectively), but the samples that contain 2% maleic anhydride (Sample 1, Sample 2, Sample 3, and Sample 6) do not show much variation in the intensity of the carbonyl peak. This suggests that when more maleic anhydride is present, then more reacts during the extrusion process, as one would expect. This is evidence of maleation and



that it depends on the amount of maleic anhydride added during the production of the MTPS samples.

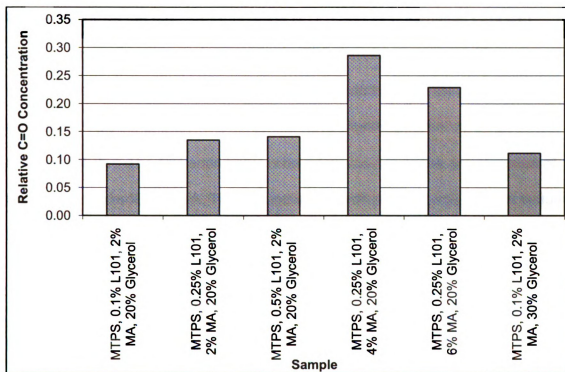


**Figure 14.** FTIR relative intensities of the carbonyl peak for the MTPS samples.

### 3.3.3 Thermal Analysis (DSC)

In the DSC analysis, the first heating showed endotherm transitions while the second heating did not. This is attributed to there being some crystallinity left in the starch structures after extrusion or from being aged for some time after being extruded and before running the DSC tests. This allows sufficient time for the materials to reform into crystal structures. However, between the first and second heatings, there is not enough time for re-crystallization to occur, and there is thus

no crystallization exotherm or subsequent melting endotherm during the second heating. Thus, all DSC observations discussed here refer to the first heating.

Figure 15 shows the thermograms of the MTPS and TPS samples. One can observe a broad melting endotherm in the TPS sample, and two melting endotherms in the MTPS sample. This has been attributed to the fact that the maleation of starch creates segments that have slightly different melting characteristics.<sup>35</sup> The first endotherm is broad and is due to the gelatinization of the starch, glycerol, and MA. The second endotherm is much sharper and is due to the fact that grafting has occurred.

Considering the effect of the amount of initiator on the DSC results, we observe that for Sample 1 (0.1% Luperox 101), the sharp endotherm is small ( $\Delta H=0.08397$  J/g) and is located at 168.07°C. As the amount of Luperox 101 increases to 0.25% (Sample 2), the sharp endotherm is larger ( $\Delta H=2.062$  J/g) and is located at 157.30°C. Finally, when the amount of Luperox 101 is 0.5% (Sample 3), the sharp endotherm is larger still ( $\Delta H=72.52$  J/g) and is located at 145.22°C. This suggests that grafting of maleic anhydride to the starch backbone and disruption of the crystalline starch structure has occurred during the reactive extrusion of the MTPS. This is consistent with our FTIR and soxhlet extraction observations.

Considering the effect of maleic anhydride on the melting endotherms of the samples, one can see the same type of trend. For Sample 2 (2% MA), the sharp endotherm ( $\Delta H=2.062$  J/g) is located at  $157.30^{\circ}\text{C}$ . As the amount of MA increases to 4% (Sample 4), the sharp endotherm is larger ( $\Delta H=36.30$  J/g) and is located at  $141.17^{\circ}\text{C}$ . Finally, when the amount of MA is 6% (Sample 5), the sharp endotherm is larger still ( $\Delta H=83.25$  J/g) and is located at  $132.60^{\circ}\text{C}$ . This also suggests that grafting of maleic anhydride to the starch backbone and disruption of the crystalline starch structure has occurred during the reactive extrusion of the MTPS. Again, this is consistent with our FTIR and soxhlet extraction observations.

Figure 15 shows the samples that were extruded at a maximum temperature of  $135^{\circ}\text{C}$ . Comparing the two thermograms, one can see that the sharp melting endotherm for the MTPS sample is at  $152.69^{\circ}\text{C}$ , while the melting endotherm for the TPS sample is at  $112.15^{\circ}\text{C}$ .

All of the MTPS samples exhibit melting endotherms that are at a higher temperature than that of the TPS sample. The fact that the maleated samples have a higher melting temperature than the TPS sample is one characteristic that will allow it to be blended with polymers, such as PLA, that have a higher melting temperature.

Another endotherm transition was observed for all of the MTPS and TPS samples close to 0°C. The transition occurred at positive values (from 0.27 to 5.43°C) in the first heating and at negative values (from -4.56 to -0.28°C) in the second heating. This transition resembles a first order transition (small endotherm peak) and is most likely due to fusion of water that is present in the samples.

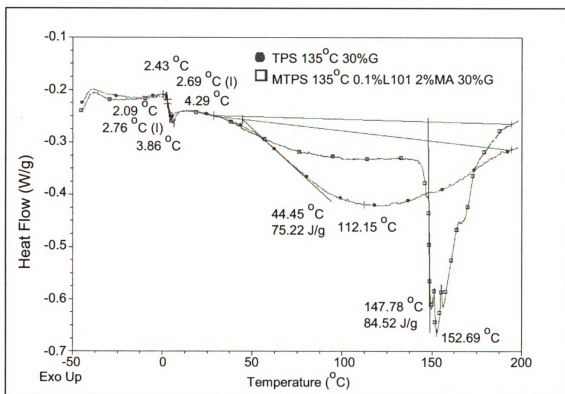


**Figure 15.** DSC thermogram of the MTPS (at 135°C and 30% glycerol) and TPS (at 135°C and 30% glycerol) samples.

### **3.3.4 Soxhlet Extraction Analysis**

The results of the soxhlet extraction in acetone of the MTPS and TPS samples are shown in Table 3. The calculated percentage of glycerol grafted to the starch is tabulated for each sample. The values are an average of four specimens that were tested for each sample.

Based on the soxhlet data, some of the maleic anhydride is hydrolyzed to maleic acid, due to the equilibrium moisture content of the starch (approximately 12%), facilitating the reaction of glycerol with the terminal C1 functionality of the starch backbone, chemically linking the starch and glycerol, as was shown in Figure 10, in Section 3.2.3.1.

For the maleated thermoplastic starch extruded at 165°C, after soxhlet extraction, 28.0 to 44.1% of the original glycerol in the samples remained. These results demonstrate that a certain amount of glycerol could not be removed after 3 days due to the fact that the glycerol has been linked to the starch backbone. This indicates that reactive extrusion has occurred. At this temperature, it was observed that the Luperox 101 content has more of an effect on the amount of glycerol extracted. When the Luperox 101 content changed from 0.1 to 0.5%, the amount of glycerol linked to the starch changes from 38.4 to 28.0%. Comparing samples 2 and 3, when the Luperox 101 content increased to 0.5%, less glycerol was linked to the starch. This could be caused by the reduction in the relative

molecular weight of the starch which makes some fraction of the maleated starch to be soluble in acetone.

The effect of the percentage of maleic anhydride on the soxhlet extraction is not evident. When the MA content changed from 2 to 6%, the amount of glycerol grafted to the starch was not significantly different.

For the maleated thermoplastic starch extruded at 135°C, after soxhlet extraction, only 9.2% of the original glycerol in the sample remained, while the TPS at the same temperature profile extracted almost all of the original glycerol in the sample, leaving only 1.3%. This is an indication that in maleated samples chemical interactions occur between starch and glycerol that hinder the extraction of the glycerol; however, these interactions are not present in TPS.

Comparing the MTPS samples with a maximum extrusion temperature of 165°C and 135°C, the samples extruded at the higher temperature have more glycerol linked to the starch (from 28.0 to 44.1%) than samples extruded at 135°C (9.2%). These results indicate that interactions between glycerol and starch, that are promoted by the reactive extrusion using MA, are more efficient at the higher temperature profile. Furthermore, the extrusion temperature profile also affected the color of the MTPS samples. Samples extruded at 165°C had a green color while the MTPS sample extruded at 135°C had a yellow color, which was more similar to the original color of the TPS sample.

**Table 3.** Percentage of glycerol grafted to the starch after soxhlet extraction of maleated thermoplastic starch in acetone for 72 hours.

Sample	Composition	Percentage of Glycerol Grafted to Starch (%)
1	MTPS, 165°C, 0.1% L101, 2% MA, 20% glycerol	38.4±1.42 <sup>c,d</sup>
2	MTPS, 165°C, 0.25% L101, 2% MA, 20% glycerol	42.4±6.49 <sup>d</sup>
3	MTPS, 165°C, 0.50% L101, 2% MA, 20% glycerol	28.0±8.32 <sup>c</sup>
4	MTPS, 165°C, 0.25% L101, 4% MA, 20% glycerol	44.1±18.04 <sup>c,d</sup>
5	MTPS, 165°C, 0.25% L101, 6% MA, 20% glycerol	38.2±13.00 <sup>c,d</sup>
6	MTPS, 135°C, 0.1% L101, 2% MA, 30% glycerol	9.2±5.66 <sup>b</sup>
7	TPS, 135°C, 30% glycerol	1.3±2.99 <sup>a</sup>

Means in same column with different letters are significantly different ( $p \leq 0.05$ ).

### 3.3.5 Environmental Scanning Electron Microscopy (ESEM) Analysis

Using the environmental scanning electron microscope (ESEM), one can understand the topography of the samples. Areas that are higher appear brighter in the image, while areas that are lower appear darker in the image. In this way, variations in light and dark areas give an indication of the roughness of the surface.

Images of the samples taken with the environmental scanning electron microscope (ESEM) are shown in Figure 16. The samples that were processed at 165°C (Figure 16 a,b,c and d) appear to be smoother than the MTPS and TPS samples that were processed at 135°C (Figure 16 e and f). This could imply that there was better plasticization of the starch at higher temperatures.

Also, since the DLS data indicates that the molecular weight of the starch is higher when the starch is extruded at 135°C, the higher molecular weight could make it more difficult for the starch to fully plasticize and regions of unplasticized starch may be present in the MTPS or TPS, thus, the TPS sample appears to have the roughest surface.

When comparing the samples extruded at 165°C, the effect of MA content is not evident. The samples appear to have comparable regions of light and dark, signifying that they have similar roughness. However, the effect of the content of free-radical initiator content is evident. The sample with 0.5% Luperox (Figure 16 c) presented a more homogeneous and a smoother surface compared to the samples with 0.1 and 0.25% Luperox (Figure 16 a and b), due to the smaller hydrodynamic radius of the sample which facilitates the plasticization of the starch. These observations are in agreement with the DLS data. Observations of the material as it was extruded showed that MTPS flowed better than TPS. This could also be an indication that there was less plasticization occurring during the extrusion of TPS compared with MTPS.



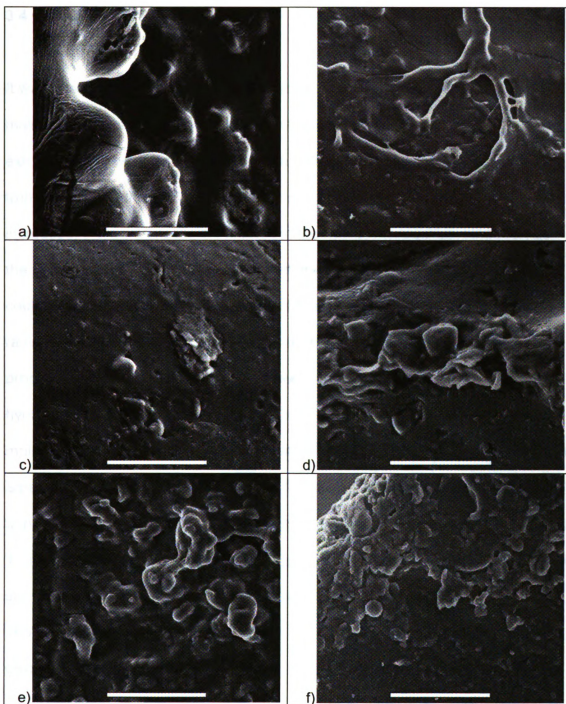


**Figure 16.** Environmental scanning electron microscope images of extrudate samples. Images shown at 750x magnification (50  $\mu\text{m}$  scale bar). a) MTPS, at 165°C, 0.1% L101, 2% MA, 20% glycerol, b) MTPS, at 165°C, 0.25% L101, 2% MA, 20% glycerol, c) MTPS, at 165°C, 0.50% L101, 2% MA, 20% glycerol, d) MTPS, at 165°C, 0.25% L101, 6% MA, 20% glycerol, e) MTPS, at 135°C, 0.1% L101, 2% MA, 30% glycerol and f) TPS, at 135°C, 70% starch and 30% glycerol.

### **3.4 CONCLUSIONS**

It was observed that MTPS had improved processability over TPS. Also, the maleation process permitted formulations with less than 30 wt% of glycerol to be extruded in the twin-screw extruder. The resulting MTPS pellets were more transparent than the TPS pellets. As the percentage of maleic anhydride increased, there was negligible change in the hydrodynamic radii. However, as the percentage of Luperox 101 increased, the hydrodynamic radii decreased. It could be inferred that the molecular weight decreased as the percentage of free-radical initiator increased. Using the maximum temperature during the extrusion process of 165°C instead of 135°C caused a drastic decrease in the hydrodynamic radius, due to the high influence of the temperature profile on the molecular weight of the thermoplastic starch. ESEM images of the samples are in agreement with the DLS data. FTIR of TPS and MTPS indicates that the maleic anhydride has reacted with the thermoplastic starch during the extrusion process. The MTPS samples presented higher melting temperatures compared to the TPS sample. The soxhlet studies indicated that using the maximum temperature of 165°C in the extrusion temperature profile resulted in more grafting between glycerol and starch than when the maximum temperature used was 135°C.

## **CHAPTER 4**

### **MTPS-PBAT BLENDS BY REACTIVE EXTRUSION PROCESSING AND THEIR APPLICATION AND PERFORMANCE FOR THERMOFORMED ARTICLES**

---

#### **4.1 RATIONALE**

This work was performed to better understand the effect of amylose content and percentage of MTPS in MTPS-PBAT blends used to produce thermoformable sheets. The materials were characterized by mechanical properties (tensile and puncture tests), thermal analysis (DSC), Fourier transform infrared spectroscopy (FTIR), and microstructural analysis (ESEM). This is, to the best of the author's knowledge, the first report of a truly biodegradable thermoformed article.

## **4.2 MATERIALS AND METHODS**

### **4.2.1 Materials**

High amylose corn starch was purchased from National Starch and Chemicals (Indianapolis, IN). Regular corn starch was obtained from Cargill Inc. (Minneapolis, MN). Poly(butylene adipate-co-terephthalate) (PBAT) was purchased from BASF Chemicals (Ludwigshafen, Germany), under the trade name Ecoflex. Anhydrous glycerol, 99.9% assay, was purchased from J.T. Baker (Phillipsburg, NJ). Maleic anhydride was purchased from Sigma-Aldrich, Inc (St. Louis, MO). The initiator, 2,5-bis(tert-butylperoxy)-2,5-dimethylhexane, also referred to as Luperox 101, was purchased from Sigma-Aldrich, Inc (St. Louis, MO).

### **4.2.2 Equipment**

A Century CX-30 co-rotating twin-screw extruder, having a length/diameter ratio (L/D) of 42 and a screw diameter of 30 mm was used to prepare the thermoplastic starch and maleated thermoplastic starch, and to blend these materials with Ecoflex. The screw configuration for the extruder is shown in Figure 7, in Section 3.2.2. A pelletizer was used to cut the extruded strands into small pellets.

The blended material was then extruded through a Killion single-screw extruder, having a length/diameter ratio of 24 and a screw diameter of 1 inch. The extrudate exited the extruder in the form of a sheet of material and was collected on a roller.

Thermoforming of the sheets of blended material was done using a Labform thermoformer by Hydro-Trim Corporation.

### **4.2.3 Procedure**

#### **4.2.3.1 Production of Thermoplastic Starch (TPS) and Maleated Thermoplastic Starch (MTPS)**

Thermoplastic starch (TPS) and maleated thermoplastic starch (MTPS) were produced in a Century CX-30 co-rotating twin-screw extruder as described in Section 3.2.3.1.

The samples either contained regular corn starch or high amylose corn starch.

With a temperature profile of 25/115/120/125/130/135/135/135/130/130°C, the composition of the samples was 70 wt% starch and 30 wt% glycerol. With a temperature profile of 25/95/125/145/160/165/165/165/150/145°C, the composition of the samples was 80 wt% starch and 20 wt% glycerol.

The amount of MA and Luperox 101 in the MTPS samples was 2 wt% and 0.1 wt%, respectively, of starch and glycerol.

The extruded strand was air cooled and pelletized in line. The pellets were dried for two days in an oven set at 65°C before being blended with Ecoflex.

The temperature profile used with the maximum temperature of 165°C was defined in preliminary tests as the best temperature for production of MTPS of high amylose corn starch with 20% glycerol. It is not possible to make TPS with 20% glycerol in the twin-screw extruder, due to its high viscosity. For comparison purposes, TPS and MTPS were also produced under the same conditions; with a temperature profile of 25/95/115/125/130/135/135/135/130/130°C and 30% glycerol. With a maximum extrusion temperature of 135°C, it is possible to produce both TPS and MTPS with 30 wt% glycerol. These samples were made in order to compare blends of maleated and non-maleated thermoplastic starch of high amylose corn starch and regular corn starch.

#### **4.2.3.2 Blend Production of TPS and MTPS with PBAT**

Blends of thermoplastic starch/PBAT or maleated thermoplastic starch/PBAT were produced in a Century CX-30 co-rotating twin-screw extruder. Pellets of TPS or MTPS were pre-mixed with PBAT in various weight of TPS (or MTPS) to weight of PBAT ratios (60:40 and 50:50) and placed in the external feeder. The feeder fed the pellets into the feed port of the extruder. Table 4 shows the

composition of each sample. The terms “HA” and “corn” in the sample names refer to high amylose corn starch and regular corn starch, respectively. The temperature profile of the extruder was set at 25/125/135/140/145/150/150/150/145/135°C from the feed throat to the die. The screw speed was set to 100 rpm. The vent port was kept open to remove any moisture. The extruded strand was air cooled and pelletized in line. The pellets were dried for one day in an oven set at 65°C before being extruded into sheets.

In previous work done by others,<sup>16</sup> the reaction between MTPS and PBAT shown in Figure 17 has been proposed.

**Table 4.** Composition of the blends of TPS and MTPS with PBAT.

<b>Samples</b>	<b>Maximum Temperature (°C)</b>	<b>Glycerol (%)</b>	<b>Luperox (%)</b>	<b>Blend Composition</b>	
				<b>TPS/MTPS (%)</b>	<b>PBAT (%)</b>
MTPS HA 165 60	165	20	0.1	60	40
MTPS HA 165 50	165	20	0.1	50	50
MTPS corn 165 50	165	20	0.1	50	50
MTPS HA 135 50	135	30	0.1	50	50
MTPS corn 135 50	135	30	0.1	50	50
TPS HA 135 50	135	30	-	50	50
TPS corn 135 50	135	30	-	50	50
PBAT	-	-	-	-	100



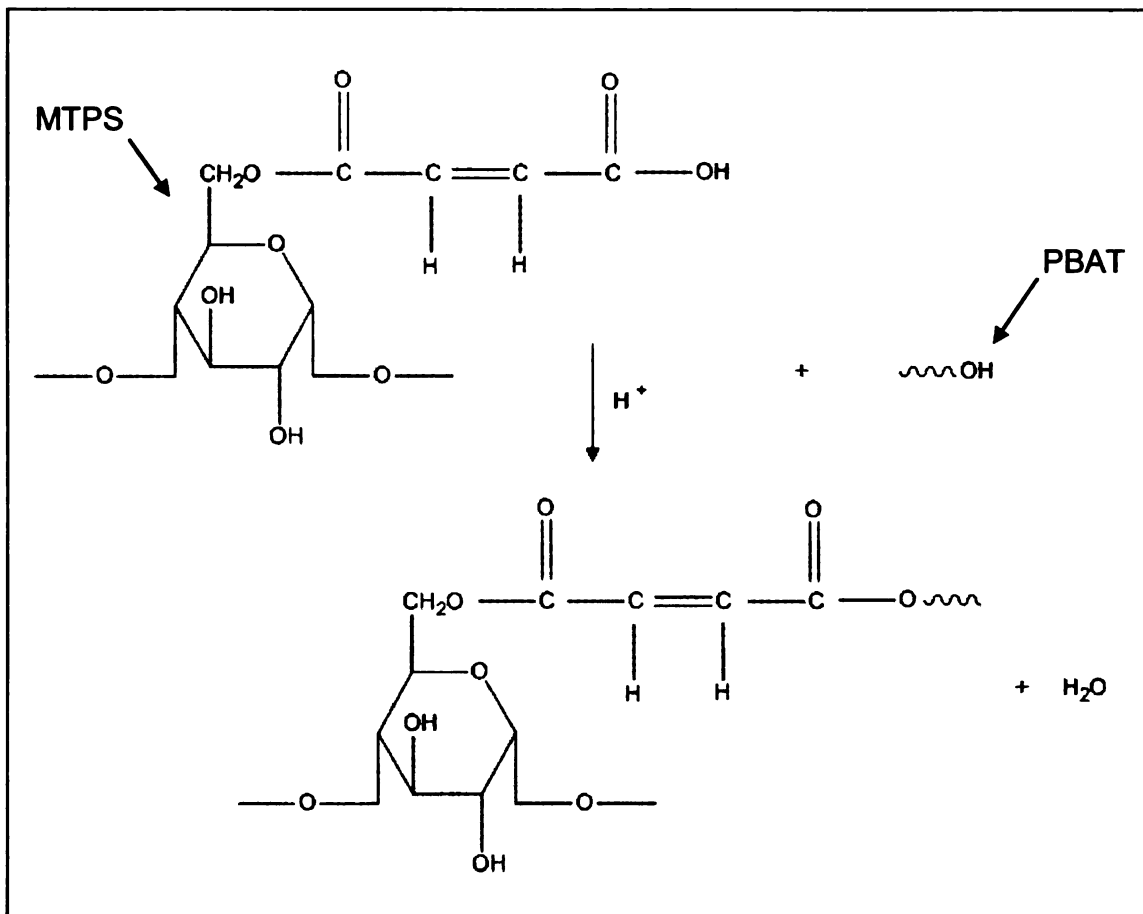


**Figure 17.** Proposed reaction scheme for MTPS and PBAT. [Adapted from Balakrishnan<sup>16</sup>]

#### 4.2.3.3 Sheet Production

Extruded sheets of the blended material were produced in a Killion single-screw extruder. The pellets were gravity-fed into the extruder at the feed throat. The temperature profile of the extruder was set to 160/160/160/160/154°C from the feed throat to the die. Cooling water was circulated through the extruder to maintain the set temperatures. The screw speed was set to 65 rpm. The extruded sheet was cooled on a chill roller set at 21<sup>0</sup>C and then collected on an

auxiliary roller. The speed of the chill roller was adjusted so as to produce a sheet with a thickness of 500 $\mu$ m.

#### 4.2.3.4 Thermoforming Process

Pieces of the sheets were cut with scissors and clamped in place in the Labform thermoformer. The upper and lower heaters of the thermoformer were both set to 154<sup>o</sup>C. The sheets were heated between the upper and lower heaters for varying lengths of time (from 24 to 40 seconds), depending on the composition of the material. The length of time was determined so as to ensure that the material was adequately heated, but did not sag too much. The material was then placed over the forming die and a vacuum of approximately 25 mmHg was pulled and held for 20 seconds. During this process, the sheet of material was drawn by the vacuum into the forming die, where it cooled and was formed into the desired shape. The thermoformed object could then be removed from the thermoformer and the excess material around the object was trimmed away with scissors. The shape of the object that was formed is shown in Figure 18, below.

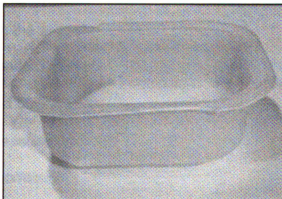


**Figure 18.** Picture of the object formed in the Labform thermoformer.

#### **4.2.3.5 Fourier Transform Infrared Spectroscopy (FTIR) Analysis**

The FTIR spectra of TPS, MTPS, starch, and blends of TPS or MTPS/PBAT pellets were scanned from  $650\text{ cm}^{-1}$  to  $4000\text{ cm}^{-1}$  using a Perkin Elmer Spectrum One FT-IR Spectrometer.

Soxhlet extraction in dichloromethane was performed on pellets of the “MTPS HA 165 60” sample in order to prove that grafting between the MTPS and the PBAT had occurred. PBAT is soluble in dichloromethane but MTPS is not, therefore, the soxhlet extraction removes the PBAT, glycerol and starch that are grafted on the PBAT backbone, leaving in the extraction thimble the MTPS that is not grafted to the PBAT. FTIR spectra of the pellets before soxhlet extraction and after soxhlet extraction were obtained. Also, the solvent was collected after the extraction and evaporated, leaving a film whose FTIR spectrum was recorded.

#### **4.2.3.6 Tensile Tests**

Tensile specimens (100mm x 25mm) of the blends of TPS and MTPS/PBAT blends were cut from the extruded sheets of material and were conditioned as recommended in standard method ASTM D4332,<sup>77</sup> in a constant environment room at  $23 \pm 1^\circ\text{C}$  and  $50 \pm 2\%$  RH for at least 40 hours before testing. The tensile tests were measured in accordance with standard method ASTM D882.<sup>78</sup> Specimens of each formulation were clamped between the grips of a United Testing Systems (Huntington Beach, CA) model SFM-20 tensile test machine.

Force-extension curves were recorded. Tensile strength and elongation were calculated for each of the samples. Seven specimens were tested for each blend.

#### **4.2.3.7 Puncture Tests**

Puncture tests were performed on the thermoformed specimens to determine puncture strength (N) and deformation (mm) using a TA.TX2i Stable Micro Systems texture analyzer (Surrey, England). Specimens measuring 40mm in diameter were affixed with tape (3M Scotch, Brazil) onto the plate of the equipment with a hole of 20mm diameter. A cylindrical probe of 5mm diameter was moved perpendicularly to the sheet surface at a constant speed of 1 mm/s until the probe passed through the film. Force-deformation curves were recorded and the force and deformation at the point of rupture were determined. Each data point represents an average of four specimens.

#### **4.2.3.8 Thermal Analysis (DSC)**

Differential scanning calorimetry (DSC) was performed using a high resolution DSC 2920 from TA Instruments. The purge gas, nitrogen, had a flow rate of 50 ml/min. Pellets of the extruded samples were cooled to -50°C and then heated to 200°C at a rate of 10°C/min, cooled to -50°C and then reheated to 200°C. The thermal transition temperatures of the blends and of PBAT were determined from analysis of the thermograms.

#### **4.2.3.8 Environmental Scanning Electron Microscopy (ESEM) Analysis**

A Phillips Electroscan 2020 environmental scanning electron microscope (ESEM) was used to make observations of the topography of the surface of the sheets of the blends.

#### **4.2.3.10 Statistical Analysis**

The PBAT sample was used as a control and was tested to evaluate the effect of blends of TPS and MTPS with PBAT on the mechanical and thermal properties of the sheets and thermoformed pieces. Analysis of variance (ANOVA) and Tukey mean comparison tests ( $p \leq 0.05$ ) were performed using Statistica software (Statsoft, Oklahoma – USA).

### **4.3 RESULTS AND DISCUSSION**

#### **4.3.1 Fourier Transform Infrared Spectroscopy Analysis (FTIR)**

In Figure 19, the FTIR spectra for high amylose (HA) starch, PBAT, and a blend of MTPS-PBAT are shown. The PBAT and the blend show a carbonyl stretch peak at  $1710\text{ cm}^{-1}$  and an ester C-O stretch peak at  $1265\text{ cm}^{-1}$ . These peaks are not observed in the HA starch sample. The HA starch and the blend samples exhibit a peak between  $3200\text{-}3400\text{ cm}^{-1}$ . This corresponds to -OH stretch from the starch and glycerol in the samples. These peaks are what one would expect to observe from the FTIR spectra.

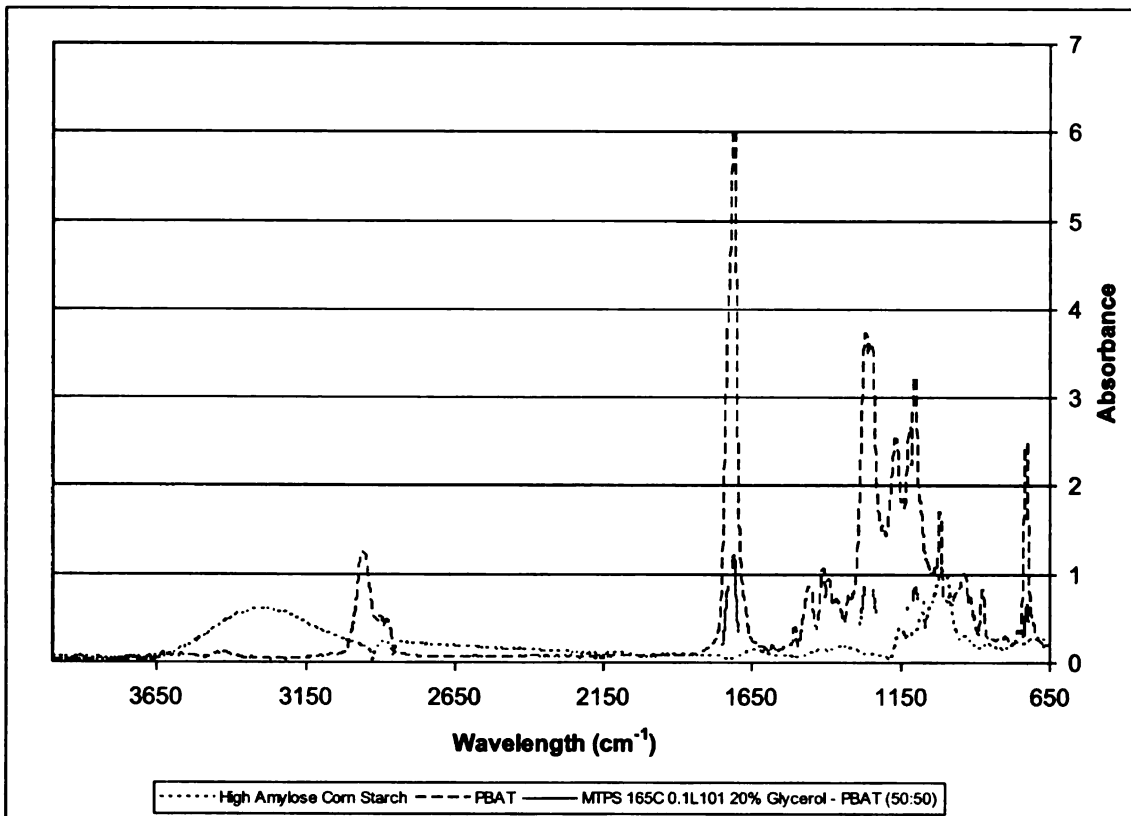


**Figure 19.** FTIR Spectra for HA Starch, PBAT, and MTPS 165°C 2%MA 0.1%L101 20%G-PBAT(50:50).

Figure 20 shows the FTIR spectra for as-extruded pellets of the sample “MTPS 165 60”, the pellets after soxhlet extraction in dichloromethane, and the film produced when the solvent was evaporated. The blend and the solvent film show a carbonyl stretch peak at  $1710\text{ cm}^{-1}$ . This is similar to what is observed for pure PBAT. Also, the ester C-O stretch at  $1265\text{ cm}^{-1}$  is exhibited in these two samples. Again, these peaks are what one would expect to observe from the FTIR spectra.

Evidence of grafting between MTPS and PBAT is shown in Figure 20, by the fact that the solvent film after soxhlet extraction exhibits a peak between  $3200\text{-}3400$

$\text{cm}^{-1}$ . This corresponds to  $-\text{OH}$  stretch from starch and glycerol and is an indication that the starch, glycerol, or both were extracted in dichloromethane with the PBAT.

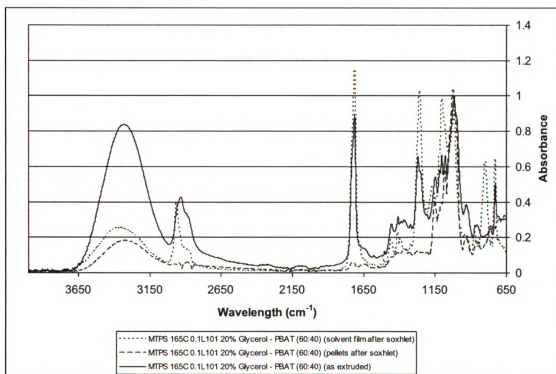


**Figure 20.** FTIR Spectra for film made after soxhlet of MTPS 165°C 0.1%L101 2%MA 20%G-PBAT(60:40), pellets left in thimble after soxhlet of MTPS 165°C 0.1%L101 2%MA 20%G-PBAT (60:40), and as extruded pellets of MTPS 165°C 0.1%L101 2%MA 20%G-PBAT (60:40).

### 4.3.2 Tensile Tests

The mechanical properties of the samples provide performance metrics for these materials. They suggest the effect of how: a) the temperature profile used in the extrusion of MTPS, b) the ratio of MTPS/PBAT of the blends, and c) the starch source impact the performance of the materials. Table 5 presents the tensile measurements of the sheets of TPS and MTPS/PBAT blends.

In examining the tensile strength of MTPS/PBAT sheets at 165°C and 20% glycerol, one observes that increasing the MTPS content to 60% caused a decrease in the tensile strength from 9.0 to 6.1MPa. Comparing the blends containing MTPS samples of high amylose and regular corn starch, observations of the effect of composition of starch on the tensile properties can be made. The blend containing MTPS of high amylose corn starch presented a higher tensile strength (9.0 MPa) than the blend containing MTPS of regular corn starch (6.2 MPa). This could be attributed to the linear structure of amylose chains.

According to Rindlav-Westling *et al.*,<sup>79</sup> the amylose network structure is very stable, having strong molecular orientation and forms films that are more dense than amylopectin films. It has been observed that higher levels of amylose in starches give stronger films, while amylopectin films generally have lower tensile strength, due to its branched structure.<sup>24, 56, 80</sup>



**Table 5.** Thickness and mechanical properties (determined by tensile tests) of sheets of blends of TPS and MTPS with PBAT.

<b>Samples</b>	<b>Thickness (<math>\mu\text{m}</math>)</b>	<b>Tensile Strength (MPa)</b>	<b>Elongation (%)</b>
MTPS HA 165 60	518.9 $\pm$ 21.64 <sup>a</sup>	6.1 $\pm$ 0.31 <sup>a</sup>	697.0 $\pm$ 50.60 <sup>a</sup>
MTPS HA 165 50	515.8 $\pm$ 6.15 <sup>a</sup>	9.0 $\pm$ 0.82 <sup>b</sup>	881.0 $\pm$ 139.13 <sup>b,c,d</sup>
MTPS corn 165 50	498.6 $\pm$ 27.50 <sup>a</sup>	6.2 $\pm$ 0.93 <sup>a</sup>	673.2 $\pm$ 131.84 <sup>a,d</sup>
MTPS HA 135 50	508.4 $\pm$ 24.56 <sup>a</sup>	8.4 $\pm$ 1.46 <sup>b</sup>	946.8 $\pm$ 151.35 <sup>b,c,d</sup>
MTPS corn 135 50	506.5 $\pm$ 9.82 <sup>a</sup>	9.2 $\pm$ 0.62 <sup>b</sup>	938.6 $\pm$ 52.27 <sup>b</sup>
TPS HA 135 50	524.7 $\pm$ 20.26 <sup>a</sup>	8.6 $\pm$ 0.57 <sup>b</sup>	852.5 $\pm$ 33.27 <sup>c</sup>
TPS corn 135 50	508.7 $\pm$ 9.81 <sup>a</sup>	8.0 $\pm$ 0.99 <sup>b</sup>	807.2 $\pm$ 111.20 <sup>c,d</sup>
PBAT	510.2 $\pm$ 24.60 <sup>a</sup>	15.3 $\pm$ 2.90 <sup>c</sup>	824.1 $\pm$ 153.45 <sup>a,b,c,d</sup>

Means in same column with different letters are significantly different ( $p \leq 0.05$ ).

There was not a statistical difference ( $p \leq 0.05$ ) between the values of tensile strength for the samples of sheets of TPS and MTPS/PBAT at 135°C and 30% glycerol. This is most likely due to the effect of glycerol. For blends of MTPS/TPS with 30% glycerol, the amount of glycerol affects the tensile properties more than the amylose/amylopectin ratio or the type of thermoplastic starch used (maleated and non-maleated).

The values of the tensile strength for the blends are higher than the values reported for blends of cassava TPS with the biodegradable polymer, PBSA (polybutylene succinate adipate). Values of 5.2 MPa for TPS/PBSA (30:70) and 7.0 MPa for TPS/PBSA (70:30) have been reported.<sup>81</sup> However, the values of the tensile strength for the blends are lower than the values reported for synthetic films such as LDPE (low density polyethylene) and HDPE (high density polyethylene), of 16 and 30 MPa, respectively.<sup>82, 83</sup>

There is not a statistical difference ( $p \leq 0.05$ ) in the values for elongation, when comparing all samples of sheets of TPS/PBAT and MTPS/PBAT with sheets of PBAT.

The elongation of test specimens depends on the interactions between the components of the blend and the elongation of the polymers used. One of the characteristics of PBAT is its high elongation (~800%). In this work, the addition of 50% of TPS or MTPS and 60% of MTPS did not change the elongation from that of the pure PBAT. The values presented here are higher than those of PLA blends with TPS that showed elongation at break between 5 to 20%,<sup>48</sup> and LDPE (low density polyethylene) and HDPE (high density polyethylene), which present strain at break of 570 and 180%, respectively.<sup>82, 83</sup>

According to Myllarinen *et al.*,<sup>29</sup> glycerol and starch interact strongly, and when the glycerol content is low (< 20%), this interaction results in more brittle and stronger networks. In the current work, the samples of 20% glycerol did not show improvement in tensile strength, most likely due to the effect of the extrusion temperature. The samples of 20 and 30% of glycerol were extruded with different temperature profiles, with maximum temperatures of 165°C and 135°C, respectively. The lower glycerol content positively affected the tensile strength while the higher temperature profile used negatively affected the tensile strength, due to higher degradation of the maleated samples at the higher temperatures.

Even though the tensile properties of TPS and MTPS blends presented similar values, the visual characteristics of the samples were very different. The MTPS blends have a more homogeneous surface and formed more transparent sheets than the TPS sheets. Also, high amylose corn starch MTPS has improved processability compared to the processability of regular corn starch MTPS. High amylose corn starch MTPS containing 20 or 30% glycerol can be pelletized in line; however, regular corn starch MTPS containing 20 or 30% glycerol cannot be pelletized in line. In this case, the materials were collected and ground into a powder before being blended with PBAT.

### **4.3.3 Puncture Tests**

In packaging applications, the resistance of the package to puncture is an important consideration if it contains products with sharp extremities or products that could be damaged by being punctured during storage or distribution. The shape and size of the thermoformed specimens produced in this work did not allow for tensile tests to be performed on the thermoformed specimens; however, puncture tests were performed on the thermoformed specimens. Table 6 shows the thickness ( $\mu\text{m}$ ), puncture strength (N), and puncture deformation (mm) for the samples.

The sample "MTPS com 165 50" produced a thermoformed object that was irregular in shape and thickness, so puncture tests were not performed on specimens of that particular blend. Also, due to the extreme flexibility of the thermoformed PBAT specimens, puncture tests were not performed on the PBAT specimens either.

**Table 6.** Mechanical properties determined by puncture tests of the thermoformed pieces of the blends of TPS and MTPS with PBAT.

Samples	Thermoformed Pieces		
	Thickness ( $\mu\text{m}$ )	Puncture Strength (N)	Puncture Deformation (mm)
MTPS HA 165 60	283 $\pm$ 9.6 <sup>a</sup>	26.0 $\pm$ 0.80 <sup>a</sup>	10.3 $\pm$ 0.44 <sup>a</sup>
MTPS HA 165 50	323 $\pm$ 15 <sup>b</sup>	47.7 $\pm$ 2.29 <sup>b</sup>	15.9 $\pm$ 0.51 <sup>b</sup>
MTPS corn 165 50	-	-	-
MTPS HA 135 50	333 $\pm$ 70 <sup>a,b,c</sup>	40.4 $\pm$ 6.91 <sup>b</sup>	19.5 $\pm$ 2.44 <sup>c,d</sup>
MTPS corn 135 50	380 $\pm$ 78 <sup>b,c</sup>	27.7 $\pm$ 5.56 <sup>a</sup>	20.0 $\pm$ 0.72 <sup>c</sup>
TPS HA 135 50	333 $\pm$ 16 <sup>b</sup>	52.3 $\pm$ 2.35 <sup>c</sup>	16.6 $\pm$ 1.37 <sup>b</sup>
TPS corn 135 50	363 $\pm$ 23 <sup>c</sup>	48.4 $\pm$ 2.41 <sup>b</sup>	18.6 $\pm$ 0.84 <sup>d</sup>
PBAT	-	-	-

Means in same column with different letters are significantly different ( $p \leq 0.05$ ).

It should be noted that the thickness of the thermoformed pieces varied by more than 5%. This could interfere with the mechanical properties of the specimens.

The puncture test results show similar behavior to the tensile test results. When one compares the samples extruded at 165°C, it is observed that the samples

containing 60% MTPS have lower puncture strength and deformation than samples containing 50% MTPS.

For the samples extruded at 135<sup>0</sup>C, the high amylose corn starch MTPS blend presented higher puncture strength and lower puncture deformation than the blend containing regular corn starch MTPS. This is also observed for the blend containing high amylose TPS, compared to the blend containing regular corn starch TPS.

#### **4.3.4 Thermal Analysis (DSC)**

The thermal transition temperatures of the MTPS/PBAT and TPS/PBAT samples are tabulated and shown in Table 7. One can observe a melting temperature for PBAT of 113.6<sup>0</sup>C. The MTPS and TPS blends all presented melting temperatures that are slightly higher than that of PBAT; varying from 115.7 to 123.3<sup>0</sup>C, measured at the second heating. The crystallization temperatures were similar for all the MTPS/TPS blends (from 72.4 to 79.5<sup>0</sup>C), while the PBAT presented a crystallization temperature of 33.0<sup>0</sup>C.

The fact that the crystallization temperature of the blends is higher than for neat PBAT is a property that will allow the blends to crystallize at a higher temperature, after being extruded and formed. This could be advantageous in a production environment.

Another endotherm transition was observed for all of the samples close to 0°C. The transition occurred at positive values (from 0.3 to 5.1°C) in the first heating and at negative values (from -6.3 to -0.7°C) in the second heating. This transition is a first order transition (small endotherm peak) and is most likely due to fusion of water that is present in the samples.

**Table 7.** DSC parameters: glass transition temperature ( $T_g$ ), crystallization temperature ( $T_c$ ), crystallization enthalpy ( $\Delta H_c$ ), and melting temperature ( $T_m$ ) of the blends of MTPS and TPS with PBAT.

Sample	First Heating	Cooling		Second Heating	
	$T_g$ (°C)	$T_c$ (°C)	$\Delta H_c$ (J/g)	$T_g$ (°C)	$T_m$ (°C)
MTPS HA 165 60	3.2	78.9	6.2	-0.7	123.1
MTPS HA 165 50	5.1	79.5	7.7	-1.0	123.3
MTPS corn 165 50	0.9	72.4	8.4	-6.3	115.7
MTPS HA 135 50	1.2	75.8	6.9	-2.8	117.8
MTPS corn 135 50	3.0	74.5	9.3	-4.9	116.8
TPS HA 135 50	2.3	79.2	7.8	-2.8	121.5
TPS corn 135 50	0.3	72.6	8.5	-4.7	121.5
PBAT	2.3	33.0	20.1	-2.4	113.6

#### **4.3.5 Environmental Scanning Electron Microscopy (ESEM) Analysis**

Environmental scanning electron microscopy (ESEM) was used to observe the surface of the sheets of the blends. Figure 21 shows the samples containing MTPS that were extruded with a maximum temperature of 165°C and Figure 22 shows the samples containing MTPS and TPS that were extruded with a maximum temperature of 135°C. In general, the blends containing maleated thermoplastic starch extruded with a maximum temperature of 165°C are more homogeneous and smoother than the blends containing MTPS and TPS extruded with a maximum temperature of 135°C. This could imply that there was better plasticization of the starch with higher temperatures. According to Mali *et al.*,<sup>84</sup> a homogeneous matrix of films is a good indicator of their structural integrity and consequently good mechanical properties would be expected. However, the samples containing MTPS extruded with a maximum temperature of 165°C did not exhibit better mechanical properties. This is most likely due to the thermoplasticization process. Although there was better plasticization of the MTPS, there was also more degradation of the starch during the reactive extrusion to produce the MTPS at the higher temperature profile.



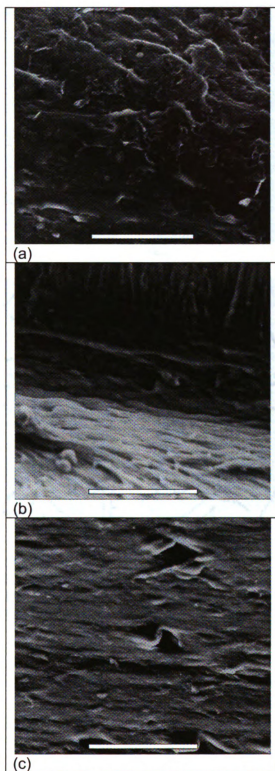


**Figure 21.** ESEM images of the samples extruded at 165°C and 20% glycerol at 750x magnification (50  $\mu\text{m}$  scale bar): (a) MTPS high amylose-PBAT (60:40), (b) MTPS high amylose-PBAT (50:50) and (c) MTPS corn starch-PBAT (50:50).

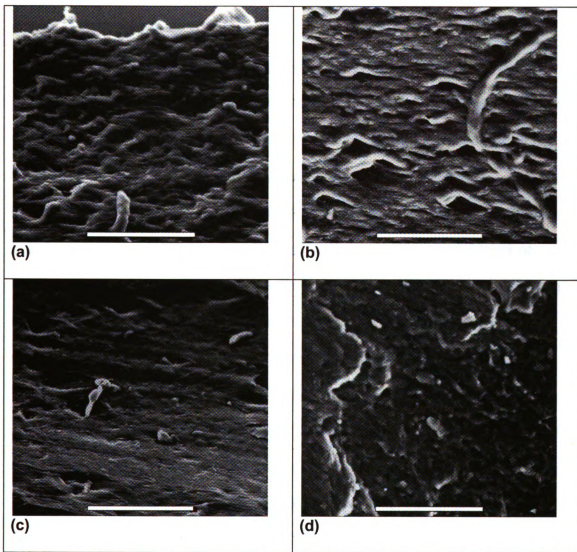


**Figure 22.** ESEM images of the samples extruded at 135°C and 30%glycerol at 750x magnification (50 μm scale bar): (a) TPS high amylose-PBAT (50:50), (b) MTPS high amylose-PBAT (50:50), (c) TPS corn starch-PBAT (50:50) and (d) MTPS corn starch-PBAT (50:50).

#### **4.4 CONCLUSIONS**

The processability of high amylose corn starch MTPS is much better than the processability of regular corn starch MTPS. Blends of plasticized starch, with or without maleation, with PBAT can form sheets which can be thermoformed. To the best of the author's knowledge, this is the first report of a 100% biodegradable thermoformed article. FTIR results show that starch, glycerol, or both have been grafted to the PBAT. The tensile properties of the blends of PBAT with TPS and MTPS extruded with a maximum temperature of 135°C are not statistically different. However, the maleated thermoplastic samples formed sheets and thermoformed pieces that were more transparent and had a more homogeneous surface. The effect of the amylose content of the starches used did not present significant differences in the tensile properties when the glycerol content was 30% and the ratio of thermoplastic starch:PBAT used was 50:50. However, when the MTPS contained 20% glycerol, the ratio of MTPS:PBAT was 50:50, and the maximum processing temperature during the extrusion of the MTPS was 165°C, the blend containing high amylose corn starch MTPS showed better tensile properties than the blend containing regular corn starch MTPS. Increasing the MTPS (high amylose corn starch) content to 60% decreased the tensile strength and elongation of the sheets. The addition of TPS or MTPS decreased the tensile strength, but did not cause a significant difference in the elongation, compared to the elongation of PBAT. The puncture test results show similar behavior to the tensile test results. DSC analysis shows that the blends all

have higher melting and crystallization temperatures than neat PBAT. Finally, ESEM shows that the blends containing MTPS extruded with a maximum temperature of 165°C are smoother and more homogeneous than the blends containing MTPS and TPS extruded with a maximum temperature of 135°C.

## **CHAPTER 5**

### **APPLICATION AND PERFORMANCE OF MTPS-PBAT BLENDS FOR FILMS**

---

#### **5.1 RATIONALE**

This work was performed to better understand the effect of the percentage of MTPS in MTPS-PBAT blends used to produce extruded films. The materials were characterized by mechanical properties (tensile and puncture tests), barrier properties (carbon dioxide, oxygen, and water vapor permeability), and microstructural analysis (transmission electron microscopy).

## **5.2 MATERIALS AND METHODS**

### **5.2.1 Materials**

High amylose corn starch was purchased from National Starch and Chemicals (Indianapolis, IN). Poly(butylene adipate-co-terephthalate) (PBAT) was purchased from BASF Chemicals (Ludwigshafen, Germany), under the trade name Ecoflex. Anhydrous glycerol, 99.9% assay, was purchased from J.T. Baker (Phillipsburg, NJ). Maleic anhydride was purchased from Sigma-Aldrich, Inc (St. Louis, MO). The initiator, 2,5-bis(tert-butylperoxy)-2,5-dimethylhexane, also referred to as Luperox 101, was purchased from Sigma-Aldrich, Inc (St. Louis, MO).

### **5.2.2 Equipment**

A Century CX-30 co-rotating twin-screw extruder, having a length/diameter ratio (L/D) of 42 and a screw diameter of 30 mm was used to prepare the maleated thermoplastic starch (MTPS) and to blend the MTPS with PBAT. Figure 7, in Section 3.2.2 shows the screw configuration for the twin-screw extruder. A pelletizer was used to cut the extrudate strands into small pellets.

The blended material was then extruded through a Killion single-screw extruder, having a length/diameter ratio of 24 and a screw diameter of 1 inch. The

extrudate exited the extruder in the form of a film of material and was collected on a roller.

### **5.2.3 Procedure**

#### **5.2.3.1 Production of Maleated Thermoplastic Starch (MTPS)**

Maleated thermoplastic starch (MTPS) was produced in a Century CX-30 co-rotating twin-screw extruder as described in Section 3.2.3.1. The concentration of maleic anhydride used was 2 wt% with respect to the total mass. The concentration of Luperox 101 used was 0.1 wt% with respect to the total mass. The feed rates of the external feeder and the peristaltic pump for the glycerol were set so as to accomplish a composition of 80 wt% starch and 20 wt% glycerol. The temperature profile of the extruder for producing maleated thermoplastic starch was 25/95/125/145/160/165/165/165/150/145°C from the feed throat to the die. The extruded strand was air cooled and pelletized in line. The pellets were dried for two days in an oven at 65°C before being blended with PBAT.

### 5.2.3.2 Blend Production of MTPS with PBAT

Blends of maleated thermoplastic starch/PBAT were produced in a Century CX-30 co-rotating twin-screw extruder. Pellets of MTPS were pre-mixed with PBAT in a 10:90, 20:80, 30:70, 40:60, or 50:50 weight of MTPS: weight of PBAT ratio (Table 8) and placed in the external feeder. The feeder fed the pellets into the feed port of the extruder. The temperature profile of the extruder was set at 25/125/135/140/145/150/150/150/145/135°C from the feed throat to the die. The screw speed was set to 100 rpm. The vent port was kept open to remove any moisture. The extruded strand was air cooled and pelletized in line. The pellets were dried for one day in an oven set at 65°C before being extruded into films.

**Table 8.** Composition of films of blends of MTPS with PBAT.

Samples	Glycerol (%)	Maleic Anhydride (%)	Luperox (%)	Blend Composition	
				MTPS (%)	PBAT (%)
1	-	-	-	-	100
2	20	2	0.1	10	90
3	20	2	0.1	20	80
4	20	2	0.1	30	70
5	20	2	0.1	40	60
6	20	2	0.1	50	50



### **5.2.3.3 Film Production**

Extruded films of the blended material as well as neat PBAT were produced in a Killion single-screw extruder. The pellets were gravity-fed into the extruder at the feed throat. The temperature profile of the extruder was set to 160/160/160/160/154°C from the feed throat to the die. Cooling water was circulated to maintain the set temperatures. The screw speed was set to 65 rpm. The extruded sheet was cooled on a chill roller set at 21°C and then collected on an auxiliary roller. The speed of the chill roller was adjusted so as to produce a film with a thickness of 150µm.

### **5.2.3.4 Determining Biobased Content**

Samples of MTPS and the 50:50 MTPS:PBAT blend were sent to Beta Analytic Inc. (Miami, FL) for biobased content analysis. This analysis was run according to standard method ASTM D6866 Method B.<sup>85</sup> In this testing, the amount of radiocarbon (<sup>14</sup>C) in a test sample is compared to that of a modern reference sample. The ratio of the unknown to the standard is reported as a percentage, having units of percent modern carbon (pMC). A sample that is a mixture of fossil carbon (ie: contains no radiocarbon) and present day radiocarbon will have a pMC value that correlates directly to the amount of biobased content in the sample.

It should be noted that the results of the biobased content analysis give a value for the percentage of carbon that is radiocarbon, out of the total amount of carbon in the sample, not the total weight of the sample.

### **5.2.3.5 Mechanical Properties**

#### **5.2.3.5.1 Tensile Tests**

Tensile specimens (100mm x 25mm) of the MTPS/PBAT blends were cut from the extruded sheets of material and were conditioned as recommended in standard method ASTM D4332,<sup>77</sup> in a constant environment room at  $23\pm 1^{\circ}\text{C}$  and  $50\pm 2\%$  RH for at least 40 hours before testing. The tensile tests were measured in accordance with standard method ASTM D882.<sup>78</sup> Specimens of each formulation, cut along the machine direction and along the transverse direction, were clamped between the grips of a United Testing Systems (Huntington Beach, CA) model SFM-20 tensile test machine. Force-extension curves were recorded. Values for the tensile strength and elongation were determined for each sample, in both the machine and transverse direction. Seven specimens were tested for each blend and direction.

#### **5.2.3.5.2 Puncture Tests**

Puncture tests were performed on the film samples to determine puncture strength (N) and deformation (mm) using a TA.TX2i Stable Micro Systems texture analyzer (Surrey, England). Specimens (40mm x 40mm) were affixed

with tape (3M Scotch, Brazil) onto the plate of the equipment with a hole of 20mm diameter. A cylindrical probe of 5mm diameter was moved perpendicularly to the film surface at a constant speed of 1 mm/s until the probe passed through the film. Force-deformation curves were recorded and the force and deformation at the point of rupture were determined. Each data point represents an average of ten specimens.

### **5.2.3.6 Barrier Properties**

#### **5.2.3.6.1 Carbon Dioxide Permeability**

Carbon dioxide (CO<sub>2</sub>) permeability tests were performed using Mocon Permatran-C Model 4/41 carbon dioxide permeability equipment. Testing was run per ASTM standard F2476.<sup>86</sup> For the CO<sub>2</sub> permeability tests, specimens of each formulation were cut from the films that were extruded. Aluminum masks (4 mil thick) were used to ensure that the area of the specimen tested was 1.41 cm<sup>2</sup>. The carrier gas used was nitrogen. Permeability tests were run using a flow rate of 50 sccm for carbon dioxide and nitrogen. All tests were run at 23°C and 0% humidity. Once the specimens were loaded into the Permatran-C, they were conditioned for 2 hours. Permeability data was then collected for 30 minutes for each specimen (one cycle each). The Permatran-C has two cells and can test two specimens at once. After every two cycles, the test module was rezeroed. Each test was run until steady-state conditions were achieved. Values for permeability of CO<sub>2</sub> for each specimen were determined by multiplying the

average thickness of the specimen area tested by the average steady-state transmission rate. The Permatran-C compensates the transmission data to 1 atm barometric pressure. The values reported are an average of 4 specimens for each sample.

#### **5.2.3.6.2 Oxygen Permeability**

Oxygen (O<sub>2</sub>) permeability tests were performed using Illinois Instruments Model 8001 oxygen permeability equipment. Testing was run per ASTM standard D3985.<sup>87</sup> For the O<sub>2</sub> permeability tests, the specimens that were used to test carbon dioxide permeability were tested. Aluminum masks (4 mil thick) were used to ensure that the area of the specimen tested was 1.41 cm<sup>2</sup>. The carrier gas used was nitrogen. Permeability tests were run using a flow rate of 10 sccm for oxygen and nitrogen. All tests were run at 23°C and 0% humidity. Once the specimens were loaded into the test equipment, the gas lines and cells were purged. Permeability data was then collected for 5 minutes for each sample (one cycle each). The Illinois Instruments equipment has two cells and can test two specimens at once. Each test was run until steady-state conditions were achieved. Values for permeability of O<sub>2</sub> for each specimen were determined by multiplying the average thickness of the specimen area tested by the average steady-state transmission rate. The Illinois Instruments equipment acquires the data at atmospheric pressure. The permeability data presented has been compensated to 1 atm barometric pressure. The values reported are an average of 4 specimens for each sample.

### **5.2.3.6.3 Water Vapor Permeability**

Water vapor (H<sub>2</sub>O) permeability tests were performed using Mocon Permatran-W Model 3/33 water vapor permeability equipment. Testing was run per ASTM standard F1249.<sup>88</sup> For the H<sub>2</sub>O permeability tests, the specimens that were used to test carbon dioxide and oxygen permeability were tested. Aluminum masks (4 mil thick) were used to ensure that the area of the specimen tested was 1.41 cm<sup>2</sup>. The carrier gas used was nitrogen. Permeability tests were run using a flow rate of 100 sccm. All tests were run at 37.8°C and 100% humidity. Once the specimens were loaded into the Permatran-W, they were conditioned for 2 hours. Permeability data was then collected for 15 minutes for each specimen (one cycle each). The Permatran-W has two cells and can test two specimens at once. After every two cycles, the test module was rezeroed. Each test was run until steady-state conditions were achieved. Values for permeability of H<sub>2</sub>O for each specimen were determined by multiplying the average thickness of the specimen area tested by the average steady-state transmission rate. The Permatran-W acquires the data at atmospheric pressure. The permeability data presented has been compensated to 1 atm barometric pressure. The values reported are an average of 4 specimens for each sample.

### **5.2.3.7 Transmission Electron Microscopy (TEM)**

A transmission electron microscope (TEM) (JEOL-100CX) was used to make observations of the morphology of the blends. Samples of PBAT and the extruded blends were cryogenically frozen with liquid nitrogen and microtomed. The samples were mounted on TEM grids and then viewed with the transmission electron microscope.

### **5.2.3.8 Statistical Analysis**

One control sample, PBAT, was tested to evaluate the effect of blends of MTPS with PBAT on mechanical and barrier properties of the films. Analysis of variance (ANOVA) and Tukey mean comparison tests ( $p \leq 0.05$ ) were performed using Minitab 15 software (Minitab Inc., State College, PA).

## **5.3 RESULTS AND DISCUSSION**

### **5.3.1 Determining Biobased Content**

The results of the biobased content analysis show that MTPS has a mean biobased result of  $96 \pm 3\%$ , while the 50:50 blend has a mean biobased result of  $32 \pm 3\%$ . That is to say that  $96 \pm 3\%$  of the carbon in the MTPS is biobased carbon, while  $32 \pm 3\%$  of the carbon in the 50:50 blend is biobased carbon.

It should be noted that PBAT is a synthetic biodegradable polyester that is not produced with any biobased content.

One can see that blending PBAT with MTPS significantly reduces the biobased content of the material. In order to maintain the greatest amount of biocontent in a material, the least amount of PBAT should be used that will provide the required material properties for a specific application.

### **5.3.2 Mechanical Properties**

#### **5.3.2.1 Tensile Tests**

The tensile tests that were performed give an indication of the effect of the ratio of MTPS:PBAT of the blends and the effect of the direction from which the specimens have been cut on the mechanical properties of the materials. These effects will be discussed here. Table 9 presents the tensile strength (MPa) and break elongation (%) for the samples.

**Table 9.** Thickness and mechanical properties (determined by tensile tests) of films of blends of MTPS with PBAT.

Sample	Direction	Thickness ( $\mu\text{m}$ )	Tensile Strength (MPa)	Elongation at Break (%)
PBAT	Machine	$148.8 \pm 6.51^A$	$19.7 \pm 3.27^A$	$789.0 \pm 179.08^A$
PBAT	Transverse	$146.4 \pm 3.45^A$	$15.3 \pm 0.90^B$	$709.6 \pm 35.79^{A,B}$
10:90	Machine	$150.4 \pm 5.63^A$	$18.9 \pm 1.59^A$	$937.5 \pm 90.11^{A,B}$
10:90	Transverse	$154.7 \pm 7.79^{A,B}$	$14.3 \pm 2.14^{B,C}$	$857.5 \pm 141.60^{A,B}$
20:80	Machine	$152.1 \pm 9.96^A$	$17.6 \pm 1.26^{A,B,D}$	$991.8 \pm 121.00^{A,C}$
20:80	Transverse	$170.9 \pm 3.14^C$	$14.3 \pm 0.90^{B,D,E}$	$877.4 \pm 34.00^{A,B,C}$
30:70	Machine	$155.8 \pm 4.59^{A,D}$	$13.5 \pm 2.50^{B,F}$	$908.6 \pm 192.09^{A,B,C}$
30:70	Transverse	$154.8 \pm 6.95^{A,E}$	$11.5 \pm 2.79^{C,E,F,G}$	$781.3 \pm 196.92^{A,B,C}$
40:60	Machine	$152.8 \pm 5.97^{A,F}$	$12.2 \pm 1.22^{B,C}$	$940.0 \pm 104.64^{A,B,C}$
40:60	Transverse	$163.3 \pm 5.26^{B,C,D,E,F,G}$	$8.9 \pm 1.25^{G,H}$	$776.0 \pm 102.23^{A,B,C}$
50:50	Machine	$144.9 \pm 4.52^A$	$8.6 \pm 1.12^{G,I}$	$736.9 \pm 99.54^{A,B}$
50:50	Transverse	$157.1 \pm 6.93^{A,G}$	$7.1 \pm 1.32^{H,I}$	$709.0 \pm 138.81^{A,B}$

Means in same column with different letters are significantly different ( $p \leq 0.05$ ).



The tensile strength values for samples tested in the machine direction are greater than samples tested in the transverse direction. Also, as the amount of MTPS in the samples increases, the tensile strength decreases. Adding MTPS to the material decreases the tensile strength of the resulting films.

Observing the elongation at break of the samples, there is not a statistical difference between the samples when comparing the composition and the direction. Adding MTPS to PBAT does not significantly change the elongation exhibited. One also observes that all samples show elongations greater than 700%. These materials can deform greatly prior to breaking.

The values for tensile strength and elongation of films containing 20% MTPS are greater than those of Parulekar and Mohanty,<sup>89</sup> in which extruded cast films of 50 wt% PHBV, 30 wt% PBAT, 12 wt% high amylose corn starch, and 8 wt% glycerol exhibited tensile strength and elongation values of 15 MPa and 368%, respectively. However, Otey and Westhoff<sup>90</sup> reported blown films consisting of 20% corn starch and 80% poly(ethylene-co-acrylic acid) having tensile strength and elongation of 28.5 MPa and 120%, respectively.

From the data presented in this work, one would expect the tensile strength of starch films to be lower than the MTPS-PBAT blends. This has been shown by Zamudio-Flores *et al.*<sup>91</sup> who reported values for tensile strength of native and

acetylated banana starch films of approximately 2.5 MPa and 3 MPa, respectively.

### 5.3.2.2 Puncture Tests

The results of the puncture tests on the film specimens are shown in Table 10, below. The thickness, force, and deformation of the samples are given. Each entry is an average of 10 specimens.

**Table 10.** Puncture test results of films of blends of MTPS with PBAT.

Sample	Thickness ( $\mu\text{m}$ )	Force (N)	Deformation (mm)
PBAT	$155 \pm 6.6^{\text{A}}$	$42.5 \pm 3.22^{\text{A}}$	$17.9 \pm 1.74^{\text{A}}$
10:90	$150 \pm 8.4^{\text{A,B}}$	$42.1 \pm 3.21^{\text{A}}$	$24.2 \pm 1.78^{\text{B}}$
20:80	$152 \pm 7.4^{\text{A,B}}$	$40.9 \pm 2.93^{\text{A}}$	$23.5 \pm 1.32^{\text{B}}$
30:70	$148 \pm 10.1^{\text{A,B}}$	$38.2 \pm 6.04^{\text{A}}$	$25.2 \pm 3.09^{\text{B}}$
40:60	$151 \pm 8.5^{\text{A,B}}$	$32.2 \pm 1.18^{\text{B}}$	$24.8 \pm 2.14^{\text{B}}$
50:50	$143 \pm 3.9^{\text{B}}$	$30.3 \pm 1.72^{\text{B}}$	$20.3 \pm 2.04^{\text{A}}$

Means in same column with different letters are significantly different ( $p \leq 0.05$ ).

One can see that as the amount of MTPS in the samples increases, the maximum force achieved prior to rupture decreases. This is the same phenomenon as was observed for the tensile tests. Adding MTPS to PBAT

decreases the amount of force that can be withstood both in a tensile type loading and puncture type loading. One would expect starch films to exhibit lower puncture strength than MTPS-PBAT films. Aguilar-Mendez *et al.*<sup>92</sup> observed that gelatine - corn starch films had, on average, lower puncture strength and deformation than what has been reported here.

With regard to the deformation, it is observed that the blends containing 10, 20, 30, and 40% MTPS have the highest deformation prior to rupture, but the PBAT sample and the 50:50 blend sample have lower values for deformation. However, all samples exhibited puncture deformation values between 17.9 and 25.2 mm.

### **5.3.3 Barrier Properties**

A main function of packaging, especially food packaging, is often to avoid or at least decrease the transfer of gases such as oxygen, carbon dioxide, and water vapor between the contents of the package and the surrounding environment. Thus, the permeability of the packaging material to oxygen, carbon dioxide, and water vapor should be as low as possible.<sup>93</sup> Values for carbon dioxide, oxygen, and water vapor permeability of the film samples are shown in Table 11.

**Table 11.** Barrier properties of films of blends of MTPS with PBAT.

<b>Sample</b>	<b>Carbon Dioxide Permeability (kg·m·m<sup>-2</sup>·s<sup>-1</sup>·Pa<sup>-1</sup>) x 10<sup>16</sup></b>	<b>Oxygen Permeability (kg·m·m<sup>-2</sup>·s<sup>-1</sup>·Pa<sup>-1</sup>) x 10<sup>18</sup></b>	<b>Water Vapor Permeability (kg·m·m<sup>-2</sup>·s<sup>-1</sup>·Pa<sup>-1</sup>) x 10<sup>15</sup></b>
PBAT	3.0 ± 0.33 <sup>A</sup>	16.8 ± 1.77 <sup>A</sup>	5.0 ± 0.50 <sup>A</sup>
10:90	2.5 ± 0.10 <sup>A,B</sup>	14.5 ± 1.27 <sup>A,B</sup>	5.9 ± 0.24 <sup>A</sup>
20:80	2.1 ± 0.17 <sup>B,C</sup>	12.2 ± 0.70 <sup>B,C</sup>	6.7 ± 0.12 <sup>B</sup>
30:70	1.8 ± 0.31 <sup>C,D</sup>	10.0 ± 1.79 <sup>C,D</sup>	8.1 ± 1.10 <sup>B,C</sup>
40:60	1.3 ± 0.10 <sup>D,E</sup>	8.0 ± 0.67 <sup>D,E</sup>	10.4 ± 0.74 <sup>C,D</sup>
50:50	1.1 ± 0.12 <sup>E</sup>	6.0 ± 0.39 <sup>E</sup>	10.4 ± 0.80 <sup>D</sup>

Means in same column with different letters are significantly different ( $p \leq 0.05$ ).

One can see that by increasing the amount of MTPS in the sample, the carbon dioxide and oxygen permeability values decrease. For carbon dioxide, the permeability value decreases from  $3.0 \times 10^{-16} \text{ kg·m·m}^{-2}\cdot\text{s}^{-1}\cdot\text{Pa}^{-1}$  for PBAT to  $1.1 \times 10^{-16} \text{ kg·m·m}^{-2}\cdot\text{s}^{-1}\cdot\text{Pa}^{-1}$  for the 50:50 blend. While, for oxygen permeability, the values decrease from  $1.68 \times 10^{-17} \text{ kg·m·m}^{-2}\cdot\text{s}^{-1}\cdot\text{Pa}^{-1}$  for PBAT to  $6.0 \times 10^{-18} \text{ kg·m·m}^{-2}\cdot\text{s}^{-1}\cdot\text{Pa}^{-1}$  for the 50:50 blend. This could be due to the fact that a second phase has been added to the material, causing the transport of the gases through the films to be hindered.

However, for water vapor permeability, one can see that the values increase from  $5.0 \times 10^{-15} \text{ kg}\cdot\text{m}\cdot\text{m}^{-2}\cdot\text{s}^{-1}\cdot\text{Pa}^{-1}$  for PBAT to  $1.04 \times 10^{-14} \text{ kg}\cdot\text{m}\cdot\text{m}^{-2}\cdot\text{s}^{-1}\cdot\text{Pa}^{-1}$  for the 50:50 blend. Starch is a hygroscopic material, and thus has a greater affinity for water than PBAT. This causes an increase in the permeability of water vapor through films with higher starch content.

One would expect starch films to have carbon dioxide and oxygen permeability values that are lower than the values for the 50:50 blends reported in this work. In fact, this is the case. Biliaderis *et al.*<sup>94</sup> observed carbon dioxide and oxygen permeability values of  $1.60 \times 10^{-18} \text{ kg}\cdot\text{m}\cdot\text{m}^{-2}\cdot\text{s}^{-1}\cdot\text{Pa}^{-1}$  and  $5.46 \times 10^{-19} \text{ kg}\cdot\text{m}\cdot\text{m}^{-2}\cdot\text{s}^{-1}\cdot\text{Pa}^{-1}$ , respectively, for polyol-plasticized pullulan-starch blend films. Bae *et al.*<sup>95</sup> reported an oxygen permeability value for mungbean starch films of  $9.22 \times 10^{-20} \text{ kg}\cdot\text{m}\cdot\text{m}^{-2}\cdot\text{s}^{-1}\cdot\text{Pa}^{-1}$ . Thirathumthavorn and Charoenrein<sup>96</sup> reported oxygen permeability values of less than  $4.38 \times 10^{-19} \text{ kg}\cdot\text{m}\cdot\text{m}^{-2}\cdot\text{s}^{-1}\cdot\text{Pa}^{-1}$  for films of tapioca starch plasticized with sorbitol.

One would also expect starch films to have water vapor permeability values that are higher than the value for the 50:50 blends reported in this work. This is also the case. Bae *et al.*<sup>95</sup> reported a water vapor permeability value of  $1.8 \times 10^{-12} \text{ kg}\cdot\text{m}\cdot\text{m}^{-2}\cdot\text{s}^{-1}\cdot\text{Pa}^{-1}$  for mungbean starch films, while Thirathumthavorn and Charoenrein<sup>96</sup> reported a value of  $3.08 \times 10^{-13} \text{ kg}\cdot\text{m}\cdot\text{m}^{-2}\cdot\text{s}^{-1}\cdot\text{Pa}^{-1}$  for films of tapioca starch plasticized with sorbitol.

With regard to other polymers, Avella *et al.*<sup>97</sup> reported carbon dioxide and oxygen permeabilities for isotactic polypropylene (iPP) of approximately  $7.4 \times 10^{-17}$   $\text{kg}\cdot\text{m}^{-2}\cdot\text{s}^{-1}\cdot\text{Pa}^{-1}$  and  $1.7 \times 10^{-17}$   $\text{kg}\cdot\text{m}^{-2}\cdot\text{s}^{-1}\cdot\text{Pa}^{-1}$ , respectively. These values are lower and slightly higher, respectively, when compared to the permeabilities of the blends reported in this work. Also, the blends reported in this work exhibit oxygen permeability values that are higher than that reported by Frounchi and Dourbash<sup>98</sup> ( $3.4 \times 10^{-19}$   $\text{kg}\cdot\text{m}^{-2}\cdot\text{s}^{-1}\cdot\text{Pa}^{-1}$ ) for films of poly(ethylene terephthalate) (PET). Shellhammer and Krochta<sup>99</sup> reported values for the water vapor permeability for low-density polyethylene (LDPE), cellophane, and whey protein plasticized with glycerol of  $3.6 \times 10^{-16}$   $\text{kg}\cdot\text{m}^{-2}\cdot\text{s}^{-1}\cdot\text{Pa}^{-1}$ ,  $8.4 \times 10^{-14}$   $\text{kg}\cdot\text{m}^{-2}\cdot\text{s}^{-1}\cdot\text{Pa}^{-1}$ , and  $5.3 \times 10^{-13}$   $\text{kg}\cdot\text{m}^{-2}\cdot\text{s}^{-1}\cdot\text{Pa}^{-1}$ , respectively. In the current work, the water vapor permeability values for the MTPS/PBAT blends are lower than cellophane and whey protein plasticized with glycerol, but higher than for LDPE.

#### **5.3.4 Transmission Electron Microscopy (TEM)**

Images of the samples taken with the transmission electron microscope are shown in Figure 23. The PBAT is the continuous phase, while the MTPS is the dispersed phase. One can see that with an increasing amount of MTPS in the samples, the dispersed phase becomes finer and more regularly spaced.

For all blends, the MTPS phase is dispersed and has not significantly agglomerated. This demonstrates that the extrusion process of blending MTPS

and PBAT has resulted in a well mixed material. This is most likely due to the fact that maleating thermoplastic starch makes it more compatible with the PBAT, thus resulting in a more consistent blend. This regularity will help to provide consistent properties for films produced using these materials.

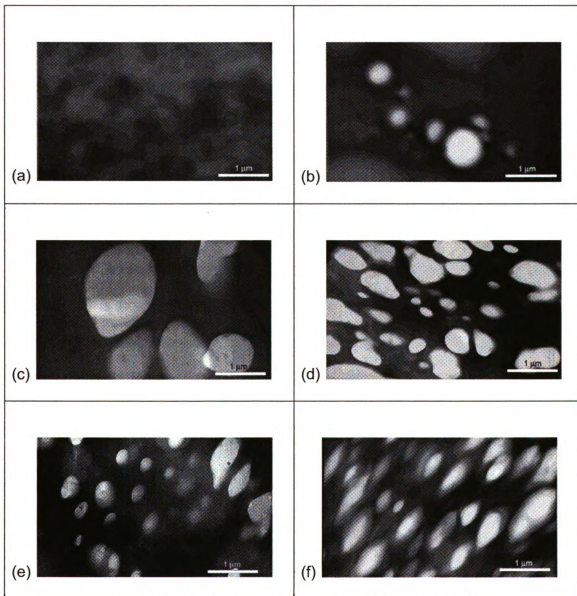


**Figure 23.** TEM images of the samples at 20,000x magnification (1 $\mu$ m scale bar): (a) PBAT, (b) MTPS:PBAT (10:90), (c) MTPS:PBAT (20:80), (d) MTPS:PBAT (30:70), (e) MTPS:PBAT (40:60), and (f) MTPS:PBAT (50:50). MTPS is the light phase and PBAT is the dark phase.

## **5.4 CONCLUSIONS**

Blends of MTPS and PBAT can be produced and formed into films. Mechanical tests of the films show that the tensile strength decreases with increasing MTPS in the samples; however, the elongation of the samples is not significantly affected by the addition of MTPS to the PBAT. Also, puncture force decreases as the amount of MTPS in the samples increases. As a barrier to carbon dioxide and oxygen, the addition of MTPS to PBAT improves the performance of the films. The permeability of carbon dioxide and oxygen decreases as the amount of MTPS in the materials increases. However, for water vapor permeability, the opposite is true. With increasing MTPS in the samples, the permeability of water vapor increases due to the hygroscopic nature of starch. Images of the samples, using transmission electron microscopy, show that MTPS is the dispersed phase while PBAT is the continuous phase. Also, as the amount of MTPS in the samples increases, the dispersed phase becomes finer and more regularly spaced. In order to use these materials for specific film applications, one must determine the necessary trade-off between mechanical properties and barrier properties. One should also keep in mind that by increasing the amount of PBAT in the material, the percent biocontent decreases. To maintain the maximum amount of biocontent in the material, the minimum amount of PBAT should be used that will still give the required material properties for the specific application.



## **CHAPTER 6**

### **APPLICATION AND PERFORMANCE OF MTPS-PBAT BLENDS FOR FOAMS**

---

#### **6.1 RATIONALE**

This work was performed to better understand the effect of the percentage of MTPS in MTPS-PBAT blends and the percentage of chemical blowing agent used on various properties of the foams produced. The foam samples were characterized by measurements of density, expansion ratio, and specific length, compressive strength, resiliency, and moisture sorption tests, and imaging using digital light microscopy.

## **6.2 MATERIALS AND METHODS**

### **6.2.1 Materials**

High amylose corn starch was purchased from National Starch and Chemicals (Indianapolis, IN). Poly(butylene adipate-co-terephthalate) (PBAT) was purchased from BASF Chemicals (Ludwigshafen, Germany), under the trade name Ecoflex. Anhydrous glycerol, 99.9% assay, was purchased from J.T. Baker (Phillipsburg, NJ). Maleic anhydride was purchased from Sigma-Aldrich, Inc (St. Louis, MO). The initiator, 2,5-bis(tert-butylperoxy)-2,5-dimethylhexane, also referred to as Luperox 101, was purchased from Sigma-Aldrich, Inc (St. Louis, MO). An endothermic chemical blowing agent, SAFTEC® UBA-60, was supplied by Reedy International Corporation (Keyport, NJ). The chemical blowing agent consists of sodium salts of carbonic and polycarboxylic acids in an ethylene-methyl acrylate copolymer carrier.<sup>100</sup>

### **6.2.2 Equipment**

A Century CX-30 co-rotating twin-screw extruder, having a length/diameter ratio (L/D) of 42 and a screw diameter of 30 mm was used to prepare the maleated thermoplastic starch, and to blend these materials with PBAT. A pelletizer was used to cut the extruded strands into pellets.

Foaming of the material was performed using a Killion single-screw extruder, having a length/diameter ratio of 24 and a screw diameter of 1 inch.

### **6.2.3 Procedure**

#### **6.2.3.1 Production of Maleated Thermoplastic Starch (MTPS)**

Maleated thermoplastic starch (MTPS) was produced in a Century CX-30 co-rotating twin-screw extruder in the same manner as described in Section 5.2.3.1.

#### **6.2.3.2 Blend Production of MTPS with PBAT**

Blends of maleated thermoplastic starch/PBAT were produced in a Century CX-30 co-rotating twin-screw extruder. Pellets of MTPS were pre-mixed with PBAT in a 50:50 and 30:70 weight of MTPS:weight of PBAT ratio and placed in the external feeder. The feeder fed the pellets into the feed port of the extruder. The temperature profile of the extruder was set at 25/125/135/140/145/150/150/150/145/135°C from the feed throat to the die. The screw speed was set to 100 rpm. The vent port was kept open to remove any moisture. The extruded strand was air cooled and pelletized in line. The pellets were dried for one day in an oven set at 65°C before being extruded into foams.

### **6.2.3.3 Foam Production**

Extruded foams of the blended material were produced in a Killion single-screw extruder. Pellets of the MTPS/PBAT blends were pre-mixed with the chemical blowing agent. The chemical blowing agent content was either 3 wt%, 5 wt%, or 7 wt% (of the blends) for production of the foams (Table 12). The pellets were gravity-fed into the extruder at the feed throat. The temperature profile of the extruder was set at 150/160/160/150°C from the feed throat to the die. Cooling water was circulated to maintain the set temperatures. The screw speed was set to 65 rpm. The extruded strands exited through a 4.72mm cylindrical die.

**Table 12.** Composition of foams of blends of MTPS and PBAT.

<b>Sample</b>	<b>Blowing Agent (%)</b>	<b>Blend Composition</b>	
		<b>MTPS (%)</b>	<b>PBAT (%)</b>
1	3	50	50
2	5	50	50
3	7	50	50
4	3	30	70
5	5	30	70
6	7	30	70
7	3	-	100
8	5	-	100
9	7	-	100

#### **6.2.3.4 Chemical Blowing Agent Thermal Decomposition**

The chemical blowing agent used in the foaming of the material had a reported process range of 100°C to 180°C. To ensure that thermal decomposition occurred within this range, thermal gravimetric analysis (TGA) was used to test a sample of the blowing agent. TGA was performed using a high resolution TGA 2950 from TA Instruments. The purge gas, nitrogen, had a flow rate of 50 ml/min. A pellet of the blowing agent was heated from room temperature to 600°C at a rate of 20°C/min.

#### **6.2.3.5 Extensional Viscosity**

Extensional viscosity measurements of PBAT and the 30:70 and 50:50 blends was performed by the Jayaraman group at Michigan State University. The PBAT was tested using an extensional viscosity fixture (EVF) mounted on an ARES melt rheometer at 150°C and tested to a strain of 3. The blends were tested using a Rheometrics Melt Elongational Rheometer (RME) at 140°C and tested to a strain of 3. If the samples broke before a strain of 3 was achieved, then that data was discarded.

### **6.2.3.6 Foam Characterization**

Foam specimens of the MTPS/PBAT blends were cut to approximately 25mm in length using a razor blade and were conditioned per standard method ASTM D4332,<sup>77</sup> in a constant environment room at  $23\pm 1^{\circ}\text{C}$  and  $50\pm 2\%$  RH for at least 72 hours before testing.

#### **6.2.3.6.1 Density**

The density of the foam samples was calculated according to ASTM test method D3575<sup>101</sup> (Method A), using the mass and volume of the specimens.<sup>12, 102, 103</sup> Ten specimens were measured for each sample. The density reported for each sample is the average of the ten specimens.

#### **6.2.3.6.2 Expansion Ratio**

The expansion ratio of the foam was calculated as the ratio of the cross-sectional area of the foam specimen to the cross-sectional area of the die.<sup>12</sup> Ten specimens were measured for each sample. The expansion ratio reported for each sample is the average of the ten specimens.

#### **6.2.3.6.3 Specific Length**

The specific length of the foam was calculated as the ratio of the length of each specimen to its mass.<sup>12</sup> The values used were those used in the density calculation. The units of specific length are centimeters per gram. Ten specimens were measured for each sample. The specific length reported for each sample is the average of the ten specimens.

#### **6.2.3.6.4 Compressive Strength and Resiliency**

Compressive strength of foam specimens were measured on a Stable Micro Systems texture analyzer (Surrey, England). Foam specimens were positioned lengthwise and compressed by a steel probe (6.35mm diameter) with a spherical end cap. The probe was lowered to the foam surface and an initial load of 0.5N was applied to the specimen. The probe was then lowered at a rate of 30 mm/min for a distance of 3mm. The probe was held at the distance of 3mm for 60 seconds. Load-deflection curves were recorded. Compressive strength was calculated by dividing the maximum load achieved by the cross-sectional area of the probe. Resiliency was calculated as the ratio of the compressive force at the end of the 60s hold period divided by the maximum force necessary to compress the foam specimen by 3mm, and is expressed as a percentage.<sup>12</sup> The compressive strength and resiliency reported for each sample are the average of five specimens.



#### **6.2.3.6.5 Moisture Sorption Analysis**

Five foam specimens of each sample were placed in a Blue M Electric Model WP-4800 (Watertown, WI) environmental humidity chamber at  $38\pm 5^{\circ}\text{C}$  and  $95\pm 5\%$  RH.<sup>12</sup> The weight and the dimensions (length and diameter) of the specimens were measured prior to entering the chamber. The weight of the specimens was monitored until steady state values were reached (approximately 60 days). The weight and dimensions were measured again at steady state. The initial weight, diameter, and length of the specimens were designated  $W_o$ ,  $D_o$ , and  $L_o$ , respectively. The steady state weight, diameter, and length of the specimens were designated  $W$ ,  $D$ , and  $L$ , respectively. Normalized values for steady state weight gain, steady state diameter, and steady state length were calculated using the initial and steady state values that were recorded. The values for normalized steady state weight gain, normalized steady state diameter, and normalized steady state length reported for each sample are an average of five specimens.

#### **6.2.3.6.6 Digital Light Microscopy**

A digital light microscope (Keyence Corporation of America, Woodcliff Lake, NJ) was used to make observations of the morphology of the cross-sectional area of the foams. A razor blade was used to section the foam samples.

### **6.2.3.7 Statistical Analysis**

One control sample, PBAT, was tested to evaluate the effect of blends of MTPS with PBAT on the properties of the foams produced. Analysis of variance (ANOVA) and Tukey mean comparison tests ( $p \leq 0.05$ ) were performed using Minitab 15 software (Minitab Inc., State College, PA).

## **6.3 RESULTS AND DISCUSSION**

### **6.3.1 Chemical Blowing Agent Thermal Decomposition**

The results of the TGA testing of the blowing agent are shown in Figure 24. The maximum rate of thermal decomposition of the blowing agent occurs at 150°C. This is towards the upper processing temperature range reported by the manufacturer. The temperature profile chosen for foaming of the materials, 150/160/160/150°C, is higher than the thermal decomposition temperature of the blowing agent, ensuring that decomposition of the blowing agent occurs during the foaming process.

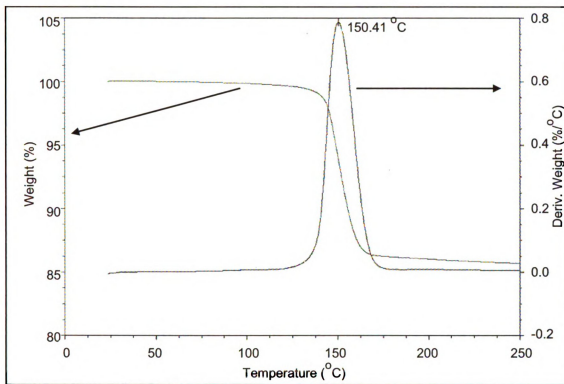


**Figure 24.** TGA graph of thermal decomposition of chemical blowing agent.

### **6.3.2 Extensional Viscosity**

Successful foaming of polymers requires a certain amount of strain hardening during extensional flow.<sup>104</sup> Figures 25 and 26 display the results of the extensional viscosity measurements of PBAT and the blends, respectively. One can see that the PBAT sample, the nonlinear viscoelastic response in extensional viscosity (strain hardening) increases as the strain rate increases. However, for the blends, the extensional viscosity rapidly decreases after it has begun to stretch (strain softening). This strain softening behavior is not conducive to foaming of the material. In the foam characterization data presented here, the differences between the melt properties of PBAT and the blends are apparent in their effect on the resulting foam properties.

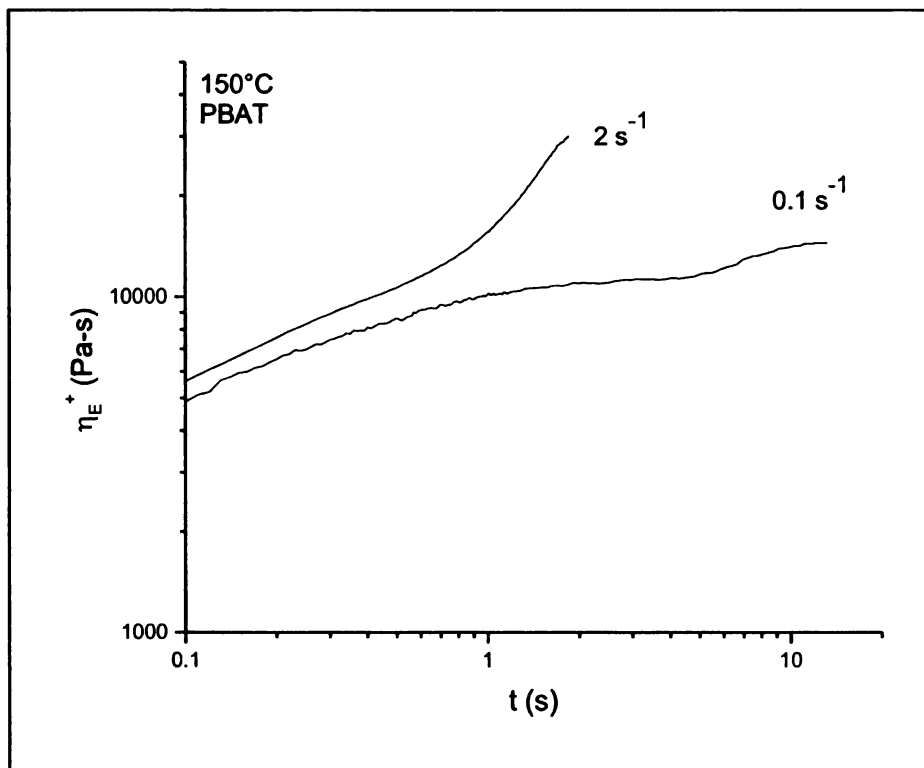


**Figure 25.** Extensional viscosity plot of PBAT at 150°C.

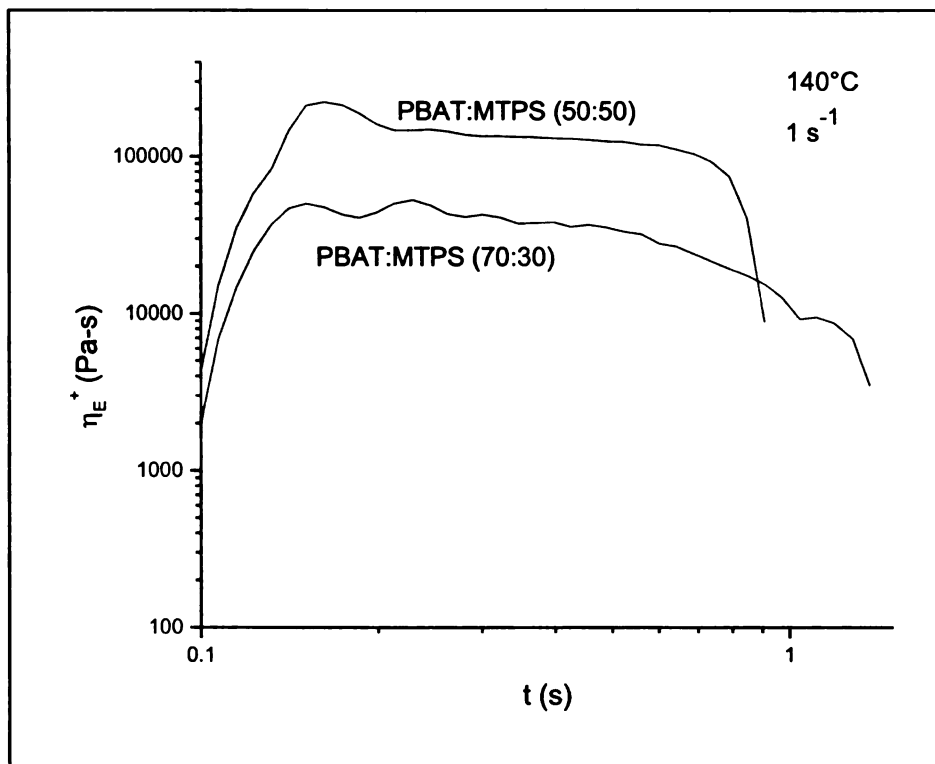


**Figure 26.** Extensional viscosity of blends at 140°C and 1<sup>s</sup>.

### **6.3.3 Density, Expansion Ratio, and Specific Length**

Table 13 displays the data for the density, expansion ratio, and specific length of the foam samples.

It should be noted that the densities of extruded, unfoamed PBAT, and 30:70 and 50:50 blends are  $1.22 \pm 0.01$ ,  $1.30 \pm 0.01$ , and  $1.37 \pm 0.03 \text{ g/cm}^3$ , respectively.

All foams showed a reduction in their densities, compared to the unfoamed material.

From Table 13, one observes that the foam samples that showed the best characteristics of lowest density, highest expansion ratio, and highest specific length are the PBAT samples. This is most likely due to the fact that the blends containing MTPS go through an additional heat cycle during the foaming process, causing the starch to degrade. This shortens the length of the starch polymer chains and decreases the ability of the blends to support the expanding cells during the foaming process. During the foaming process, it was observed that the foamed blends shrunk more than the foamed PBAT upon exiting the extruder and cooling.

Looking at the effect of the amount of blowing agent on the density of the foams shows that for PBAT samples, increasing the blowing agent from 3% to 5% decreases the density, however, increasing the blowing agent to 7% does not affect the density of the foam. For the 30:70 blend, the density of the foams is not

affected by the amount of blowing agent added. As will be discussed in the digital light microscopy results, this is most likely due to the fact that with only 3% blowing agent, there is not enough gas liberated during the blowing agent decomposition; however, when 5% and 7% blowing agent are used, the melt properties of the blends are inadequate to support the expanding cells, leading to cell collapse and the formation of voids in the center of the samples. These same observations are made for the 50:50 blend samples, however, with 7% blowing agent, the cell collapse actually causes the density to increase slightly.

The data reported here shows values for density, expansion ratio, and specific length of the foams that are quite high, low, and low, respectively, when compared with foam extrusion of starch, using water as the blowing agent.<sup>12, 68</sup>

When one compares the densities to studies using chemical blowing agents to foam HDPE,<sup>73</sup> they are more closely related. Using chemical blowing agents with PBAT and blends of MTPS:PBAT show a comparable reduction in density to the work by Li and Matuana<sup>73</sup> foaming HDPE and HDPE composites using chemical blowing agents.



**Table 13.** Density, expansion ratio, and specific length of foams of blends of MTPS and PBAT.

<b>Sample</b>	<b>Density (g/cm<sup>3</sup>)</b>	<b>Expansion Ratio</b>	<b>Specific Length (cm/g)</b>
PBAT 3%	0.73 ± 0.06 <sup>A</sup>	2.49 ± 0.48 <sup>A</sup>	3.28 ± 0.70 <sup>A,B</sup>
PBAT 5%	0.49 ± 0.02 <sup>B</sup>	2.95 ± 0.28 <sup>B</sup>	4.00 ± 0.45 <sup>C,D</sup>
PBAT 7%	0.50 ± 0.05 <sup>B</sup>	2.72 ± 0.30 <sup>A,B</sup>	4.29 ± 0.46 <sup>D</sup>
30:70 3%	0.84 ± 0.03 <sup>C</sup>	1.92 ± 0.09 <sup>C</sup>	3.54 ± 0.19 <sup>A,C</sup>
30:70 5%	0.91 ± 0.08 <sup>C,D</sup>	1.87 ± 0.15 <sup>C</sup>	3.40 ± 0.31 <sup>A</sup>
30:70 7%	0.83 ± 0.05 <sup>C</sup>	1.91 ± 0.13 <sup>C</sup>	3.63 ± 0.12 <sup>A,C</sup>
50:50 3%	0.89 ± 0.07 <sup>C,E</sup>	2.60 ± 0.26 <sup>A,B</sup>	2.50 ± 0.10 <sup>E</sup>
50:50 5%	0.94 ± 0.10 <sup>D,E</sup>	2.22 ± 0.24 <sup>A,C,D</sup>	2.78 ± 0.16 <sup>E</sup>
50:50 7%	1.08 ± 0.05 <sup>F</sup>	1.86 ± 0.10 <sup>C,D</sup>	2.85 ± 0.10 <sup>B,E</sup>

Means in same column with different letters are significantly different ( $p \leq 0.05$ ).

### 6.3.4 Compressive Strength and Resiliency

Foams can better resist deformation during loading if they are denser and have thicker cell walls, as opposed to less dense foams that have thinner walls. A power-law relationship has been observed between compressive strength,  $\sigma_c$ , and foam density,  $\rho$ , where  $\sigma_c \sim \rho^n$ . In Figure 27 below, one observes a strong relationship between compressive strength and foam density. The slope of the regression line was calculated to be  $n=0.94$ . A value of  $n=0.92$  was reported by Nabar *et al.*<sup>12</sup> and Willet *et al.*,<sup>68</sup> however, Hutchinson *et al.*<sup>105</sup> reported values of  $n=1.5-1.6$  for foams made from maize grits. In the current work, the value of  $n$  is in agreement with the values calculated by Nabar *et al.* and Willett *et al.* It should be noted; however, that this value is dependent on the extrusion system and the materials used.<sup>12</sup>

In Figure 27, the point at (6.59, 14.81) is an outlier (Dixon's Q-test for outliers, with 95% confidence interval). This point has not been used to calculate the regression line.

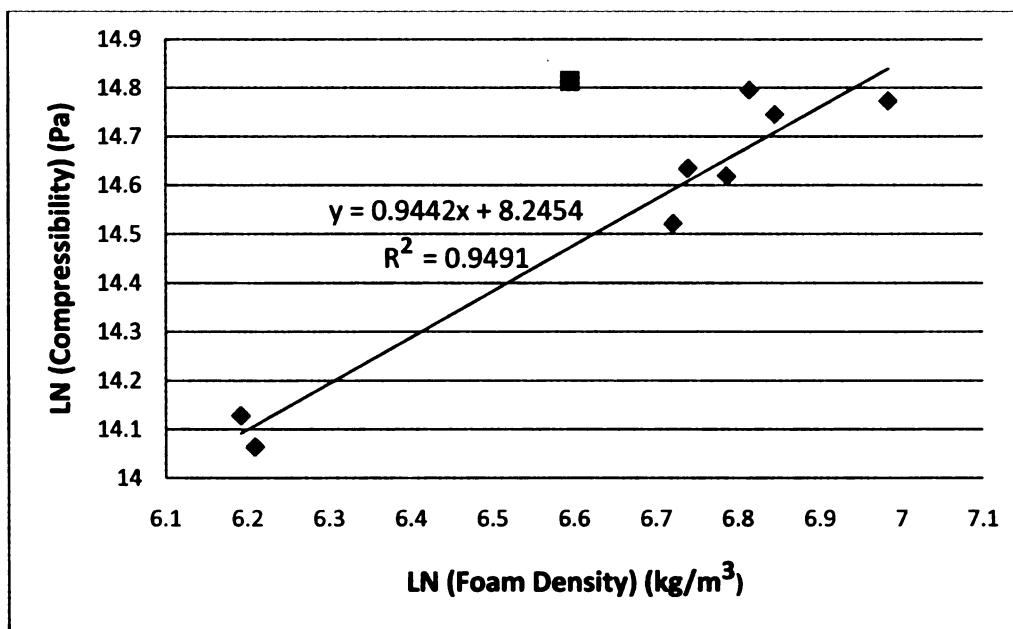


**Figure 27.** Logarithmic plot of compressive strength as a function of foam density.

The resiliency values of the foam samples are shown in Table 14. From the values of resiliency listed, one observes that resiliency improves when there is more PBAT present in the samples. The foamed samples of PBAT have the greatest resiliency, 82.14% - 80.82%, while the foamed samples of the blends have a much lower resiliency; 57.50%-61.58% for the 30:70 blend, and 54.73%-51.33% for the 50:50 blend. The effect of the amount of blowing agent added is not evident.

When one compares the densities and the resiliencies, one observes that foams of PBAT have lower densities and higher resiliency values than foams of blends of MTPS and PBAT.

**Table 14.** Resiliency of foams of blends of MTPS and PBAT.

<b>Sample</b>	<b>Resiliency (%)</b>
PBAT 3%	82.14 ± 1.23 <sup>A</sup>
PBAT 5%	81.51 ± 0.35 <sup>A</sup>
PBAT 7%	80.82 ± 1.07 <sup>A</sup>
30:70 3%	59.57 ± 5.16 <sup>B,D</sup>
30:70 5%	57.50 ± 6.51 <sup>B,C,D</sup>
30:70 7%	61.58 ± 2.05 <sup>B,D</sup>
50:50 3%	54.73 ± 0.89 <sup>B,E</sup>
50:50 5%	53.46 ± 1.34 <sup>B,E</sup>
50:50 7%	51.33 ± 2.01 <sup>C,E</sup>

Means in same column with different letters are significantly different ( $p \leq 0.05$ ).

### 6.3.5 Moisture Sorption Analysis

The results of the moisture sorption tests are shown in Table 15. In other work that has been performed previously,<sup>12</sup> foams consisting of starch shrink during moisture sorption tests. Arif *et al.*<sup>106</sup> also observed the shrinkage of starch foam when it was subjected to conditions of 30°C and 89% relative humidity. This was not observed in the current work. This unexpected result is due to the fact that PBAT forms the matrix for the materials that were foamed. The PBAT is the

continuous phase, while the MTPS is the dispersed phase. PBAT expands when it sorbs water. Since the PBAT is the continuous phase in these samples, they also expand when they sorb water.

Starch is a hygroscopic material, so adding MTPS to PBAT (30:70 blend and 50:50 blend) causes an increase in the normalized steady state weight gain. The "50:50 7%" sample shows a much lower steady state weight gain value than the other two 50:50 blend samples. This is most likely due to the fact that the density is highest in this sample, which does not allow moisture to be sorbed well throughout the sample.

The performance of starch foam (cushioning and insulation) is negatively affected by the shrinkage that usually occurs during moisture sorption of starch-based foams.<sup>12</sup> From the results of this study, it would appear that foams which contain higher amounts of PBAT would not see this adverse affect. Starch can be added to the PBAT (which would decrease the cost of the material), and the resulting foam still does not shrink during moisture sorption.

**Table 15.** Moisture sorption steady-state weight gain, diameter, and length of foams of blends of MTPS and PBAT.

<b>Sample</b>	<b>Normalized Steady State Weight Gain<sup>a</sup></b>	<b>Normalized Steady State Diameter<sup>b</sup></b>	<b>Normalized Steady State Length<sup>c</sup></b>
PBAT 3%	3.54 ± 0.47 <sup>A</sup>	203.94 ± 11.95 <sup>A,C</sup>	100.38 ± 0.46 <sup>A,B</sup>
PBAT 5%	7.13 ± 0.24 <sup>A,B</sup>	182.49 ± 5.54 <sup>B</sup>	100.88 ± 0.56 <sup>A</sup>
PBAT 7%	8.67 ± 0.87 <sup>A,C</sup>	186.99 ± 8.00 <sup>B</sup>	100.87 ± 0.52 <sup>A</sup>
30:70 3%	24.08 ± 0.57 <sup>D,E,F</sup>	214.62 ± 2.50 <sup>A</sup>	103.19 ± 0.56 <sup>C</sup>
30:70 5%	26.98 ± 0.44 <sup>E,F</sup>	217.30 ± 6.95 <sup>A</sup>	103.43 ± 0.22 <sup>C</sup>
30:70 7%	32.01 ± 1.19 <sup>F</sup>	217.16 ± 6.53 <sup>A</sup>	103.34 ± 0.48 <sup>C</sup>
50:50 3%	22.92 ± 5.33 <sup>D,E</sup>	188.69 ± 4.57 <sup>B</sup>	99.03 ± 0.26 <sup>D</sup>
50:50 5%	20.03 ± 6.38 <sup>D</sup>	195.36 ± 7.49 <sup>B,C</sup>	99.45 ± 0.16 <sup>D</sup>
50:50 7%	9.56 ± 1.18 <sup>B,C</sup>	214.06 ± 2.82 <sup>A</sup>	99.74 ± 0.28 <sup>B,D</sup>

<sup>a</sup> $[(W-W_0)/W_0] \times 100\%$ , <sup>b</sup> $[D/D_0] \times 100\%$ , <sup>c</sup> $[L/L_0] \times 100\%$

Means in same column with different uppercase letters are significantly different ( $p \leq 0.05$ ).

### **6.3.6 Digital Light Microscopy**

Images of the foam samples are shown in Figure 28. One can see that the foams of PBAT have a more regular cell structure. For the sample with 3% blowing agent, there are some areas of unfoamed PBAT. However, for the samples containing 5% and 7% blowing agent, the cells appear to be throughout the matrix.

For the foams of 30:70 blends, one can see that with 3% blowing agent there are some areas of unfoamed 30:70 material. However, for the samples containing 5% and 7% blowing agent, the cells appear to become larger and more of an open cell structure is observed.

For the foams of the 50:50 blends, one can see that with 3% blowing agent there are some areas of unfoamed 50:50 material (as was seen with the PBAT and 30:70 blend). Also, like the 30:70 blend, the samples containing 5% and 7% blowing agent show cells that appear to be an opened cell structure. The samples also show evidence of cell collapse and aggregation to large voids in the center of the sample.

These images suggest that PBAT has better melt properties than the blends which allow the cells to grow but not collapse. The blends; however, show large irregular cells that have joined to form an open cell structure. This is observed in the blends with greater than 3% blowing agent in them; however, with 3%

blowing agent there are still areas that have not been foamed. This is not an optimum condition.

The results of the density measurements agree with the images that have been shown above. For the PBAT, one can see that with 5% and 7% blowing agent, we see similar densities and they are less than the density of PBAT with 3% blowing agent. With 3% blowing agent, there is not enough gas liberated by the decomposition of the blowing agent to fully foam all of the material. With 5% and 7% blowing agent, there is enough gas present, and foaming occurs throughout the material.

For both the 30:70 and 50:50 blends, one notices that the densities are similar, independent of the amount of blowing agent added. This is due to the fact that with only 3% blowing agent, there is not enough gas liberated during blowing agent decomposition; however, when 5% and 7% blowing agent are used, the melt properties of the blends are inadequate to support the expanding cells, leading to cell collapse and the formation of large voids.



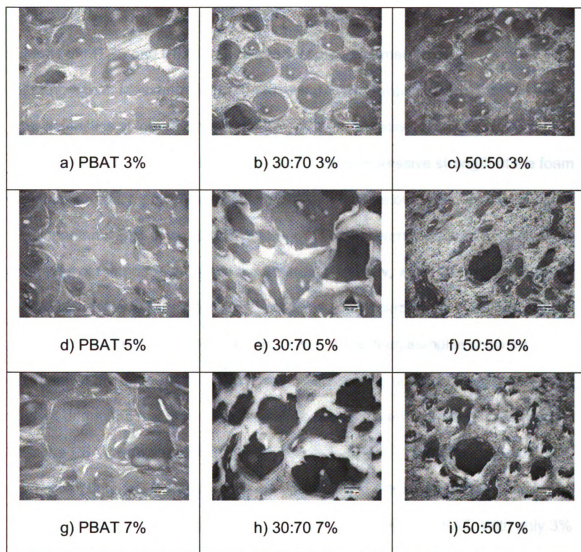


**Figure 28.** Digital light microscope images of foams of blends of MTPS and PBAT (250  $\mu\text{m}$  scale bar) showing the cell structure of the foams.

## 6.4 CONCLUSIONS

Blends of MTPS and PBAT can be produced and foamed using a chemical blowing agent. Measurement of the resulting foam samples shows that the best characteristics of lowest density, highest expansion ratio, and highest specific length are observed in the PBAT samples. The compressive strength of the foam samples follows a power-law relationship, with a slope of the regression line of the logarithmic plot of compressive strength versus foam density of  $n=0.94$ . Samples of foamed PBAT have the greatest resiliency, while samples of foamed 30:70 blends have lower resiliency, and samples of foamed 50:50 blends have the lowest resiliency. Moisture sorption tests of the foam samples show an increase in the diameter of the samples as moisture is sorbed. All samples gain weight during the moisture sorption testing, with the blends gaining more weight than the PBAT samples, due to the hygroscopic nature of MTPS. Images of the samples using a digital light microscope show that PBAT foams have a more regular cell structure than the foams of blends of MTPS and PBAT. With only 3% blowing agent, there appears to be regions of unfoamed material in all of the samples. For the blended materials, with 5% and 7% blowing agent, the cells become larger and show more of an open cell structure. Blending MTPS with PBAT decreases the cost of using only PBAT, however, one can see that this affects the properties of the foam. In order to use these materials for specific applications, one must determine the necessary trade-off between required properties and cost of the material.

## **CHAPTER 7**

### **SUMMARY AND CONCLUSIONS**

---

#### **7.1 SUMMARY**

The engineering significance of the work that has been performed is that it shows that blends of starch and the biodegradable polyester, PBAT, can be produced and formed into thermoformed objects, films, and foams. These objects can be used to replace current objects made from petroleum-based plastics that are not biodegradable. By blending the starch and PBAT together, one receives advantages over using either component separately; namely, improved mechanical properties through the addition of the PBAT to the starch, and lower cost through the addition of the starch to the PBAT. As well, improvements in

some barrier properties of films have also been observed by blending MTPS with PBAT.

The materials produced in this work have the potential to decrease the carbon footprint of the manufacturers who produce the products, as well as the consumers who use the products. Also, since the products are biodegradable, they can be composted and will not add to the garbage that is in landfills.

## **7.2 CONCLUSIONS**

Upon completion of this work, one can make the following conclusions:

### **7.2.1 Maleated Thermoplastic Starch by Reactive Extrusion Processing**

- MTPS had improved processability over TPS.
- The maleation process permitted formulations with less than 30% of glycerol to be extruded in the twin-screw extruder, resulting in pellets that were more transparent than thermoplastic starches not modified with maleic anhydride.
- As the percentage of maleic anhydride increased, there was negligible change in the hydrodynamic radii. However, as the percentage of Luperox 101 increased, the hydrodynamic radii decreased.
- Using the maximum temperature during the extrusion process of 165°C instead of 135°C caused a drastic decrease in the hydrodynamic radius,

due to the high influence of the temperature profile on the molecular weight of the thermoplastic starch.

- The MTPS samples presented higher melting temperatures compared to the TPS sample.
- The soxhlet studies indicated that using the maximum temperature of 165°C in the extrusion temperature profile resulted in more grafting between glycerol and starch than when the maximum temperature used was 135°C.
- There is an increased understanding of maleation of high amylose corn starch and the effect of maleic anhydride and initiator content.

### **7.2.2 MTPS-PBAT Blends by Reactive Extrusion Processing and Their Application and Performance for Thermoformed Articles**

- The processability of high amylose corn starch MTPS is much better than the processability of regular corn starch MTPS.
- Blends of plasticized starch, with or without maleation, with PBAT can form sheets which can be thermoformed.
- To the best of the author's knowledge, this is the first report of thermoforming of 100% biodegradable material.
- The tensile properties are similar for blends of PBAT with TPS and MTPS that have been extruded at a maximum temperature of 135°C. However, the maleated thermoplastic samples formed sheets and thermoformed pieces that were more transparent and had a more homogeneous surface.

- The effect of amylose content of the different starches used did not present significant differences in the tensile properties when the glycerol content was 30% and the ratio of thermoplastic starch/PBAT used was 50:50.
- When the MTPS contained 20% glycerol and the maximum processing temperature was 165°C, the blend containing MTPS of high amylose corn starch showed better tensile properties than the blend containing MTPS of regular corn starch, when the ratio of thermoplastic starch/PBAT used was 50:50.
- Increasing the MTPS (high amylose corn starch) content to 60% decreased the tensile strength and elongation of the sheets.
- The addition of TPS or MTPS decreased the tensile strength, but did not cause a significant difference in the elongation, compared to the elongation of PBAT.
- The puncture test results show similar behavior to the tensile test results.
- DSC analysis shows that the blends all have higher melting and crystallization temperatures than neat PBAT.
- ESEM shows that blends containing MTPS extruded with a maximum temperature of 165°C are smoother and more homogeneous than the blends containing MTPS and TPS extruded with a maximum temperature of 135°C.

### **7.2.3 Application and Performance of MTPS-PBAT Blends for Films**

- Blends of MTPS and PBAT can be produced and formed into films.
- Increasing the amount of PBAT in the material causes a decrease in the percent biocontent.
- Mechanical tests of the films show that the tensile strength decreases with increasing MTPS in the samples, however, the elongation of the samples is not significantly affected by the addition of MTPS to the PBAT.
- The puncture force of the films decreases as the amount of MTPS in the samples increases.
- As a barrier to carbon dioxide and oxygen, the addition of MTPS to PBAT improves the performance of the films. The permeability of carbon dioxide and oxygen decreases as the amount of MTPS in the materials increases.
- With increasing MTPS in the samples, the permeability of water vapor increases due to the hygroscopic nature of starch.
- Images of the samples, using transmission electron microscopy, show that MTPS is the dispersed phase while PBAT is the continuous phase.
- As the amount of MTPS in the samples increases, the dispersed phase becomes finer and more regularly spaced.

#### **7.2.4 Application and Performance of MTPS-PBAT Blends for Foams**

- Blends of MTPS and PBAT can be produced and foamed using a chemical blowing agent.
- Measurement of the resulting foam samples shows that the best characteristics of lowest density, highest expansion ratio, and highest specific length are observed in the PBAT samples.
- The compressive strength of the foam samples follows a power-law relationship, with a slope of the regression line of the logarithmic plot of compressive strength versus foam density of  $n=0.94$ .
- Samples of foamed PBAT have the greatest resiliency, while samples of foamed 30:70 blends have lower resiliency, and samples of foamed 50:50 blends have the lowest resiliency.
- Moisture sorption tests of the foam samples show an increase in the diameter of the samples as moisture is sorbed.
- All samples gain weight during the moisture sorption testing, with the blends gaining more weight than the PBAT samples, due to the hygroscopic nature of MTPS.
- Images of the samples using a digital light microscope show that PBAT foams have a more regular cell structure than the foams of blends of MTPS and PBAT.
- With only 3% blowing agent, there appears to be regions of unfoamed material in all of the samples.



- For the blended materials, with 5% and 7% blowing agent, the cells become larger and show more of an open cell structure.
- Blending MTPS with PBAT decreases the cost of using only PBAT; however, one can see that this affects the properties of the foam.
- In order to use these materials for specific applications, one must determine the necessary trade-off between required properties and cost of the material.

## **CHAPTER 8**

### **RECOMMENDATIONS FOR FUTURE WORK**

---

#### **8.1 RECOMMENDATIONS FOR FUTURE WORK**

The work presented here describes much of the materials testing performed on MTPS and MTPS-PBAT blends. These materials have the potential to be used to produce thermoformed objects, films, and foams. Future work could focus on testing the materials for specific applications to ensure that they meet the requirements for each application. This testing could include product durability, product dimensional, and product environmental testing.

Heat has been shown to decrease the molecular weight of starch during the extrusion process. In the procedures described in this work, starch was extruded

to produce MTPS, then it was blended with PBAT in another extrusion process, and finally, it was formed into sheets, films, or foams in a third extrusion process. A procedure could be developed in which the starch, glycerol, maleic anhydride, Luperox 101, and PBAT are reactively extruded at once, and formed into sheets, films, or foams upon exit from the extruder.

Polymeric materials are often injection molded to form various products. Injection molding of the MTPS-PBAT blends described in this work could be performed. Mechanical and thermal testing of the resulting injection molded products would give an indication of the usefulness of these materials for injection molded applications. Furthermore, adding fibers to the materials during the extrusion process could be investigated to determine if composites of MTPS-PBAT blends have improved characteristics for injection molding, versus MTPS-PBAT blends without fibers.

Biodegradability studies were not performed on these materials. Although it is known that the materials are biodegradable, testing should be performed to better understand the length of time required for biodegradation to occur.

Biodegradability can be measured according to ASTM standard test method D5338, "Standard Test Method for Determining Aerobic Biodegradation of Plastic Materials Under Controlled Composting Conditions",<sup>107</sup> and in combination with ASTM standard test method D6400, "Standard Specification for Compostable

Plastics".<sup>108</sup> In this way, the biodegradability performance of these materials can be compared to other biodegradable products.

A life cycle analysis of the MTPS and MTPS-PBAT blends was not performed. A recommendation for future work would be to perform a life cycle analysis for the materials produced in this work. ASTM standard test method D7075, "Standard Practice for Evaluating and Reporting Environmental Performance of Biobased Products",<sup>109</sup> should be used to perform this evaluation. Having a life cycle analysis of the materials would allow potential manufacturers to better understand the impact of these materials and how the impacts compare to conventional polymeric materials.

## REFERENCES

- [1] Narayan, R. Environmental footprint/profile of biobased, biodegradable products. <http://www3.abe.iastate.edu/biobased/LCAFootprint.pdf>.
- [2] IPCC, 2007: Summary for Policymakers. In: Climate Change 2007: The Physical Science Basis. Contribution of Working Group I to the Fourth Assessment Report of the Intergovernmental Panel on Climate Change; Solomon, S.; Qin, D.; Manning, M.; Chen, Z.; Marquis, M.; Averyt, K.B.; Tignor, M.; Miller, H.L., Eds.; Cambridge University Press: Cambridge, United Kingdom, 2007.
- [3] United Nations, 1998: Kyoto protocol to the United Nations framework convention on climate change.
- [4] Narayan, R. In Drivers for biodegradable/compostable plastics & role of composting in waste management & sustainable agriculture, Proceedings of the International Conference on Biodegradable Polymers: Production, market utilization, and residue management, Wolfsburg, Germany, 2000 (EXPO 2000).
- [5] Narayan, R. In Rationale, drivers, and design for biodegradable & biobased plastics, Proceedings of the 2002 Polymers, Laminations & Coatings Conference (TAPPI), Boston, Massachusetts, September 7-12, 2002.
- [6] Narayan, R. In Biodegradable/Compostable Plastics, USDA Food Plastic Ware Composting Workshop, 2005.
- [7] Thompson, R.C.; Olsen, Y.; Mitchell, R.P.; Davis, A.; Rowland, S.J.; John, A.W.G.; McGonigle, D.; Russell, A.E. Science 2004, 304, 838.
- [8] Algalita Marine Research Foundation.  
[http://www.algalita.org/pelagic\\_plastic.html](http://www.algalita.org/pelagic_plastic.html) (accessed March 4, 2008).
- [9] Narayan, R. In Biobased & biodegradable polymer materials: Rationale, drivers, and technology exemplars, Presented at the National American Chemical Society, Division of Polymer Chemistry meeting, San Diego (2005); ACS Symposium Series Book Chapter – 2005, In Press.
- [10] Narayan, R. In Overview of biodegradable & biobased plastics technologies, Proceedings of the 2002 Polymers, Laminations & Coatings Conference (TAPPI), Boston, Massachusetts, September 7-12, 2002.

- [11] Yamamoto, M.; Witt, U.; Skupin, G.; Beimborn, D.; Müller, R.-J. Biodegradable aliphatic-aromatic polyesters: "Ecoflex®". In *Biopolymers Volume 4 – Polyesters III: Applications and Commercial Products*; Steinbüchel, A., Ed.; Wiley-VCH: Weinheim, 2003.
- [12] Nabar, Y.; Raquez, J.M.; Dubois, P.; Narayan, R. *Biomacromolecules* 2005, 6, 807-817.
- [13] BASF, Ecoflex® F BX 7011 – Biodegradable polyester for compostable film, Product Information, Version 1.3, April, 2007.
- [14] White, J.L.; Potente, H.; Eds. *Screw Extrusion*; Hanser: Cincinnati, 2003.
- [15] Selke, S.E.M.; Culter, J.D.; Hernandez, R.J. *Plastics Packaging – Properties, Processing, Applications and Regulations, Second Edition*; Hanser: Cincinnati, 2004.
- [16] Balakrishnan, S. *Studies in reactive extrusion processing of biodegradable polymeric materials*. PhD Dissertation, Michigan State University, 2004.
- [17] Rauwendaal, C. *Polymer Extrusion*; Hanser: Cincinnati, 2001.
- [18] Kienzle, S.Y. *Polymer Blends and Alloys: Guidebook to Commercial Products*; Technomic Publishing Co., Inc.: Lancaster, Pennsylvania, 1988.
- [19] Paul, D.R.; Barlow, J.W. *Polymer Blends: Introductory Overview and Future Developments*. In *Polymer Compatibility and Incompatibility: Principles and Practices*; Solc, K., Ed.; Harwood Academic Publishers: Chur, Switzerland, 1982.
- [20] Bonner, J.G.; Hope, P.S. *Compatibilization and Reactive Blending*. In *Polymer Blends and Alloys*; Folkes, M.J.; Hope, P.S., Eds.; Blackie Academic & Professional: London, 1993.
- [21] Khare, A.; Deshmukh, S. *Journal of Plastic Film & Sheeting* 2006, 22, 193-211.
- [22] Thuwall, M.; Boldizar, A.; Rigdahl, M. *Carbohydrate Polymers* 2006, 65, 441-446.
- [23] George, E.R.; Sullivan, T.M.; Park, E.H. *Polymer Engineering and Science* 1994, 34, 17-23.
- [24] Dias Alves, V.; Mali, S.; Beleia, A.; Grossmann, M.V.E. *Journal of Food Engineering* 2007, 78, 941-946.

- [25] Kalambur, S.; Rizvi, S.S.H. *Journal of Plastic Film & Sheeting* 2006, 22, 39-58.
- [26] Hung, P.V.; Maeda, T.; and Morita, N. *Trends in Food Science & Technology* 2006, 17, 448-456.
- [27] Copeland, L.; Blazek, J.; Salman, H.; Tang, M.C. *Food Hydrocolloids* 2009, 23 (6), 1527-1534.
- [28] Bertoft, E.; Piyachomkwan, K.; Chatakanonda, P.; Sriroth, K. *Carbohydrate Polymers* 2008, 74 (3), 527-543.
- [29] Myllärinen, P.; Partanem, R.; Sppälä, J.; Forssell, P. *Carbohydrate Polymers* 2002, 50, 355-361.
- [30] Muller, C.M.O.; Yamashita, F.; Laurindo, J.B. *Carbohydrate Polymers* 2007, 72, 82-87.
- [31] Lourdin, D.; Della Valle, G.; Colonna, P.; Poussin, D. *Revue Generale des Caoutchoucs & Plastiques* 1999, 780, 39-42.
- [32] Narayan, R. *Commercialization Technology: A Case Study of Starch Based Biodegradable Plastics*. In *Paradigm for Successful Utilization of Renewable Resources*; Sessa, D.J., Willett, J.L., Eds.; AOCS Press: Champaign, Illinois, 1998; p 78.
- [33] Narayan, R. *Biodegradable Multi-Component Polymeric Materials Based on Unmodified Starch-Like Polysaccharides*. U.S. Patent 5,500,465, October 31, 1995.
- [34] Narayan, R. *Chemically Modified Plasticized Starch Compositions by Extrusion Processing*. U.S. Patent 7,153,354, December 26, 2006.
- [35] Nabar, Y. *Design and engineering of novel starch-based foam and film products*. PhD Dissertation, Michigan State University, 2004.
- [36] Tuil, R.V.; Fowler, P.; Lawrher, M.; Weber, C.J. *Properties of biobased packaging materials*. In *Biobased Packaging Materials for the Food Industry – Status and Perspectives*; Weber, C.J., Ed.; KVL Department of Dairy and Food Science: Denmark, 2000.
- [37] Kalambur, S.; Rizvi, S.S.H. *Journal of Plastic Film & Sheeting* 2006, 22, 39-58.
- [38] Averous, L.; Fringant, C.; Moro, L. *Starch/Starke* 2001, 53, 368-371.

- [39] Zobel, H.F. *Starch/Starke* 1988, 40, 44-50.
- [40] Van Soest, J.J.G.; Knooren, N. *Journal of Applied Polymer Science* 1997, 64, 1411-1422.
- [41] Bogoeva-Gaceva, G.; Avella, M.; Malinconico, M.; Buzarovska, A.; Grozdanov, A.; Gentile, G.; Errico, M.E. *Polymer Composites* 2007, 28, 98-107.
- [42] Vaidya, U.R.; Bhattacharya, M. *Journal of Applied Polymer Science* 1994, 52, 617-628.
- [43] Bhattacharya, M.; Vaidya, U.R.; Zhang, D.; Narayan, R. *Journal of Applied Polymer Science* 1995, 57, 539-554.
- [44] Mani, R.; Bhattacharya, M. *European Polymer Journal* 1998, 34, 1467-1475.
- [45] Carlson, D.L.; Nie, L.; Narayan, R.; Dubois, P. *Journal of Applied Polymer Science* 1999, 72, 477-485.
- [46] Wu, C.-S. *Polymer Degradation and Stability* 2003, 80, 127-134.
- [47] Dubois, P.; Narayan, R. *Macromolecular Symposia* 2003, 198, 233-243.
- [48] Huneault, M.A.; Li, H. *Polymer* 2007, 48, 270-280.
- [49] Chandra, R.; Rustgi, R. *Polymer Degradation and Stability* 1997, 56, 185-202.
- [50] Shujun, W.; Jiugao, Y.; Jinglin, Y. *Polymer Degradation and Stability* 2005, 87, 395-401.
- [51] Paramawati, R. In Effect of maleic anhydride on biodegradable film of poly(butylenes adipate-co-terephthalate) blended with thermoplastic tapioca, *Proceedings of Inno Bioplast, Bangkok, Thailand, September 21-24, 2006*; Techawiboonwong, A., Ellis, W., Eds.; National Innovation Agency: Bangkok, Thailand, 2006.
- [52] Jiang, L.; Wolcott, M.P.; Zhang, J. *Biomacromolecules* 2006, 7, 199-207.
- [53] Le Digabel, F.; Averous, L. *Carbohydrate Polymers* 2006, 66, 537-545.
- [54] Averous, L.; Le Digabel, F. *Carbohydrate Polymers* 2006, 66, 480-493.
- [55] Bodros, E.; Pillin, I.; Montrelay, N.; Baley, C. *Composites Science and Technology* 2007, 67, 462-470.



- [56] Lourdin, D.; Della Valle, G.; Colonna, P. *Carbohydrate Polymers* 1995, 27, 261–270.
- [57] Arvanitoyannis, I.; Biliaderis, C.G.; Ogawa, H.; Kawasaki, N. *Carbohydrate Polymers* 1998, 36, 89-104.
- [58] García, M.A.; Martino, M.N.; Zaritzky, N.E. *Scanning* 1999, 21, 348-353.
- [59] Mali, S.; Grossmann, M.V.E.; García, M.A.; Martino, M.N.; Zaritzky, N.E. *Food Hydrocolloids* 2005, 19, 157-164.
- [60] Mali, S.; Grossmann, M.V.E. *Journal of Agricultural and Food Chemistry* 2003, 51, 7005-7011.
- [61] Narayan, R. *Kunststoffe* 1989, 79, 1022.
- [62] Rowell, P.; Schultz, T.; Narayan, R. *Emerging Technologies for Materials and Chemicals from Biomass*; ACS Symposium Series 467; American Chemical Society: Washington, DC, 1991.
- [63] Narayan, R. *Polymeric Materials from Agricultural Feedstocks*. In *Polymers from Agricultural Coproducts*; Fishman, M. L., Friedman, R. B., Huang, S. J., Eds.; ACS Symposium Series 575; American Chemical Society: Washington, DC, 1994; p 2.
- [64] Bastioli, C.; Bellotti, V.; Del Giudice, L.; Lombi, R.; Rallis, A.; Del Tredici, G.; Montino, A.; Ponti, R. *Expanded articles of biodegradable plastics materials and a method for their production*. U.S. Patent 5,288,765, February 22, 1994.
- [65] Bastioli, C.; Bellotti, V.; Del Giudice, L.; Lombi, R.; Rallis, A. *Expanded articles of biodegradable plastic materials*. U.S. Patent 5,360,830, November 1, 1994.
- [66] Bastioli, C.; Bellotti, V.; Del Tredici, G.; Montino, A.; Ponti, R. *Biodegradable foamed plastic materials*. U.S. Patent 5,736,586, April 7, 1998.
- [67] Bastioli, C.; Bellotti, V.; Del Tredici, G.; Rallis, A. *Biodegradable foamed articles and process for the preparation thereof*. U.S. Patent 5,801,207, September 1, 1998.
- [68] Willett, J.L.; Shogren, R.L. *Polymer* 2002, 43, 5935-5947.
- [69] Fang, Q; Hanna, MA. *Bioresource Technology* 2001, 78, 115–122.
- [70] Zirkel, L.; Munstedt, H. *Polymer Engineering and Science* 2007, 47, 1740-1749.

- [71] Demir, H.; Sipahioglu, M.; Balkose, D.; Ulku, S. *Journal of Materials Processing Technology* 2008, 195, 144-153.
- [72] Guan, L.T.; Xiao, M.; Meng, Y.Z. *Polymer Engineering and Science* 2006, 46, 153-159.
- [73] Li, Q.; Matuana, L.M. *Journal of Applied Polymer Science* 2003, 88 (14), 3139-3150.
- [74] Raquez, J-M.; Nabar, Y.; Srinivasan, M.; Shin, B-Y.; Narayan, R.; Dubois, P. *Carbohydrate Polymers* 2008, 74, 159-169.
- [75] Carlson, D.; Dubois, P.; Nie, L.; Narayan, R. *Polymer Engineering and Science* 1998, 38, 311-321.
- [76] Roger, P.; Tran, V.; Lesec, J.; Colonna, P. *Journal of Cereal Science* 1996, 24, 247-262.
- [77] American Standard Test Methods, "Standard Practice for Conditioning Containers, Packages, or Packaging Components for Testing", In *Annual Book of ASTM Standards, D4332, 15.10*, ASTM, Philadelphia, PA (2007).
- [78] American Standard Test Methods, "Standard Test Method for Tensile Properties of Thin Plastic Sheeting", In *Annual Book of ASTM Standards, D882, 08.01*, ASTM, Philadelphia, PA (2006).
- [79] Rindlav-Westling, A.; Stading, M.; Hermansson, A.M.; Gatenholm, P. *Carbohydrate Polymers* 1998, 36, 217-224.
- [80] Tharanathan, R.N. *Trends in Food Science & Technology* 2003, 14, 71-78.
- [81] Sakanaka, L. *Filmes biodegradáveis de blendas de amido termoplástico e polibutileno succinato co-adipato (PBSA)*. Thesis. Universidade Estadual de Londrina, Brazil, 2007.
- [82] Garg, S.; Jana, A.K. *European Polymer Journal* 2007, 43 (9), 3976-3987.
- [83] Kang, B.G.; Yoon, S.H.; Lee, S.H.; Yie, J.E.; Yoon, B.S.; Suh, M.H. *Journal of Applied Polymer Science* 1996, 60 (11), 1977-1984.
- [84] Mali, S.; Grossmann, M.V.E.; García, M.A.; Martino, M.M.; Zaritzky, N.E. *Carbohydrate Polymers* 2002, 50, 379-386.

- [85] American Standard Test Methods, "Standard Test Methods for Determining the Biobased Content of Natural Range Materials Using Radiocarbon and Isotope Ratio Mass Spectrometry Analysis", In *Annual Book of ASTM Standards*, D6866, 08.03, ASTM, Philadelphia, PA (2006).
- [86] American Standard Test Methods, "Test Method for the Determination of Carbon Dioxide Gas Transmission Rate (CO<sub>2</sub>TR) Through Barrier Materials Using An Infrared Detector", In *Annual Book of ASTM Standards*, F2476, 15.10, ASTM, Philadelphia, PA (2007).
- [87] American Standard Test Methods, "Standard Test Method for Oxygen Gas Transmission Rate Through Plastic Film and Sheeting Using a Coulometric Sensor", In *Annual Book of ASTM Standards*, D3985, 15.10, ASTM, Philadelphia, PA (2007).
- [88] American Standard Test Methods, "Standard Test Method for Water Vapor Transmission Rate Through Plastic Film and Sheeting Using a Modulated Infrared Sensor", In *Annual Book of ASTM Standards*, F1249, 15.10, ASTM, Philadelphia, PA (2007).
- [89] Parulekar, Y.; Mohanty, A.K. *Macromolecular Materials and Engineering* 2007, 292, 1218-1228.
- [90] Otey, F.H.; Westhoff, R.P.; Doane, W.M. *Industrial & Engineering Chemistry Product Research and Development* 1980, 19 (4), 592-595.
- [91] Zamudio-Flores, P.B.; Bautista-Banos, S.; Salgado-Delgado, R.; Bello-Perez, L.A. *Journal of Applied Polymer Science* 2009, 112 (2), 822-829.
- [92] Aguilar-Mendez, M.A.; San Martin-Martinez, E.; Tomas, S.A.; Cruz-Orea, A.; Jaime-Fonseca, M.R. *Journal of the Science of Food and Agriculture* 2008, 88 (2), 185-193.
- [93] Salame, M. Barrier Polymers. In *The Wiley Encyclopedia of Packaging Technology*; Bakker, M., Ed.; Wiley: New York, 1986; pp 48-54.
- [94] Biliaderis, C.G.; Lazaridou, A.; Arvanitoyannis, I. *Carbohydrate Polymers* 1999, 40 (1), 29-47.
- [95] Bae, H.J.; Cha, D.S.; Whiteside, W.S.; Park, H.J. *Food Chemistry* 2008, 106 (1), 96-105.
- [96] Thirathumthavorn, D.; Charoenrein, S. *Starch* 2007, 59 (10), 493-497.
- [97] Avella, M.; Bruno, G.; Errico, M.E.; Gentile, G.; Piciocchi, N.; Sorrentino, A.; Volpe, M.G. *Packaging Technology and Science* 2007, 20 (5), 325-335.

[98] Frounchi, M.; Dourbash, A. *Macromolecular Materials and Engineering* 2009, 294 (1), 68-74.

[99] Shellhammer, T.H.; Krochta, J.M. *Journal of Food Science* 1997, 62 (2), 390-394.

[100] Saftec® UBA-60; Trade Secret Registration Number 763 098 00-5000P, 763 098 00-5001P, 763 098 00-5002P, 763 098 00-5003P, 763 098 00-5004P; Reedy International Corporation: Keyport, NJ, April, 2008.

[101] American Standard Test Methods, "Standard Test Methods for Flexible Cellular Materials Made From Olefin Polymers", In *Annual Book of ASTM Standards*, D3575, 08.02, ASTM, Philadelphia, PA (2006).

[102] Glenn, G.M.; Irving, D.W. *Cereal Chemistry* 1995, 72 (2), 155-161.

[103] Zhang, J.-F.; Sun, X. *Journal of Applied Polymer Science* 2007, 106 (5), 3058-3062.

[104] Xanthos, M.; Wan, C.; Dhavalikar, R.; Karayannidis, G.P.; Bikiaris, D.N. *Polymer International* 2004, 53 (8), 1161-1168.

[105] Hutchinson, R.J.; Siodlak, G.D.E.; Smith, A.C. *Journal of Material Science* 1987, 22, 3956-3962.

[106] Arif, S.; Burgess, G.; Narayan, R.; Harte, B. *Packaging Technology and Science* 2007, 20 (6), 413-419.

[107] American Standard Test Methods, "Standard Test Method for Determining Aerobic Biodegradation of Plastic Materials Under Controlled Composting Conditions", In *Annual Book of ASTM Standards*, D5338, 08.03, ASTM, Philadelphia, PA (2006).

[108] American Standard Test Methods, "Standard Specification for Compostable Plastics", In *Annual Book of ASTM Standards*, D6400, 08.03, ASTM, Philadelphia, PA (2006).

[109] American Standard Test Methods, "Standard Practice for Evaluating and Reporting Environmental Performance of Biobased Products", In *Annual Book of ASTM Standards*, D7075, 08.03, ASTM, Philadelphia, PA (2006).

MICHIGAN STATE UNIVERSITY LIBRARIES



3 1293 03063 1604